SUPPORTING INFORMATION

Conformation control through concurrent N–H···S and N–H···O=C hydrogen bonding and hyperconjugation effects

Zeynab Imani, Venkateswara Rao Mundlapati, Gildas Goldsztejn, Valérie Brenner, Eric Gloaguen, Régis Guillot, Jean-Pierre Baltaze, Katia Le Barbu-Debus, Sylvie Robin, Anne Zehnacker, Michel Mons,* David J. Aitken*

Table of Contents

1. Synthesis

1.1 General information: instrumentation and materials

Melting points were measured in open capillary tubes on a Büchi B-540 apparatus and are uncorrected. ^{1}H and ^{13}C NMR spectra were recorded on Bruker spectrometers operating at 400/360/300 MHz for ^{1}H and at 100/90/75 MHz for ^{13}C. For ^{1}H NMR spectra, chemical shifts (δ) are reported in parts per million (ppm) with reference to tetramethylsilane (δ = 0.00 ppm) or residual protonated solvent (δ = 7.26 ppm for $CDCl_3$, δ = 2.50 ppm for DMSO-d_6, δ = 4.79 ppm for D_2O) as internal standards. Splitting patterns for ^{1}H signals are designated as s (singlet), bs (broad singlet), d (doublet) or m (multiplet), and coupling constants (J) are reported in hertz. For ^{13}C NMR spectra, chemical shifts (δ) are reported in parts per million (ppm) with reference to the deuterated solvent (δ = 77.16 ppm for $CDCl_3$, δ = 39.52 ppm for DMSO-d_6) as an internal standard. Fourier-transform infrared (IR) spectra were recorded on a FT-IR Perkin Elmer Spectrum Two spectrometer; maximum absorbances (ν) are given in cm^{-1}. Spectra of neat samples, liquids or solids, were recorded using an ATR diamond accessory; solution state spectra were recorded for $CHCl_3$ solutions in an Omni-cell Specac 0.2 mm path-length NaCl solution cell, with background solvent subtraction. High-resolution mass spectrometry (HRMS) data were recorded using a spectrometer equipped with an electrospray ionisation source in positive mode (ESI+) associated with a tandem Q-TOF analyser.

Thietane-3-one (95%), isobutyl chloroformate (IBCF) (98%), Boc_2O (99%) and TFA (peptide grade) were purchased from Fluorochem; potassium cyanide (97%), ammonium cyanide (for analysis), benzyl chloroformate (CbzCl) (97 wt%), triethylamine (extra pure), 4-dimethylaminopyridine (DMAP) and sodium carbonate (bioreagent) were purchased from Acros; magnesium sulfate (98%) was purchased from VWR Chemicals; *N*-methylmorpholine (NMM) (99%), methylamine (40% aqueous solution) and Dowex 50WX8 cation-exchange resin (H^+ form, 50-100 mesh) were purchased from Sigma-Aldrich; *N*-(3-dimethylaminopropyl)-*N*′-ethylcarbodiimide hydrochloride (EDCI·HCl) (>98%) and 4 M HCl solution in 1,4-dioxane were purchased from TCI. These reagents were used without further purification, except as follows: NMM was dried over KOH then fractionally distilled at 120 °C (atmospheric pressure); triethylamine was dried over KOH then fractionally distilled at 90 °C (atmospheric pressure). Hydrochloric acid (36 wt%) and sodium hydroxide (98.5%) were purchased from Sigma-Aldrich and used to make aqueous solutions. THF was distilled from

sodium/benzophenone under argon. DMF was dried over CaH_2, then fractionally distilled at 109 °C under reduced pressure and kept under argon. Dichloromethane was passed through a column of activated alumina immediately before use. Other commercial solvents were used as received from VWR Chemicals or Carlo Erba. All reactions requiring anhydrous conditions were performed under argon. Flash chromatography was performed on silica gel columns (40–63 μm). Analytical thin-layer chromatography was carried out with 0.25 mm commercial silica gel plates (EMD, Silica Gel $60F_{254}$) TLC plates were visualized by fluorescence at 254 nm then revealed using an acidic *p*-anisaldehyde solution (5% in EtOH), a ninhydrin solution (14 mM in EtOH) or a $KMnO_4$ solution (7.5% in water). Retention factors (R_f) are given for such TLC analyses. The final purification of compound **3** was performed using a UV-directed (210 nm) HPLC with a thermostated (30 °C) reverse phase 5 μm Lux Cellulose-1 semi-preparative column (250 × 10 mm) at a flow rate of 5 mL/min.

1.2 Synthesis of Cbz-Attc-NHMe, 1 and Cbz-Attc-OMe, 4

Compounds **1** and **4** were synthesized according to Scheme S1. The first two steps are based on the literature.[S1]

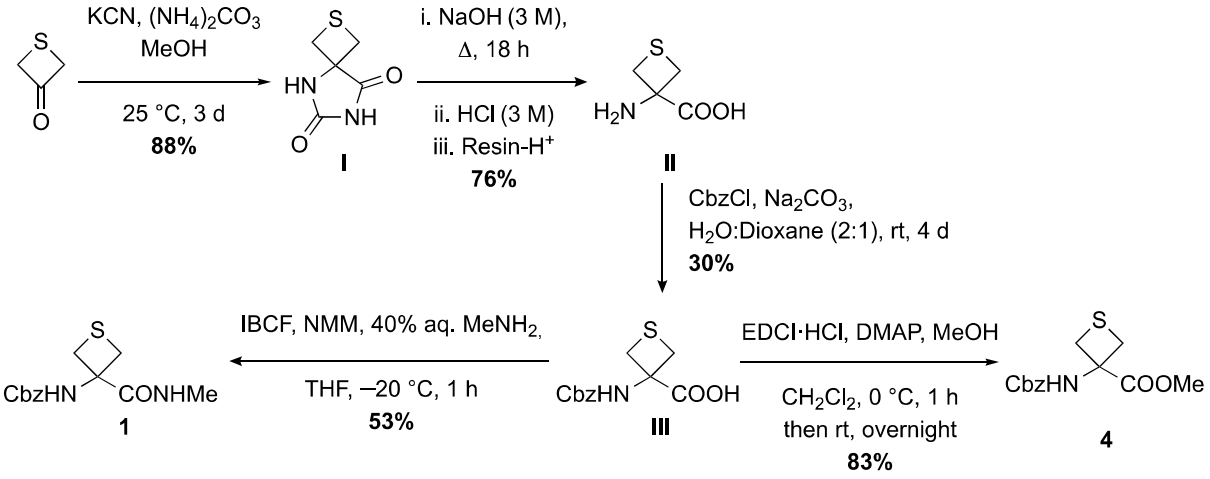

Scheme S1.

2-Thia-5,7-diazaspiro[3.4]octane-6,8-dione I. To a suspension of $(NH_4)_2CO_3$ (4.80 g, 50.0 mmol, 2.2 eq.) in MeOH (114 mL) in a 250 mL one-necked flask was added KCN (1.63 g, 25.0 mmol, 1.1 eq.). The suspension was stirred for 30 min at 40 °C until a limpid solution was obtained. A solution of thietane-3-one (2.00 g, 22.6 mmol, 1 eq.) in MeOH (27 mL) was added to the previous mixture. The mixture was stirred 30 min at 40 °C then 3 d at 25 °C (controlled with a water bath). The solvent was evaporated. The resulting brown sticky solid was treated with 6 M aqueous HCl solution to reach pH 1-2 under a fume hood. The resulting light brown solid was filtered and washed with a small amount of cold water to give the crude hydantoin **I** (3.14 g, 88%). The product was purified by recrystallization from H_2O:EtOH (5:1) (after filtration of the hot solution to remove a dark brown polymer) to give the hydantoin **I** (2.04 g, 57%) as light beige solid. In general the crude product can be used without recrystallization.

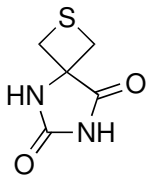

R_f = 0.61 (EtOAc:MeOH = 98:2), **Mp =** 234–238 °C.

^{1}H NMR (360 MHz, DMSO-d_6, 300 K) δ 10.73 (bs, 1H, NH^7), 8.80 (bs, 1H, NH^5), 3.47 (d, ^2J = 10.1 Hz, 2H, $C^{\beta}H^a$), 3.42 (d, ^2J = 10.4 Hz, 2H, $C^{\beta}H^b$).

^{13}C NMR (90 MHz, DMSO-d_6, 300 K) δ 175.35 (C^8O), 155.12 (C^6O), 63.24 (C^{α}), 34.63 ($C^{\beta}H_2$).

IR (neat) ν 3136, 3052, 2937, 2770, 1735, 1407, 1394 cm^{-1}.

HRMS [ESI(+)] *m/z* $[M+Na]^+$ calculated for $[C_5H_6N_2NaO_2S]^+$: 181.0042, found: 181.0041.

3-Aminothietane-3-carboxylic acid, Attc II. A solution of **I** (256 mg, 1.62 mmol, 1 eq.) in 3 M NaOH (6 mL, 11 eq.) was heated at reflux for 18 h in a 10 mL one-necked flask. Ammonia and water were removed under reduced pressure. The light yellow residue was treated with 3 M aqueous HCl solution (6 mL) to reach pH 1-2. This solution was applied to a column of cation-exchange resin (H^+ form) and eluted with 1 M NH_4OH aqueous solution to give the amino acid **II** as a beige solid (82 mg, 76%).

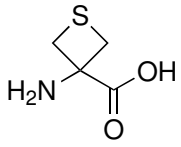

Mp = 227–230 °C.

^{1}H NMR (360 MHz, D_2O, 300 K) δ 3.68 (d, ^2J = 11.0 Hz, 2H, $C^{\beta}H^{a}$), 3.25 (d, ^2J = 11.4 Hz, 2H, $C^{\beta}H^{b}$).

^{13}C NMR (90 MHz, D_2O, 300 K) δ 170.92 (CO), 60.90 (C^{α}), 31.31 ($C^{\beta}H_2$).

IR (neat) ν 2700-3600 (br), 1628 cm^{-1}.

HRMS [ESI(+)] *m/z* $[M+H]^+$ calculated for $[C_4H_8NO_2S]^+$: 134.0276, found: 134.0270.

3-(((Benzyloxy)carbonyl)amino)thietane-3-carboxylic acid III. To a suspension of **II** (200 mg, 1.50 mmol, 1 eq.) in H_2O (8 mL) and 1,4-dioxane (4 mL) in a 25 mL one-necked flask was added Na_2CO_3 (477 mg, 4.50 mmol, 4.5 eq.). The suspension was stirred until all the solid was dissolved. The solution was cooled to 0 °C and CbzCl (107 µL, 0.75 mmol, 0.5 eq.) was added dropwise; the solution was then stirred for 24 h at room temperature. The solution was then cooled to 0 °C and more CbzCl was added dropwise (107 µL, 0.75 mmol, 0.5 eq.). This procedure was repeated two more times until a total of 2 eq. of CbzCl had been added to the solution. After a further 24 h at room temperature, 1,4-dioxane was removed under reduced pressure. The residual aqueous layer was washed with hexane (3 × 20 mL) then slowly acidified at 0 °C with a 2 M aqueous HCl solution to reach pH 1. The aqueous layer was extracted with EtOAc (6 × 20 mL). The organic layer was dried over $MgSO_4$, filtrated and concentrated under reduced pressure. The purification was carried out by flash chromatography (gradient from CH_2Cl_2:MeOH:AcOH = 98:2:1 to 90:10:1) to give **III** as a light yellow solid (116 mg, 30%).

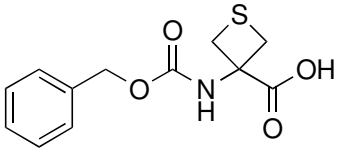

R_f = 0.28 (CH_2Cl_2:MeOH:AcOH = 95:5:1), **Mp** = 124–126 °C.

^{1}H NMR (400 MHz, $CDCl_3$, 300 K) δ 10.24 (bs, 1H, OH), 7.35 (m, 5H, CH^{Ar}), 5.79 (bs, 1H, NH), 5.13 (s, 2H, CH_2^Z), 3.75 (d, ^2J = 9.6 Hz, 2H, $C^\beta H^a$), 3.45 (d, ^2J = 9.6 Hz, 2H, $C^\beta H^b$).

^{13}C NMR (100 MHz, $CDCl_3$, 300 K) δ 175.05 (C^1O), 155.19 (C^ZO), 135.59 (C^{Ar}), 128.59, 128.48, 128.24 ($C^{Ar}H$), 67.53 (C^ZH_2), 61.77 (C^α), 33.42 ($C^\beta H_2$).

IR (neat) ν 3324, 3030, 2964, 1722, 1651, 1523 cm^{-1}.

HRMS [ESI(+)] *m/z* $[M+Na]^+$ calculated for $[C_{12}H_{13}NNaO_4S]^+$: 290.0458, found: 290.0453.

Benzyl (3-(methylcarbamoyl)thietan-3-yl)carbamate, Cbz-Attc-NHMe 1. To a cold (– 20 °C) solution of **III** (607 mg, 2.27 mmol, 1 eq.) in THF (5 mL) in an argon-flushed 25 mL one-necked flask were added successively NMM (275 µL, 2.50 mmol, 1.1 eq.) and IBCF (331 µL, 2.50 mmol, 1.1 eq.). Following the activation period of 10 min at –20 °C, a solution of 40% aqueous $MeNH_2$ (2 mL, 22.7 mmol, 10 eq.) in THF (3 mL) was added. The resulting mixture was stirred for 1 h 30 at –20 °C then 5% aqueous $NaHCO_3$ (5 mL) was added. The resulting solution was stirred for 1 h at room temperature, then was extracted with CH_2Cl_2 (6 × 15 mL). The combined organic layers were washed with 5% aqueous $NaHCO_3$ (2 × 5 mL), dried over $MgSO_4$, filtrated and concentrated under reduced pressure. The purification was carried out by flash chromatography (gradient from PE:EtOAc = 7:3 to 0:1) to give **1** as a light yellow solid (335 mg, 53%).

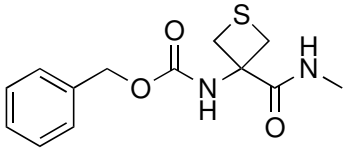

R_f = 0.60 (PE:EtOAc = 2:8), **Mp** = 172–175 °C.

^{1}H NMR (360 MHz, $CDCl_3$, 300 K) δ 7.98 (bs, 1H, NH^2), 7.38-7.30 (m, 5H, CH^{Ar}), 6.46 (bs, 1H, NH^1), 5.14 (s, 2H, CH_2^Z), 4.28 (d, ^2J = 8.8 Hz, 2H, $C^\beta H^a$), 3.24 (d, ^2J = 9.6 Hz, 2H, $C^\beta H^b$), 2.95 (d, ^3J = 4.7 Hz, 3H, CH_3).

^{13}C NMR (90 MHz, $CDCl_3$, 300 K) δ 172.34 (C^1O), 155.09 (C^ZO), 136.25 (C^{Ar}), 128.71, 128.39, 128.25 ($C^{Ar}H$), 66.89 (C^ZH_2), 61.00 (C^α), 33.61 ($C^\beta H_2$), 26.97 (CH_3).

IR (neat) *v* 3373, 3215, 3037, 1689, 1638, 1536, 1499, 1461 cm^{-1}.

HRMS [ESI(+)] *m/z* $[M+Na]^+$ calculated for $[C_{13}H_{16}N_2NaO_3S]^+$: 303.0767, found: 303.0774.

Benzyl (3-(methoxycarbonyl)thietan-3-yl)carbamate, Cbz-Attc-OMe 4. To an ice-bath cooled solution of **III** (40 mg, 0,15 mmol, 1 eq.) in CH_2Cl_2 (2 mL) in an argon-flushed one-necked 10 mL flask were added successively DMAP (2 mg, 0,10 mmol, 0.1 eq.), MeOH (18 µL, 0.45 mmol, 3 eq.) and EDCI·HCl (32 mg, 0.16 mmol, 1.1 eq.). The resulting mixture was stirred for 1 h at 0 °C then overnight at room temperature. The solvent was removed under reduced pressure. The purification was carried out by flash chromatography (gradient from PE:EtOAc = 8:2 to 4:6) to give **IV** as a cream solid (35 mg, 83%).

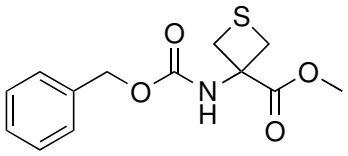

R_f = 0.40 (PE:EtOAc = 8:2), **Mp** = 80–82 °C.

^{1}H NMR (360 MHz, $CDCl_3$, 300 K) δ 7.41-7.28 (m, 5H, CH^{Ar}), 5.66 (bs, 1H, NH^1), 5.11 (s, 2H, CH_2^Z), 3.83 (bs, 3H, CH_3), 3.71 (d, ^2J = 10.1 Hz, 2H, $C^\beta H^a$), 3.43 (d, ^2J = 8.4 Hz, 2H, $C^\beta H^b$).

^{13}C NMR (90 MHz, $CDCl_3$, 300 K) δ 171.61 (C^1O), 154.82 (C^ZO), 135.98 (C^{Ar}), 128.72, 128.49, 128.34 ($C^{Ar}H$), 67.32 (C^ZH_2), 62.07 (C^α), 53.43 (CH_3), 33.96 ($C^\beta H_2$).

IR (neat) *v* 3259, 3144, 2950, 1736, 1704 cm^{-1}.

HRMS [ESI(+)] *m/z* $[M+Na]^+$ calculated for $[C_{13}H_{15}NNaO_4S]^+$: 304.0614, found: 304.0613.

1.3 Synthesis of Cbz-(Attc)$_2$-NHMe, 2

Compound **2** was synthesized according to Scheme S2.

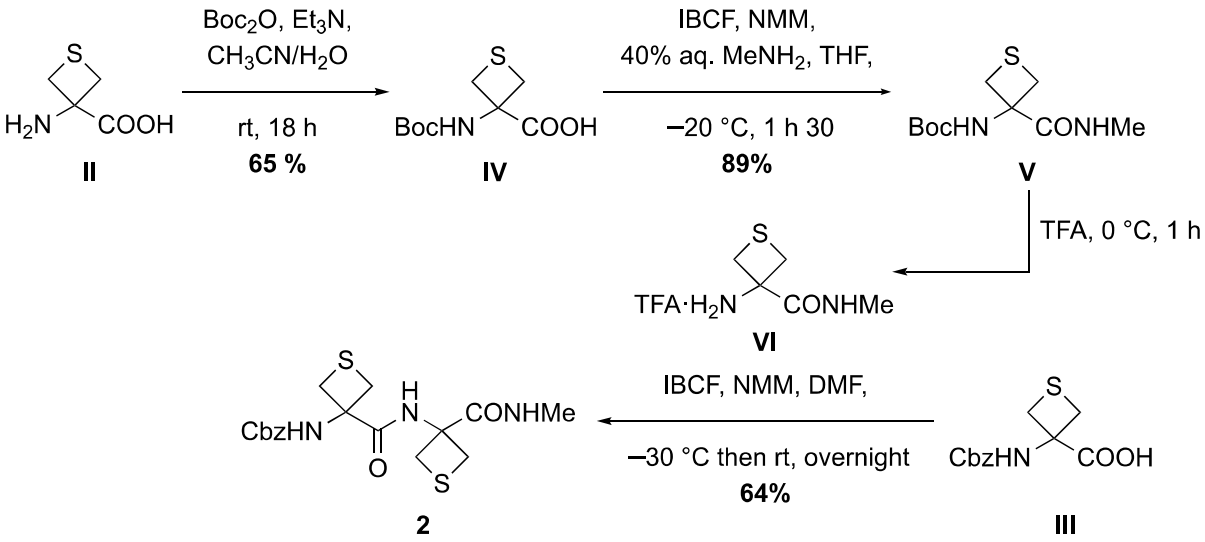

Scheme S2.

3-((*tert*-butoxycarbonyl)amino)thietane-3-carboxylic acid IV. To a solution of **II** (400 mg, 3 mmol, 1 eq.) in a 1:1 mixture of CH_3CN:H_2O (7 mL) in a 25 mL one-necked flask was added Et_3N (490 µL, 3.51 mmol, 1.2 eq.). To the resulting solution was added a solution of Boc_2O (681 mg, 3.12 mmol, 1.04 eq.) in CH_3CN (2 mL). The resulting mixture was stirred overnight at room temperature then CH_3CN was evaporated under reduced pressure. The aqueous layer was acidified with 1 M aqueous HCl solution to reach pH 1, then extracted with $CHCl_3$ (6 × 15 mL). The organic layer was washed with water (2 × 15 mL) then with brine (15 mL), dried over $MgSO_4$, filtrated and concentrated under reduced pressure. The purification was carried out by flash chromatography (gradient from PE:EtOAc = 80:20 to 0:1 then EtOAc:MeOH = 95:5) to give **IV** as a light yellow solid (421 mg, 65%).

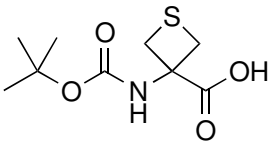

R_f = 0.37 (CH_2Cl_2:MeOH:AcOH = 94:5:1), **Mp** = 134–135 °C.

^{1}H NMR (360 MHz, $CDCl_3$, 300 K) δ 10.67 (bs, 1H, OH), 7.23 (bs, ½H, NH rotamer), 5.63 (bs, ½H, NH, rotamer), 3.72 (d, ^2J = 7.7 Hz, 2H, $C^{\beta}H^{a}$), 3.38 (bs, 2H, $C^{\beta}H^{b}$), 1.42 (s, 9H, *t*Bu).

^{13}C NMR (90 MHz, $CDCl_3$, 300 K) δ 175.19 ($C^{1}O$), 155.02 ($C^{Boc}O$), 77,35 (CMe_3), 61.83 (C^{α}), 33.78 (C^{β}), 1.42 (CH_3).

IR (neat) ν 3248, 3137, 2981, 1698, 1364 cm^{-1}.

HRMS [ESI(+)] *m/z* $[M+Na]^+$ calculated for $[C_9H_{15}NNaO_4S]^+$: 256.0614, found: 256.0612.

***tert*-butyl (3-(methylcarbamoyl)thietan-3-yl)carbamate V.** To a cold (–20 °C) solution of **IV** (146 mg, 0.68 mmol, 1 eq.) in THF (2 mL) in an argon-flushed 10 mL one-necked flask were added successively NMM (75 µL, 0.68 mmol, 1 eq.) and IBCF (88 µL, 0.68 mmol, 1 eq.). Following the activation period of 10 min at –20 °C, a solution of 40% aqueous $MeNH_2$ (620 µL, 6.97 mmol, 10 eq.) in THF (1 mL) was added. The resulting mixture was stirred for 1 h 30 at –20 °C then 5% aqueous $NaHCO_3$ (3 mL) was added. The resulting solution was stirred for 1 h at room temperature, then was extracted with CH_2Cl_2 (6 × 15 mL). The combined organic layers were washed with 5% aqueous $NaHCO_3$ (2 × 5 mL), dried over $MgSO_4$, filtrated and concentrated under reduced pressure. The purification was carried out by flash chromatography (gradient from PE:EtOAc = 7:3 to 0:1) to give **V** as a light yellow solid (138 mg, 89%).

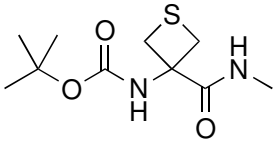

R_f = 0.20 (PE:EtOAc = 7:3), **Mp** = 171–173 °C.

^{1}H NMR (360 MHz, $CDCl_3$, 300 K) δ 7.88 (bs, 1H, NH^2), 6.09 (bs, 1H, NH^1), 4.19 (d, ^2J = 7.5 Hz, 2H, $C^{\beta}H^{a}$), 3.27 (d, ^2J = 8.1 Hz, 2H, $C^{\beta}H^{b}$), 2.95 (d, ^3J = 4.8 Hz, 3H, NCH_3), 1.47 (s, 9H, *t*Bu).

^{13}C NMR (100 MHz, $CDCl_3$, 300 K) δ 172.58 ($C^{1}O$), 154.68 ($C^{Boc}O$), 80.46 (CMe_3), 61.24 (C^{α}), 35.45 ($C^{\beta}H_2$), 28.44 ($C^{Boc}H_3$), 28.85 (NCH_3).

IR (neat) *v* 3317, 3289, 2967, 1677, 1653, 1553, 1528, 1366 cm^{-1}.

HRMS [ESI(+)] *m/z* $[M+Na]^+$ calculated for $[C_{10}H_{18}N_2NaO_3S]^+$: 269.0930, found: 269.0922.

Benzyl (3-((3-(methylcarbamoyl)thietan-3-yl)carbamoyl)thietan-3-yl)carbamate, Cbz-(Attc)$_2$-NHMe 2. To an ice-cooled solution of **V** (98 mg, 0.38 mmol, 1 eq.) in CH_2Cl_2 (9.5 mL) in an argon-flushed 25 mL one-necked flask was added dropwise TFA (895 µL, 11.70 mmol, 30 eq.). The resulting solution was stirred for 3 h at room temperature. The solvent and residual TFA were co-evaporated with $CHCl_3$ under reduced pressure to leave a sticky solid. The resulting TFA salt **VI** was used directly in the next reaction.

To a cold (–30 °C) solution of **III** (85 mg, 0.32 mmol, 1 eq.) in DMF (5 mL) in an argon-flushed 25 mL one-necked flask were added successively NMM (1.1 mL, 10.24 mmol, 32 eq.) and IBCF (44 µL, 0.34 mmol, 1.07 eq.). The solution was stirred for 1 h just below –20 °C. Then a solution of TFA salt **VI** in DMF (5 mL) was added. Residual salts were taken up by rinsing with dry DMF (0.5 mL) and added to the reaction mixture. The resulting mixture was stirred overnight and allowed to warm from –30 °C to room temperature. The reaction mixture was co-evaporated under reduced pressure with $CHCl_3$. The residue was taken up in CH_2Cl_2 (15 mL) and 5% aqueous $NaHCO_3$ (15 mL). Then, the aqueous layer was extracted with CH_2Cl_2 (6 × 10 mL). The organic layer was washed with 5% aqueous $NaHCO_3$ (2 × 10 mL), dried over $MgSO_4$, filtrated and concentrated under reduced pressure. The purification was carried out by flash chromatography (gradient from PE:EtOAc = 7:3 to 0:1) to give **2** as a light brown solid (67 mg, 52%).

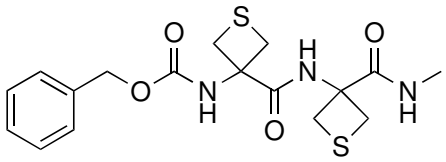

R_f = 0.58 (PE:EtOAc = 2:8), **Mp** = 165–168 °C.

^{1}H NMR (400 MHz, $CDCl_3$) δ 8.88 (bs, 1H, NH^2), 7.81 (bs, 1H, NH^3), 7.42-7.29 (m, 5H, CH^{Ar}), 6.30 (bs, 1H, NH^1), 5.14 (s, 2H, CH_2^Z), 4.09 (d, ^2J = 9.7 Hz, 2H, $C^\beta H^a$-2), 3.97 (d, 2H, ^2J = 8.3 Hz, $C^\beta H^a$-1), 3.44 (d, ^2J = 9.9 Hz, 2H, $C^\beta H^b$-1), 3.38 (d, ^2J = 8.0 Hz, 2H, $C^\beta H^b$-2), 2.96 (d, ^2J = 4 Hz, 3H, CH_3).

^{13}C NMR (100 MHz, $CDCl_3$) δ 172.10 (C^2O), 171.15 (C^1O), 155.11 (C^ZO), 136.13 (C^{Ar}), 128.73, 128.46, 128.25 ($C^{Ar}H$), 67.17 (C^ZH_2), 61.96 (C^α-2), 61.91 (C^α-1), 34.87 (C^β-1), 34.52 (C^β-2), 26.98 (CH_3).

IR (neat) *v* 3370, 3295, 3232, 2918, 1703, 1689, 1646, 1514, 1444 cm^{-1}.

HRMS [ESI(+)] *m/z* $[M+Na]^+$ calculated for $[C_{17}H_{21}N_3NaO_4S]^+$: 418.0853, found: 418.0866.

1.4 Synthesis of Cbz-(Attc)$_3$-NHMe, 3

Compound **3** was synthesized according to Scheme S3.

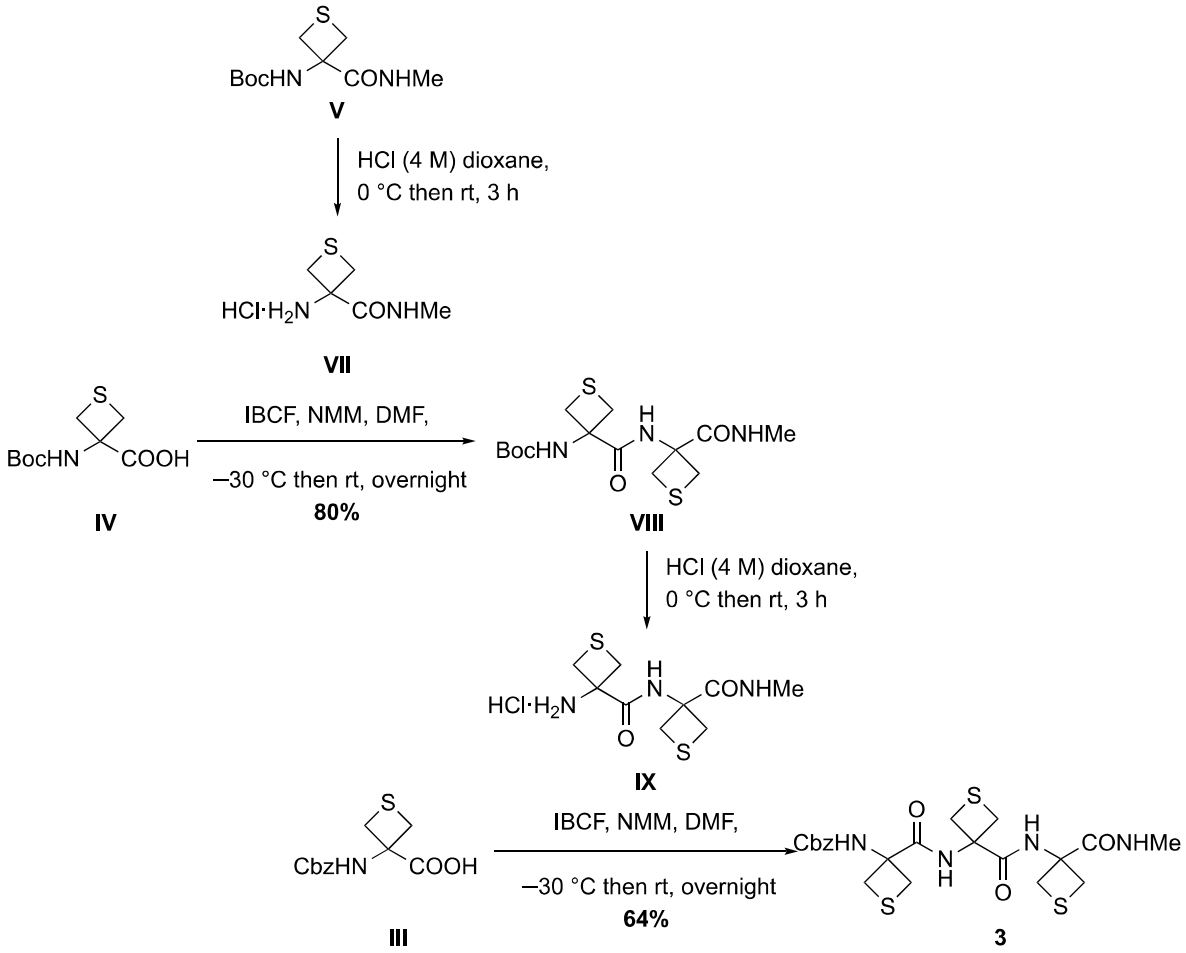

Scheme S3.

***tert*-butyl (3-((3-(methylcarbamoyl)thietan-3-yl)carbamoyl)thietan-3-yl)carbamate VIII.** To an ice-cooled neat **V** (247 mg, 1 mmol, 1 eq.) in an argon-flushed 50 mL one-necked flask was added dropwise 4 M HCl solution in 1,4-dioxane (20 mL, 80 mmol, 80 eq.). The resulting solution was stirred for 3 h at room temperature. The residual HCl and solvent were co-evaporated with $CHCl_3$ under reduced pressure to leave a sticky solid. The resulting hydrochloride salt **VII** was used directly in the next reaction.

To a cold (–30 °C) solution of **IV** (227 mg, 0.85 mmol, 0.85 eq.) in DMF (5 mL) in an argon-flushed 25 mL one-necked flask were added successively NMM (330 µL, 3 mmol, 3 eq.) and IBCF (118 µL, 0.90 mmol, 0.9 eq.). The solution was stirred for 1 h then a solution of hydrochloride salt **VII** in dry DMF (5 mL) was added. Residual salts were taken up by rinsing

with DMF (0.5 mL) and added to the reaction mixture. The resulting mixture was stirred overnight and allowed to warm from –30 °C to room temperature. The reaction mixture was co-evaporated under reduced pressure with $CHCl_3$. The residue was taken up in CH_2Cl_2 (15 mL) and 5% aqueous $NaHCO_3$ (15 mL). Then, the aqueous layer was extracted with CH_2Cl_2 (6 × 10 mL). The organic layer was washed with 5% aqueous $NaHCO_3$ (2 × 10 mL), dried over $MgSO_4$, filtrated and concentrated under reduced pressure. The purification was carried out by flash chromatography (gradient from CH_2Cl_2:CH_3CN = 1:0, 8:2, 5:5 to 0:1) to give **VIII** as a light yellow solid (246 mg, 80%).

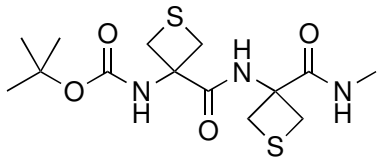

R_f = 0.11 (PE:EtOAc = 3:7), **Mp** = 220–223 °C

^{1}H NMR (400 MHz, $CDCl_3$) δ 8.59 (bs, 1H, NH^2), 7.75 (bs, 1H, NH^3), 5.94 (bs, 1H, NH^1), 4.01 (d, ^2J = 7.0 Hz, 2H, $C^\beta H^a$-2), 3.80 (d, ^2J = 8.1 Hz, 2H, $C^\beta H^a$-1), 3.51 (d, ^2J = 10.0 Hz, 2H, $C^\beta H^b$-1), 3.45 (d, ^2J = 7.8 Hz, 2H, $C^\beta H^b$-2), 2.94 (d, ^3J = 4.8 Hz, 3H, NCH_3), 1.46 (s, 9H, *t*Bu).

^{13}C NMR (100 MHz, $CDCl_3$) δ 172.06 (C^2O), 171.69 (C^1O), 154.76 ($C^{Boc}O$), 81.10 (C^{Boc}), 62.07 (C^α-1 and C^α-2), 34.74 (C^β-1), 34.45 (C^β-2), 28.42 ($C^{Boc}H_3$), 26.96 (NCH_3).

IR (neat) ν 3354, 3296, 2973, 1686, 1648, 1518 cm^{-1}.

HRMS [ESI(+)] *m/z* $[M+Na]^+$ calculated for $[C_{14}H_{23}N_3NaO_4S_2]^+$: 384.1022, found: 384.1011.

Benzyl (3-((3-((3-(methylcarbamoyl)thietan-3-yl)carbamoyl)thietan-3-yl)carbamoyl)thietan-3-yl)carbamate, Cbz-(Attc)$_3$-NHMe 3. To a solid sample of **VIII** (130 mg, 0.36 mmol, 1 eq.) in an ice-bath cooled argon-flushed 25 mL one-necked flask was added dropwise 4 M HCl solution in 1,4-dioxane (7.2 mL, 28.8 mmol, 80 eq.). The resulting solution was stirred for 3 h at room temperature. The mixture was co-evaporated with $CHCl_3$ under reduced pressure to leave a sticky solid. This hydrochloride salt **IX** was used directly in the next reaction.

To a cold (–30 °C) solution of **III** (96 mg, 0.36 mmol, 1 eq.) in DMF (5 mL) in an argon-flushed 25 mL one-necked flask were added successively NMM (119 µL, 1.08 mmol, 3 eq.) and IBCF (50 µL, 0.39 mmol, 1.07 eq.). The solution was stirred for 1 h then a solution of hydrochloride salt **IX** in DMF (5 mL) was added; residual salts were taken up by rinsing with DMF (0.5 mL) and added to the reaction mixture. The resulting mixture was stirred overnight and allowed to warm from –30 °C to room temperature. The reaction mixture was co-evaporated with $CHCl_3$ under reduced pressure. The residue was taken up in CH_2Cl_2 (15 mL) and 5% aqueous $NaHCO_3$ (15 mL). Then, the aqueous layer was extracted with CH_2Cl_2 (6 × 10 mL). The organic layer was washed with 5% aqueous $NaHCO_3$ (2 × 10 mL), dried over $MgSO_4$, filtrated and concentrated under reduced pressure. The purification was carried out by flash chromatography (gradient from PE:EtOAc = 7:3 to 0:1). Further purification was carried out by HPLC using CH_3CN:H_2O = 95:5 for 6 min to give **3** as a light yellow solid (120 mg, 64%).

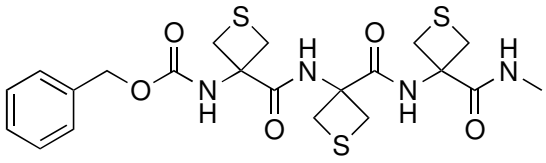

R_f = 0.55 (PE:EtOAc = 2:8), **Mp** = 200–203 °C.

^{1}H NMR (400 MHz, $CDCl_3$, 300 K) δ 8.39 (bs, 1H, NH^3), 8.32 (bs, 1H, NH^2), 7.52 (bs, 1H, NH^4), 7.42-7.30 (m, 5H, CH^{Ar}), 6.26 (bs, 1H, NH^1), 5.15 (s, 2H, CH_2^Z), 3.97-3.46 (m, 12H, $C^\beta H^{a,b}$-1,2,3), 2.93 (d, ^3J = 4 Hz, 3H, CH_3).

^{13}C NMR (100 MHz, $CDCl_3$ + 2% DMSO-d_6, 300 K) δ 172.08 (C^1O), 171.59 (C^3O), 169.98 (C^2O), 156.24 (C^ZO), 135.67 (C^{Ar}), 128.78, 128.63, 128.22 ($C^{Ar}H$), 67.60 (C^ZH_2), 63.35, 63.11, 62.59 (3 × C^α), 33.34, 33.19, 33.03 (3 × C^β), 26.78 (CH_3).

IR (neat) ν 3311, 3236, 2935, 1691, 1649, 1518, 1444 cm^{-1}.

HRMS [ESI(+)] *m/z* $[M+Na]^+$ calculated for $[C_{21}H_{26}N_4NaO_5S_3]^+$: 533.0958, found: 533.0943

1.5 Copies of ^{1}H and ^{13}C NMR of 1-4

Cbz-Attc-NHMe **1**

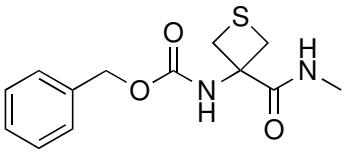

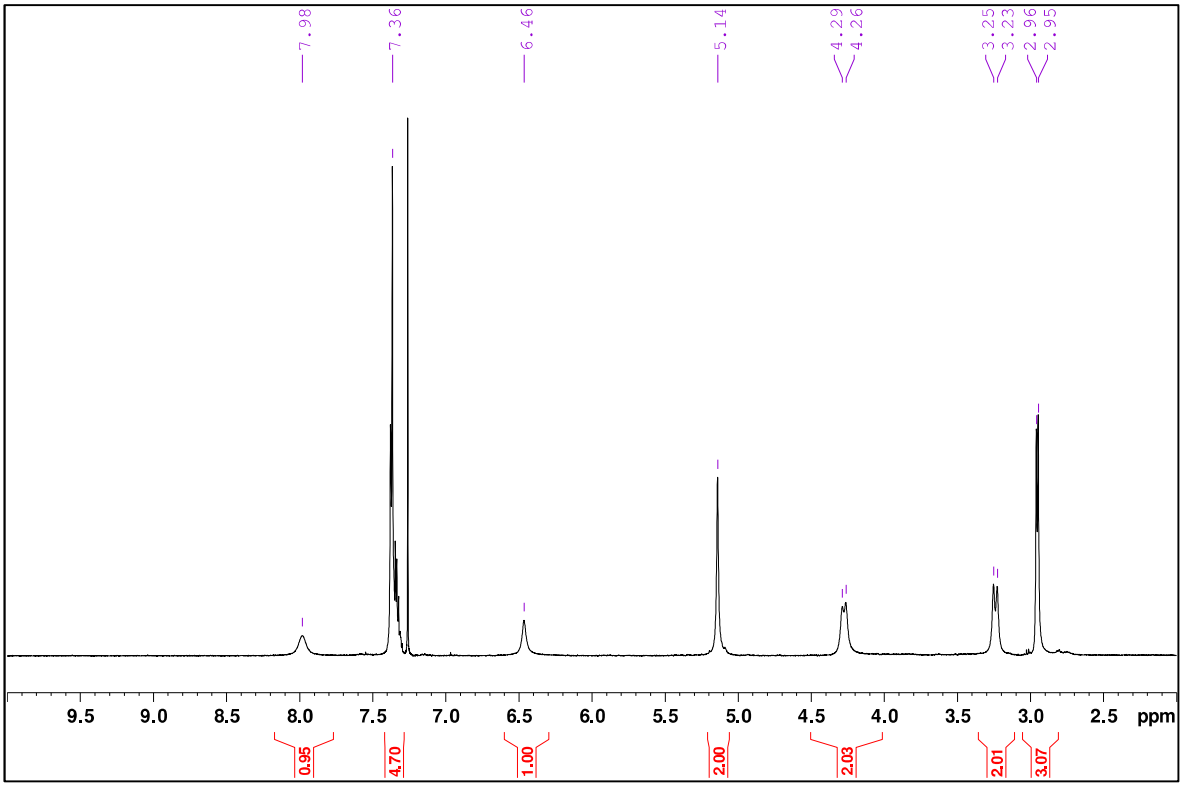

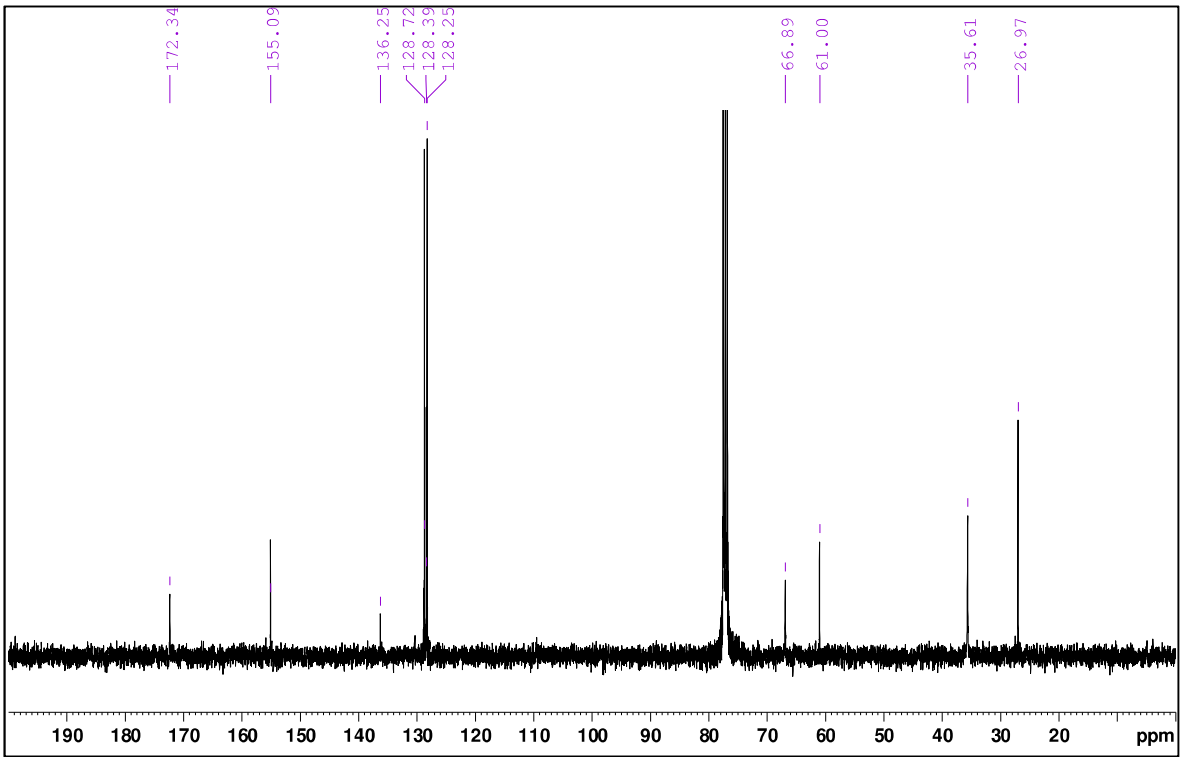

Cbz-(Attc)$_2$-NHMe **2**

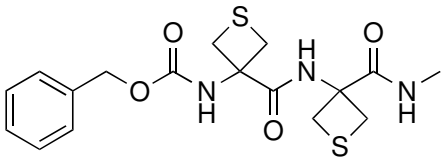

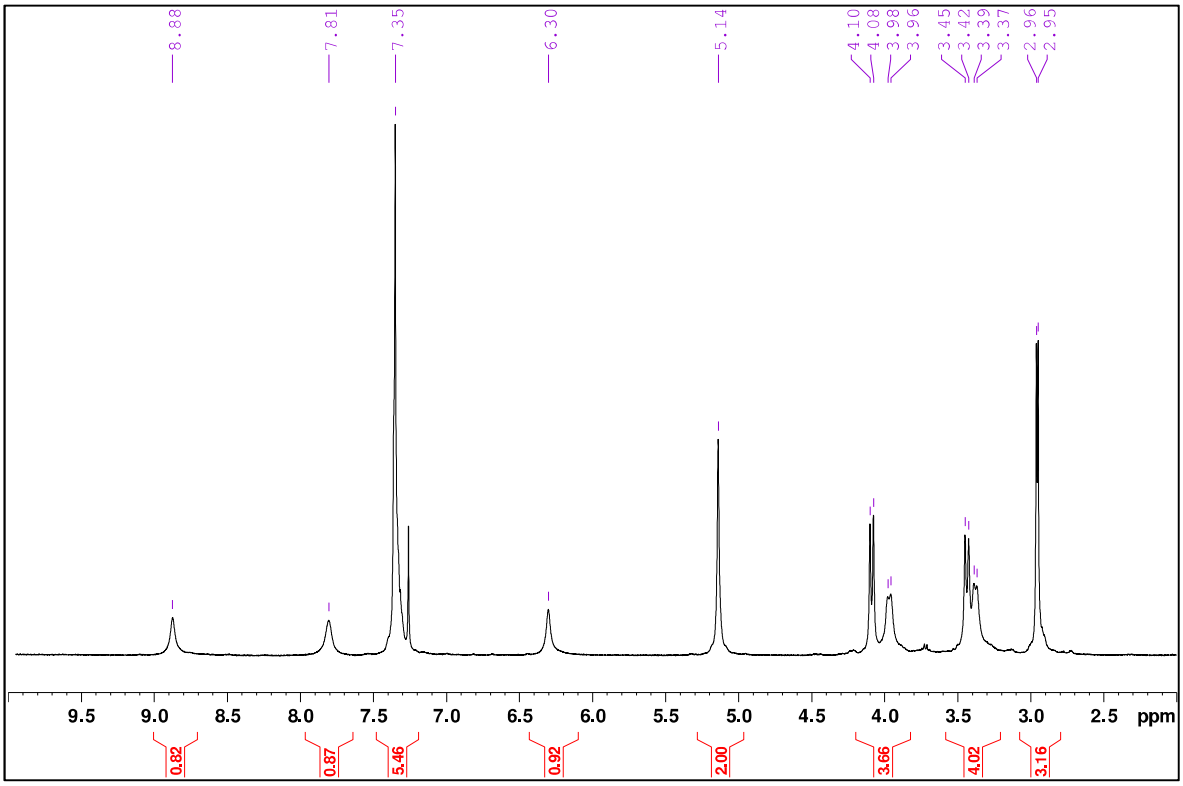

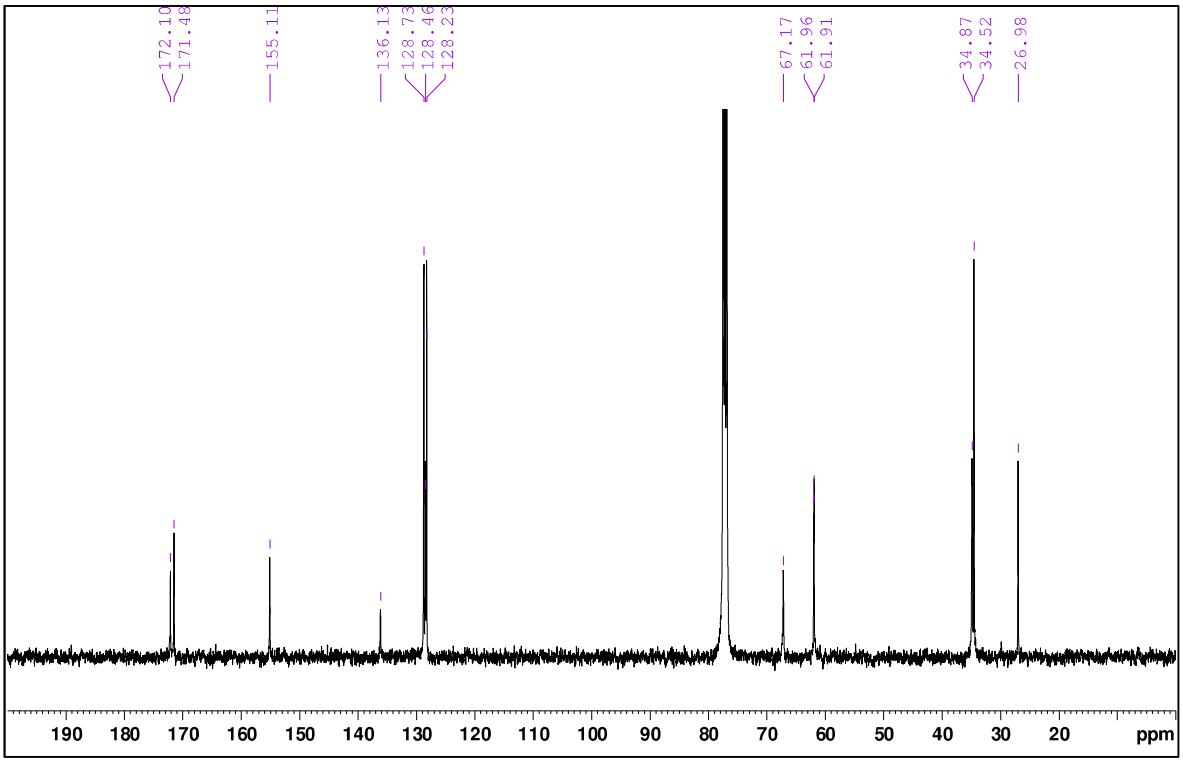

Cbz-(Attc)$_3$-NHMe **3**

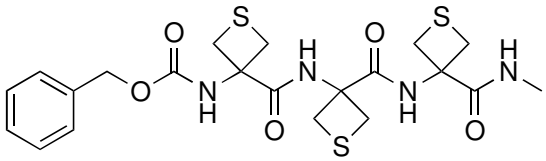

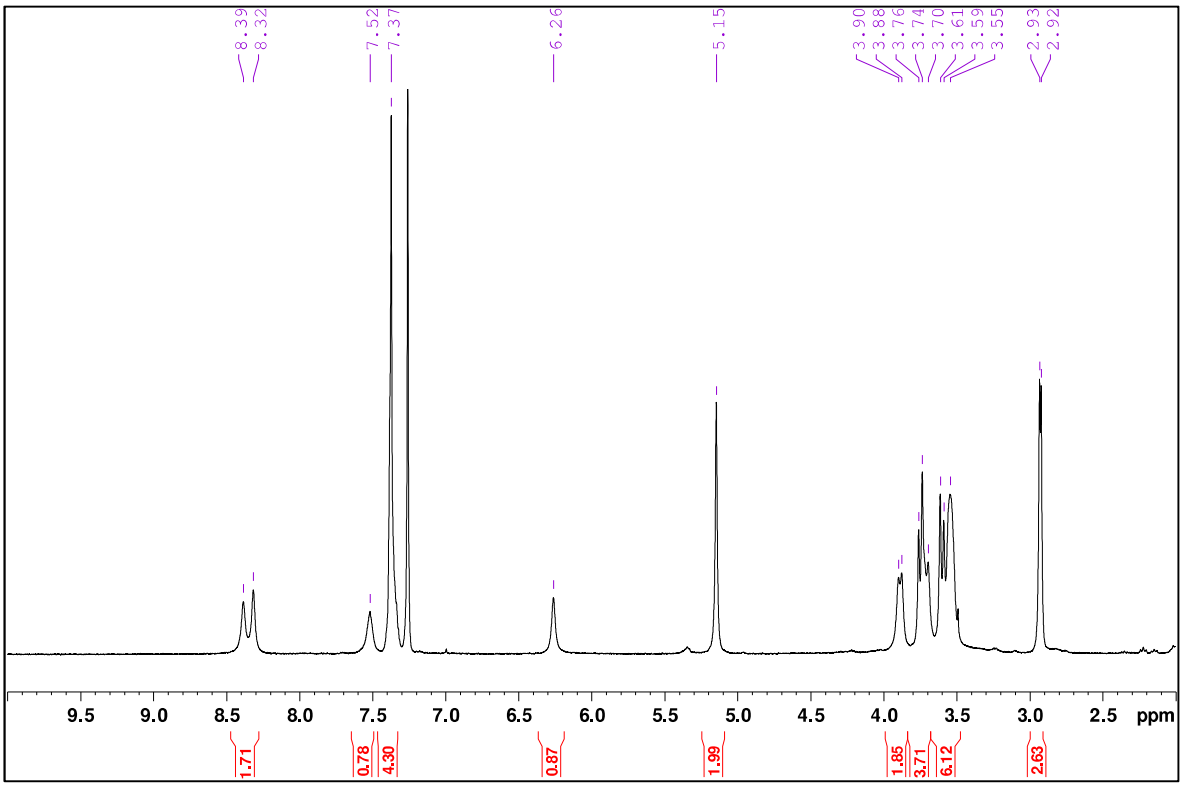

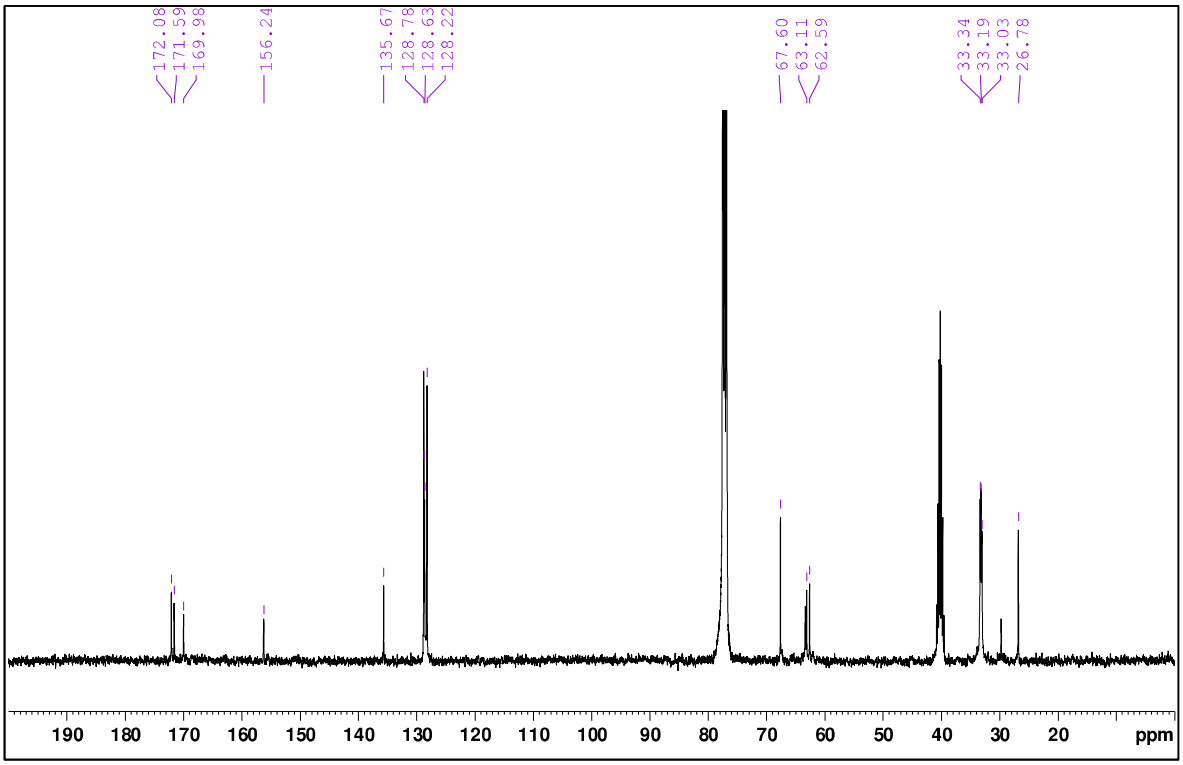

Cbz-Attc-OMe **4**

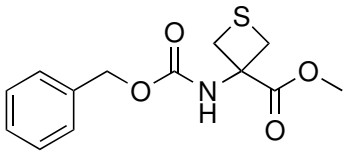

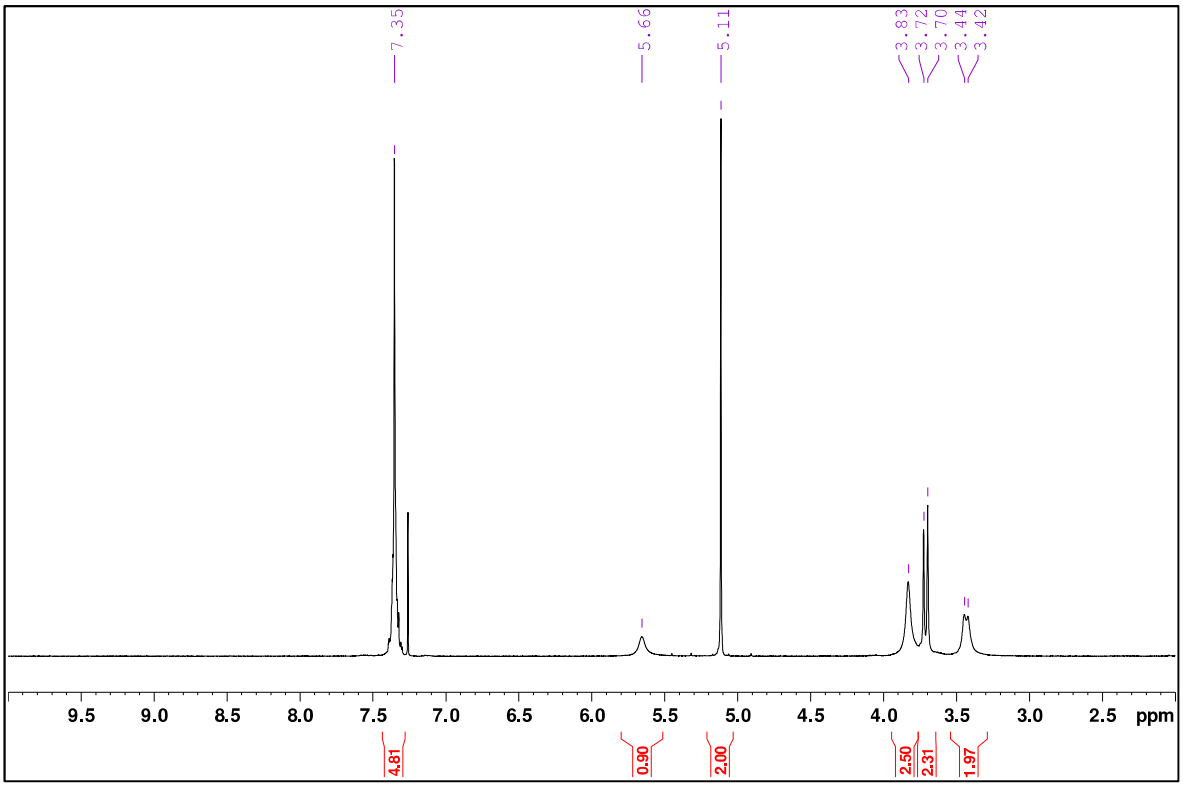

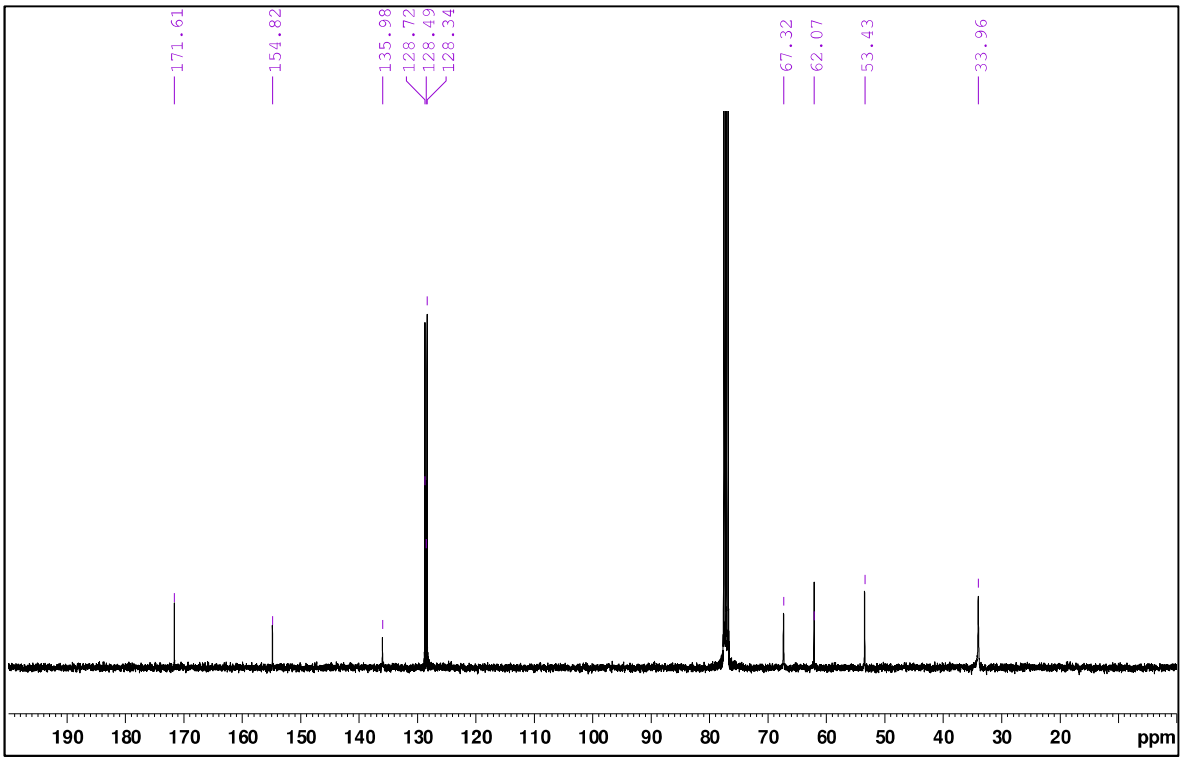

2. Gas phase experimental methods

Cbz-(Attc)$_n$-NHMe derivatives **1-3** were introduced into the gas phase using laser-desorption coupled to a supersonic expansion. Laser-desorption was carried out downstream from a pulsed nozzle by shining the frequency-doubled output of a pulsed Nd:YAG laser (Minilite Continuum, 10 Hz, 0.1–3 mJ/pulse) on the surface of a mixed graphite:sample (4:1 molar ratio) 6 mm-diameter pellet. The vaporized molecules were cooled by interaction with the supersonic molecular beam generated from the expansion of 30:70 Ne:He mixture carrier gas at a 18 bar pressure through a 1 mm diameter nozzle, before entering the source of a time-of-flight mass spectrometer. Molecules were then excited and ionized by the output of a frequency-doubled dye laser (NarrowScan, Radiant Dyes) (~0.4-0.7 mJ in the UV), pumped by a frequency tripled Nd:YAG (Powerlite, Continuum). Ions generated were then collected on the detector of a reflectron-type mass spectrometer, ensuring mass analysis. UV spectra of each molecule in the origin region of the $\pi \rightarrow \pi^*$ transition of the aromatic ring of the Cbz-cap were obtained by resonant two-photon ionization (R2PI) spectroscopy (Figure S1), *i.e.* by recording the ion signal in their corresponding mass channels (*m/z* = 281, 396 and 511 respectively) as a function of the laser UV frequency. The UV spectra showed two transitions, at around 37583 cm^{-1} and 37595 cm^{-1} (labelled A and A$_1$ respectively), which are common to all three compounds **1-3**, together with a third transition, in compound **2** at 37470 cm^{-1} (B) and in compound **3** at 37579 cm^{-1} (A'). The assignment of these UV bands to either the same or to different conformers was done on the basis of double resonance IR/UV spectroscopic data.

Gas phase conformer-specific IR spectra of compounds **1-3** were recorded using this latter technique,[S2,S3] taking advantage of the UV spectroscopy to selectively probe a well-defined conformer population. The depletion caused by a pulsed IR laser scanned in an IR absorption region of interest was then probed by the pulsed UV laser, selectively tuned on this population. The IR beam was generated either directly from the idler output (typically 10 mJ in the 3200-3600 cm^{-1} Amide A range) of a Nd:YAG-pumped (Continuum Surelite, 740 mJ/pulse at 1064 nm) OPO/OPA (Laservision), or from the output of a Difference Frequency Generation (DFG) stage, where OPA idler and signal were converted to a 1300-1800 cm^{-1} radiation (1 mJ output) in order to probe the Amide I and II regions.

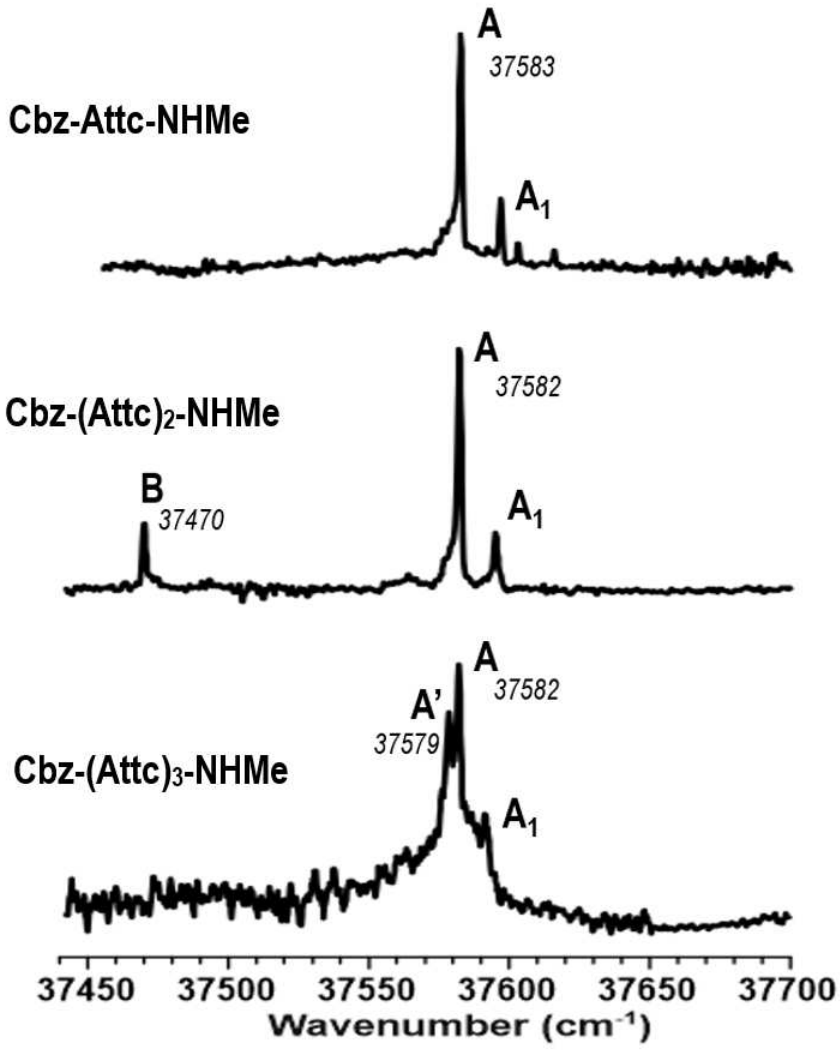

Figure S1. Mass-selected R2PI spectra of compounds **1-3** recorded under isolated conditions in the UV absorption region of the Cbz-cap. Using IR/UV double resonance spectroscopic data, the bands labelled A and A_1 in **1** and **2** were respectively assigned to the band origin and a vibronic band of a *gauche* Cbz-cap rotamer, while B was assigned to a different backbone. In **3**, the same analysis led us to assign bands A and A' to the origin of the two *gauche* Cbz-cap rotamers (for assignment details, see section 4.5). The accuracy of the UV frequency values is ± 5 cm^{-1}.

3. Quantum chemistry methods

The combination of a force field exploration and quantum chemistry was used to provide a complete picture of the conformational energy landscape of compounds **1-3**, which was used for the assignment of the experimentally observed conformations based on IR spectroscopy. For each compound, a conformational search was carried out to identify starting structures for further structure optimization and frequency calculations using quantum chemical methods. This exploration was done with the OPLS-2005 force field using the Monte-Carlo Multiple Minima procedure in the MacroModel suite.[S4] Geometry optimization and frequency calculations were done using the Density Functional Theory (DFT) at RI-B97-D3(BJ)-abc/def2-TZVPPD level of theory[S5-S7] with the Turbomole 7.2 package.[S8] (gridsize m3; SCF convergence threshold 10^{-8} u.a.; gradient norm convergence threshold 10^{-5} u.a.). The determination of the Amide A theoretical IR spectra was based on harmonic frequencies, obtained by quantum chemistry at the same level of theory, then rescaled using scaling factors of 0.978 in the NH stretching region. This strategy generally provides theoretical frequencies in good agreement with experimental frequencies (within 20 cm^{-1} for NH stretches in NH···O bonds[S3] and typically within ~30 cm^{-1} for NH···S bonds[S9]). In the Amide I and II regions, the scaling factors used (1.004 and 1.008, respectively) were chosen to fit the corresponding spectra of **1**, for which an unambiguous assignment to a planar backbone was derived from the Amide A region.

In this work, the nomenclature used to describe the conformations is based on a sequential analysis of the H-bonding status of the NH groups along the peptide chain. When a hydrogen bond occurs, a number indicates the number of atoms involved in the ring formed by the H-bond between the NH being considered and its H-bond acceptor (carbonyl O or S atom). A subscript to the number of an N–H···O=C H-bond (*e.g.* 7_D) stands for the configurational stereochemistry type for a chiral conformation. A superscript (N or O) to the number of an N–H···S H-bond (*e.g.* 7_D^N) designates the puckering orientation of the 4-membered ring in the residue, according to the nearest neighbor of the ring S atom: either the N atom of the previous amide group or the O atom of the next amide. An NH group free from any hydrogen bonding is designated by the label "f". For each backbone conformation, three Cbz-cap rotamers were found and designated according to their C_{sp2}-C_{sp3}-O-C(=O) dihedral, namely *gauche*+ (g^+; φ = +60°), *gauche*– (g^-; φ = –60°) and *trans* (t; φ = ± 180°). When the backbone exhibited a plane of symmetry, g^+ and g^- forms are enantiomers and spectroscopically indistinguishable.

A Natural Bond Orbital (NBO) analysis,[S10-S12] which enabled quantification of the stabilizing role of electron delocalization through hyperconjugation and H-bonding effects, was carried out on the B97-D3(BJ)-abc/def2-TZVPPD structures using the NBO module[S13] of the Gaussian 09 software.[S14] The NBO analysis was carried out at both HF/TZVPP and MP2/TZVPP levels. The donor and acceptor NBO occupancies considered in the following are those obtained at the MP2/TZVPP level whereas the HF level was used to calculate, for each donor NBO(i) and acceptor NBO(j), the E(2) stabilization energy through the second order perturbation theory:

$$E(2) = \Delta E_{ij} = q_i \frac{F(i,j)^2}{|\varepsilon_i - \varepsilon_j|}$$

where q_i is the donor orbital occupancy, F(i, j) is the off-diagonal NBO Fock matrix element and ε_i (resp. ε_j) is the diagonal element, *i.e.* the donor (acceptor) orbital energy; the threshold for considering the interactions as significant being equal to 0.05 kcal/mol.

Previous work has shown that the MP2/TZVPP level of theory used here provides a good compromise between accuracy and computation times.[S15]

4. Gas phase characterizations

4.1. Characterization of Cbz-Attc-NHMe, 1

Theory. The potential energy landscape exhibited three backbone families, sorted according to their hydrogen bonding content: C5-C6$^{\gamma}$, f-C7$_{(L/D)}$, f-π_{am1} (am = amide/carbamate) as shown for compound **1** (Figure S2). The most stable form was an extended, planar backbone conformation followed, more than 14 kJ/mol higher in energy, by two types of folded conformations: a γ-turn f-C7$_{L/D}$, and a Ramachandran α-type backbone, stabilized by a weak π interaction (noted π_{am1}) between the second amide NH and the π system of the carbamate group. The presence of a Cbz-cap (the benzyl carbamate) gave rise to the occurrence of three rotamers (referred to as Cbz-cap rotamers), of comparable energetics as suggested by Figure S2 and Table S1. The three rotamers indeed showed very similar vibrational frequencies (Table S2), indicating the same backbone structural characteristics. The remarkable extended C5-C6$^{\gamma}$ motif adopts a planar backbone structure, stabilized by two H-bonds, namely an N–H···O=C interaction (C5) between the amide-NH and carbonyl CO of the Attc residue and an N–H···S (C6$^{\gamma}$) interaction between the methylamide NH and the side chain cyclic ring S-atom in a γ-position.

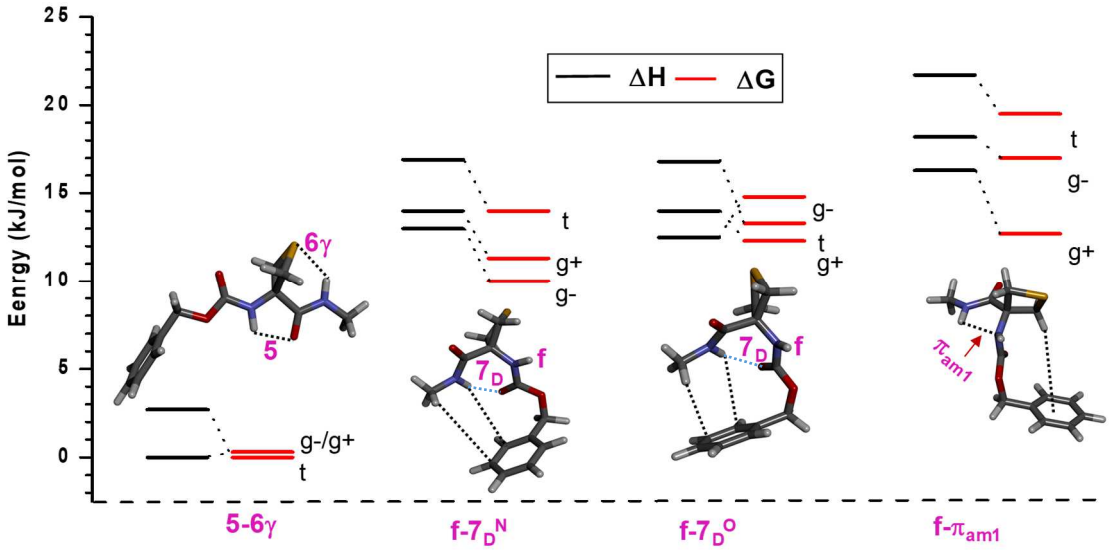

Figure S2. Conformational landscape of Cbz-Attc-NHMe (**1**). Only one Cbz-cap rotamer is shown for each backbone family. Only one member of each enantiomer pair is shown (when such pairs exist).

IR spectroscopy. The experimental conformer-specific gas phase IR spectra were recorded by probing the conformational population on the two UV features of Figure S1, A (37582 cm^{-1}) and A' (37597 cm^{-1}), using IR-UV double resonance spectroscopy (Figure S3). Both conformers exhibited two strong bands in the NH stretch region, at around 3360 cm^{-1} and 3398 cm^{-1}, as well as bands in the Amide I region at around 1703 and 1737 cm^{-1} and the Amide II region at around 1548 and 1494 cm^{-1}. These similarities made the spectra barely distinguishable, compatible, owing to the experimental uncertainty on the frequencies, with the assignment of A to the origin band of a Cbz-cap rotamer and A' to a vibronic band of the same rotamer, involving a low frequency torsional mode of the cap. Comparison of the theoretical and experimental IR spectra allowed their unambiguous assignment to the most stable backbone conformers, exhibiting the C5-C6$^{\gamma}$ motif, since the average and maximum deviations between experiment and theory are 8 and 26 cm^{-1} and 12 and 35 cm^{-1}, respectively, for the *gauche* and *trans* Cbz-cap rotamers of this form, *i.e.* much less than for all the other low energy conformations of the landscape (Figure S3 and Table S2). Owing to the similarity of both experimental and theoretical spectra, a further assignment in terms of Cbz-cap rotamer cannot be achieved in this way. Alternatively, the significant stabilization of the gauche rotamers at low temperature suggests they might be the best candidates: because of the planar backbone, the *gauche*+ and *gauche*– rotamers are enantiomers and exhibit the same UV and IR spectra. In any case, compound **1** exists as extended and planar C5-C6$^{\gamma}$ structure in gas phase and its H-bond distances and NBO energies are comparable to related derivatives shown in Figure S4 and in Table 1 of the manuscript.

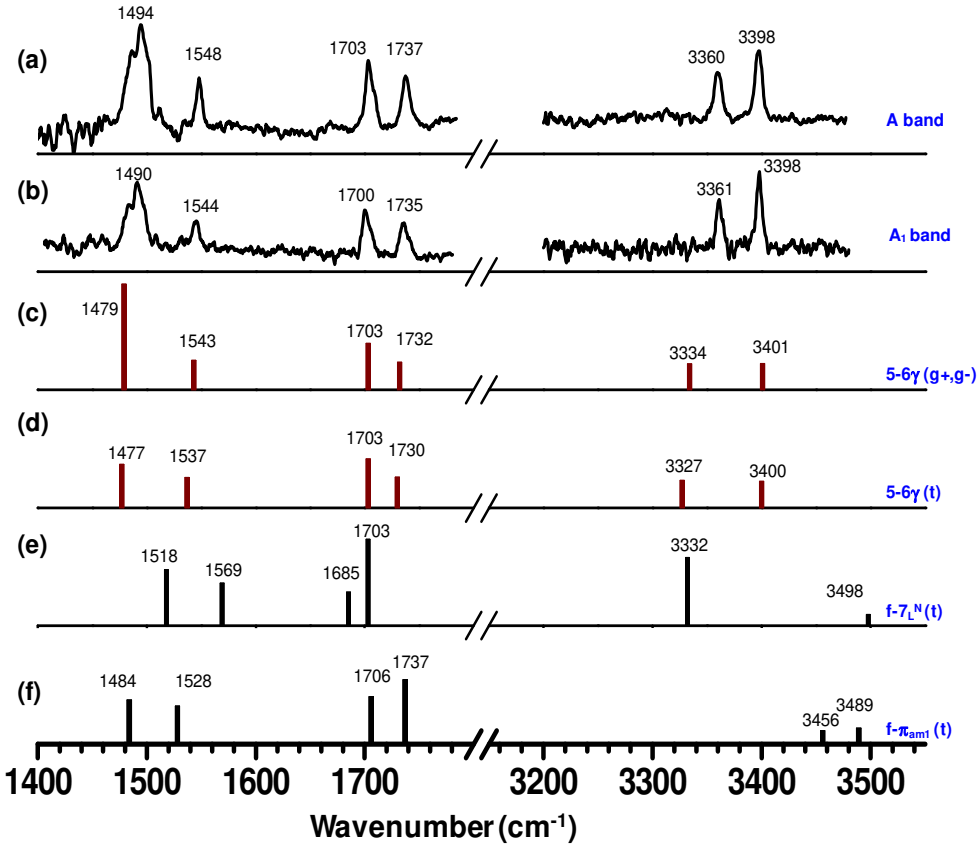

Figure S3. (a-b) Experimental conformer-specific IR/UV spectra obtained by probing the UV transitions A and A_1. (c-f) Theoretical IR spectra of selected stable conformations. The accuracy of the experimental IR frequency values is ± 3 cm^{-1}.

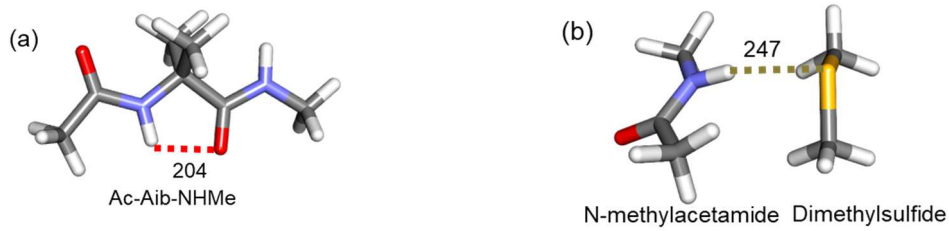

Figure S4. Model systems exhibiting similar interactions to **1**. (a) The extended conformation of capped aminoisobutyric acid, Ac-Aib-NHMe, with its C5 H-bond; (b) The *N*-methylacetamide·SMe_2 intermolecular complex, with an unconstrained amide N–H···S H-bond.

Table S1. Structural and energetic parameters of the lowest energy conformers of compound **1**: H-bond network, relative enthalpies (ΔH, at 0 K) in kJ/mol; Gibbs free energies (ΔG, 300 K) in kJ/mol; Ramachandran dihedral angles (ϕ, ψ) in degree; other dihedral angles $\chi1 = \angle N1\text{-}C_\alpha\text{-}C_{\beta1}\text{-}S^\gamma$, $\chi2 = \angle N1\text{-}C_\alpha\text{-}C_{\beta2}\text{-}S^\gamma$, $\varphi = \angle C_{sp2}\text{-}C_{sp3}\text{-}O\text{-}C(=O)$ in degree; H-bond angles (θ) in degree and H-bond distances in pm. A light grey background is used to distinguish the conformational families.

Conformers	Type of H-bond	ΔH	ΔG	ϕ	ψ	χ1	χ2	φ	θ∠NHS	θ∠NHS	d(H···S)	d(H···OC)
1-01_t	5-6γ	2.7	0	-179.8	179.9	-140.7	140.7	178.2	133.2	111.3	240	204
1-01_g$^+$/g$^-$	5-6γ	0	0.3	178.9	179.5	-140.3	140.3	-86.6	132.8	111.0	241	205
1-02_t	f-7$_D^N$	16.9	14.0	77.5	-66.8	-94.6	97.5	-180.0	-	150.0	-	193
1-02_g$^+$	f-7$_D^N$	14.0	11.3	77.6	-65.6	-94.7	97.6	85.9	-	150.9	-	192
1-02_g$^-$	f-7$_D^N$	13.0	10.0	75.9	-66.0	-95.4	98.1	-79.6	-	150.2	-	193
1-03_t	f-7$_D^O$	16.8	13.3	76.9	-75.2	-136.8	138.8	-176.6	-	143.9	-	204
1-03_g$^+$	f-7$_D^O$	14.0	12.3	77.6	-74.6	-136.5	138.5	87.9	-	144.0	-	204
1-03_g$^-$	f-7$_D^O$	12.5	14.8	73.8	-76.5	-137.7	139.6	-69.3	-	142.2		206
1-04_t	f-π$_{am1}$	21.7	19.5	-69.6	-29.2	-97.1	93.7	-174.1	-	-	-	229
1-04_g$^+$	f-π$_{am1}$	16.3	12.7	-67.4	-27.7	-97.4	94.1	83.2	-	-	-	228
1-04_g$^-$	f-π$_{am1}$	18.2	17.0	-69.6	-29.3	-97.1	93.8	-86.0	-	-	-	228

Table S2. For compound **1**: experimental and theoretical vibrational frequencies (cm^{-1}) in the N-H stretch, Amide I and Amide II regions and average and maximum deviation of the theoretical frequencies with respect to experimental frequencies on A transition (the average deviation was calculated by considering all the frequencies). Best fits to experiment are highlighted in grey.

Conformers	Type of H-bond	NH Stretching		Amide I		Amide II		Average deviation w.r.t Exp. A	Max. deviation w.r.t Exp. A
		ν_{N1H}	ν_{N2H}	ν_{CO1}	ν_{CO2}	ν_{N1H}	ν_{N2H}		
Experiment									
On A UV band		3360	3398	1738	1703	1548	1494		
On B UV band		3361	3398	1736	1700	1546	1491		
Theory									
1-01_t	5-6γ	3327	3400	1730	1703	1537	1477	12	35
1-01_g$^+$/g$^-$	5-6γ	3336	3404	1731	1703	1546	1485	8	26
1-02_t	f-7$_D^N$	3334	3498	1716	1698	1561	1513	31	100
1-02_g$^+$	f-7$_D^N$	3332	3498	1715	1697	1565	1504	31	100
1-02_g$^-$	f-7$_D^N$	3332	3497	1715	1697	1562	1512	32	99
1-03_t	f-7$_D^O$	3386	3488	1720	1702	1557	1494	24	90
1-03_g$^+$	f-7$_D^O$	3390	3493	1720	1701	1552	1493	25	95
1-03_g$^-$	f-7$_D^O$	3402	3470	1722	1706	1549	1485	23	72
1-04_t	f-π$_{am1}$	3456	3489	1750	1717	1521	1479	42	94
1-04_g$^+$	f-π$_{am1}$	3473	3490	1747	1717	1525	1484	43	111
1-04_g$^-$	f-π$_{am1}$	3459	3491	1748	1716	1525	1480	42	97

4.2. Characterization of Cbz-(Attc)$_2$-NHMe, 2

Theory. The potential energy landscape (Figure S5) exhibited five main backbone types, composed of 12 different H-bond networks: completely folded (double γ-turns and β-turns; families 4-11 and 12), partially extended (f-π_{am1}/C5-C6$^{\gamma}$, C5-C6$^{\gamma}$-C7; families 2 and 3) and fully extended C5-C6$^{\gamma}$/C5-C6$^{\gamma}$ (family 1). The fully extended C5-C6$^{\gamma}$/C5-C6$^{\gamma}$ conformer, which corresponded to the juxtaposition of two C5-C6$^{\gamma}$ "monomer" motifs, exhibited a planar backbone and was the most stable conformation. It was followed by partially (5-10 kJ/mol) and completely (10-15 kJ/mol) folded structures (families 2-3 and 4-12, respectively). The double γ-turn (f-C7-C7) type was found to have many different forms (4-11), due to the stereoisomers of the C7 folds and the two thietane ring puckering orientations (referred to as O and N, *i.e.* the O or N amide atom closest to the S atom). In these families, one of the Cbz-cap rotamers was found to be more stable than the others (at low temperature) due to a direct contact interaction between the Cbz-cap and the rest of the molecule, made possible by this particular orientation.

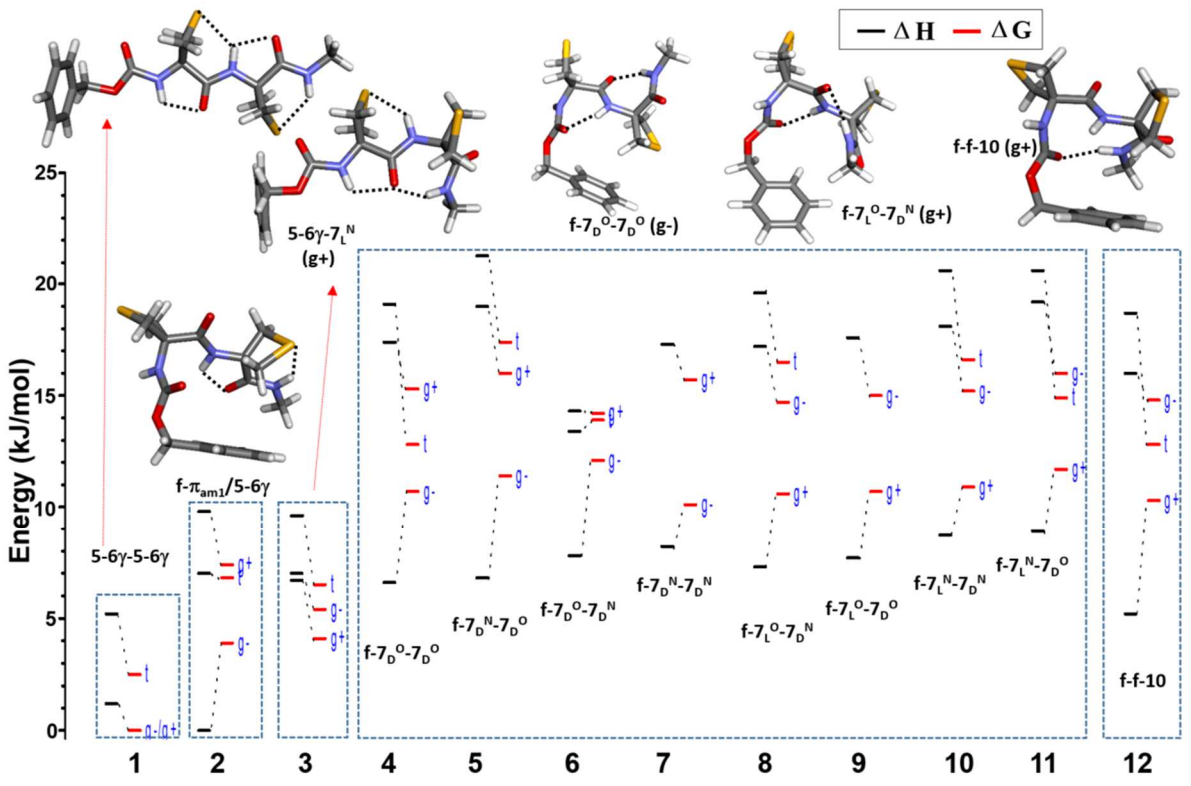

Figure S5. Conformational landscape of Cbz-(Attc)$_2$-NHMe (**2**) with the 12 families discussed. Only one member of each enantiomer pair is shown (all families apart from the achiral 1). For each backbone type, only one Cbz-cap rotamer is depicted.

IR Spectroscopy. Figure S6 depicts the conformer-selective IR spectra on each UV feature (A, A_1 and B bands) of compound **2** and their assignments with theoretical IR spectra. As for compound **1**, the experimental IR spectra of the A and A_1 UV bands were experimentally identical, suggesting the origin and vibronic bands of a same rotamer, whereas the B UV band exhibited a very different IR spectrum. The experimental frequencies of A and A_1 (Figure S6) were in good agreement with the scaled harmonic frequencies for the rotamers of the most stable extended C5-C6$^{\gamma}$/C5-C6$^{\gamma}$ backbone (top grey boxes in Table S3; 7 and 18 cm^{-1} av. & max. deviations, respectively). Again the stability at low temperature of the *gauche* rotamers made them the best candidates. The IR spectrum of B band did not match the theoretical IR spectra of the next families (2-3) in the energetic scale, especially in the Amide I region. Conversely, a better agreement was found (both in the Amide A and I regions) within the double γ-turn families (4-11), in which the most stable conformers (at low temperature) of the 4, 8, 9 and 11 families (i.e. with $\Delta H < 10$ kJ/mol) exhibited av. & max. deviations lower than 12 and 30 cm^{-1}, respectively (bottom grey boxes in Table S3). The observation of such a unique double γ-turn form can be rationalized by the numerous contributions thereto, together with the existence of modest barriers between conformations, which can be overcome during the supersonic expansion, giving rise to extensive conformational relaxation, through which the whole set of families funnels into a unique, locally most stable conformation at low temperature.

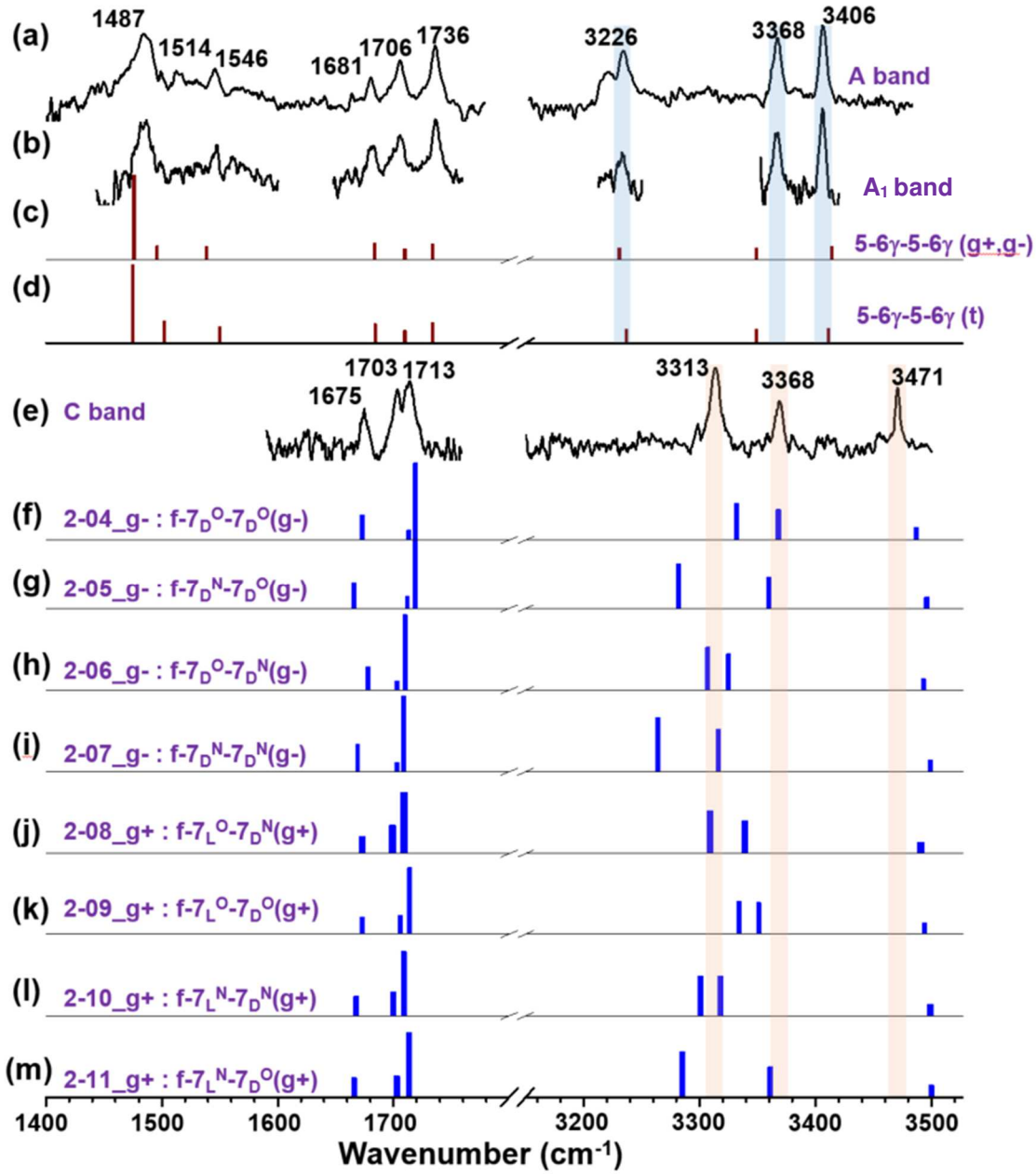

Figure S6. (a-b) Experimental conformer-specific IR/UV spectra of **2** obtained by probing the UV A and A_1 bands. (c-d) Theoretical IR spectra of two Cbz-cap rotamers of the extended conformer. (e) Experimental conformer-specific IR/UV spectra obtained by probing the UV B band. (f-m) Theoretical IR spectra of the most stable forms (0 K) in each family of double γ-turns (f-C7-C7).

Table S3. For compound **2**: relative enthalpies (ΔH) at 0 K in kJ/mol; relative Gibbs free energies (ΔG) at 300 K in kJ/mol; experimental and scaled harmonic vibrational frequencies (cm^{-1}) in the N-H stretch, Amide I and Amide II regions and average and maximum deviation of the scaled harmonic frequencies with respect to experimental spectra on A and B UV bands (the average deviation was calculated by considering NH stretch and Amide I range frequencies for both A and B). Best fits to experiment are highlighted in grey (last four columns). A light grey background is used to distinguish the conformational families.

Conformers	Type of H-bond	ΔH	ΔG	NH Stretching			Amide I			Amide II			With respect to Expt. A		With respect to Expt. B	
				ν_{N1H}	ν_{N2H}	ν_{N3H}	ν_{CO1}	ν_{CO2}	ν_{CO3}	ν_{N1H}	ν_{N2H}	ν_{N3H}	Average deviation	Max. deviation	Average deviation	Max. deviation
Exp.A				3406	3367	3226	1736	1706	1680	1546	1513	1487				
Exp.C				3471	3369	3313	1714	1704	1675							
Theory																
2-01_g^-/g^+	5-6γ-5-6γ	1.2	0.0	3414	3349	3231	1734	1710	1684	1540	1497	1477	7	18	32	82
2-01_t	5-6γ-5-6γ	5.2	2.5	3411	3349	3237	1734	1710	1684	1551	1503	1476	7	18	32	76
2-02_g^-	f-π_{am1}/5-6γ	0.0	3.9	3492	3376	3314	1745	1715	1700	1570	1492	1215	37	88	16	31
2-02_g^+	f-π_{am1}/5-6γ	9.8	7.4	3469	3375	3334	1743	1709	1696	1547	1485	1480	34	108	14	29
2-02_t	f-π_{am1}/5-6γ	7.0	6.8	3466	3376	3326	1745	1710	1694	1550	1483	1208	33	100	14	31
2-03_g^-	5-6γ-7_L^N	7.0	5.4	3428	3339	3269	1733	1709	1672	1567	1560	1484	18	43	24	44
2-03_g^+	5-6γ-7_L^N	6.7	4.1	3425	3341	3264	1734	1709	1672	1571	1556	1481	16	38	25	49
2-03_t	5-6γ-7_L^N	9.6	6.5	3423	3338	3264	1733	1709	1672	1566	1556	1476	16	38	26	49
2-04_g^-	f-7_D^O-7_D^O	6.6	10.7	3487	3368	3332	1719	1713	1673	1555	1527	1491	37	106	9	19
2-04_g^+	f-7_D^O-7_D^O	17.4	15.3	3492	3354	3337	1719	1705	1676	1556	1525	1491	39	111	11	24
2-04_t	f-7_D^O-7_D^O	19.1	12.8	3490	3349	3335	1718	1706	1675	1556	1525	1491	41	124	14	37
2-05_g-	f-7_D^N-7_D^O	6.8	11.4	3496	3360	3282	1719	1712	1666	1556	1541	1506	32	90	15	31
2-05_g+	f-7_D^N-7_D^O	19.0	16.0	3496	3351	3268	1717	1707	1667	1550	1547	1507	30	90	17	45
2-05_t	f-7_D^N-7_D^O	21.3	17.4	3497	3349	3271	1717	1704	1668	1562	1553	1512	31	91	17	42
2-06_g^-	f-7_D^O-7_D^N	7.8	12.1	3493	3325	3307	1710	1703	1678	1492	1562	1567	40	87	14	44
2-06_g^+	f-7_D^O-7_D^N	14.3	14.2	3486	3317	3310	1710	1703	1677	1565	1555	1490	41	84	13	52
2-06_t	f-7_D^O-7_D^N	13.4	13.9	3479	3316	3309	1710	1703	1676	1565	1550	1490	40	83	12	53
2-07_g^-	f-7_D^N-7_D^N	8.2	10.1	3499	3316	3264	1709	1703	1669	1567	1563	1505	37	93	25	53
2-07_g^+	f-7_D^N-7_D^N	17.3	15.7	3499	3310	3274	1709	1702	1674	1579	1566	1504	39	93	22	59
2-08_g^-	f-7_L^O-7_D^N	17.2	14.7	3497	3311	3303	1710	1701	1676	1559	1555	1492	43	91	17	58
2-08_g^+	f-7_L^O-7_D^N	7.3	10.6	3491	3339	3309	1709	1699	1673	1566	1546	1493	40	85	11	30
2-08_t	f-7_L^O-7_D^N	19.6	16.5	3496	3307	3298	1710	1701	1675	1562	1553	1495	43	90	18	62
2-09_g^-	f-7_L^O-7_D^O	17.6	15.0	3496	3368	3320	1717	1705	1675	1556	1532	1492	35	94	6	25
2-09_g^+	f-7_L^O-7_D^O	7.7	10.7	3494	3351	3334	1714	1706	1673	1563	1540	1488	40	108	11	23
2-10_g^-	f-7_L^N-7_D^N	18.1	15.2	3495	3321	3262	1710	1703	1668	1571	1568	1505	36	89	22	51
2-10_g^+	f-7_L^N-7_D^N	8.7	10.9	3499	3318	3301	1709	1700	1668	1569	1560	1507	44	93	18	51
2-10_t	f-7_L^N-7_D^N	20.6	16.6	3496	3315	3262	1711	1704	1668	1569	1555	1507	36	90	24	54
2-11_g^-	f-7_L^N-7_D^O	19.2	16.0	3498	3361	3263	1718	1705	1666	1559	1550	1474	28	92	17	50
2-11_g^+	f-7_L^N-7_D^O	8.9	11.7	3500	3361	3285	1713	1703	1666	1559	1549	1503	33	94	12	29
2-11_t	f-7_L^N-7_D^O	20.6	14.9	3499	3367	3261	1716	1703	1667	1556	1540	1504	27	93	15	52
2-12_g^-	f-f-10	16.0	14.8	3477	3453	3427	1727	1716	1704	1541	1498	1491	67	201	43	114
2-12_g^+	f-f-10	5.2	10.3	3480	3483	3427	1726	1715	1698	1485	1504	1542	7	201	47	114
2-12_t	f-f-10	18.7	12.8	3479	3454	3427	1727	1716	1703	1535	1496	1490	67	201	43	114

4.3. Characterization of Cbz-(Attc)$_3$-NHMe, 3

Theory. For compound **3**, as expected, the conformational landscape increased in complexity with the increased size of the molecule. Many composite H-bond patterns were observed, among which the C5-C6$^{\gamma}$ motif was ubiquitous (Figure S7). The two most stable conformer families had (a) an extended, planar C5-C6$^{\gamma}$/C5-C6$^{\gamma}$/C5-C6$^{\gamma}$ backbone and (b) a half-extended C5-C6$^{\gamma}$-π_{am2}/C5-C6$^{\gamma}$ backbone. The former differed from the latter by virtue of the central residue, which was folded in a Ramachandran α-type backbone local conformation. Energetics calculations showed that the half-extended form was the most stable, challenged by the fully extended one, at around 3-5 kJ/mol higher in energy, suggesting that both forms could be observed in the supersonic expansion.

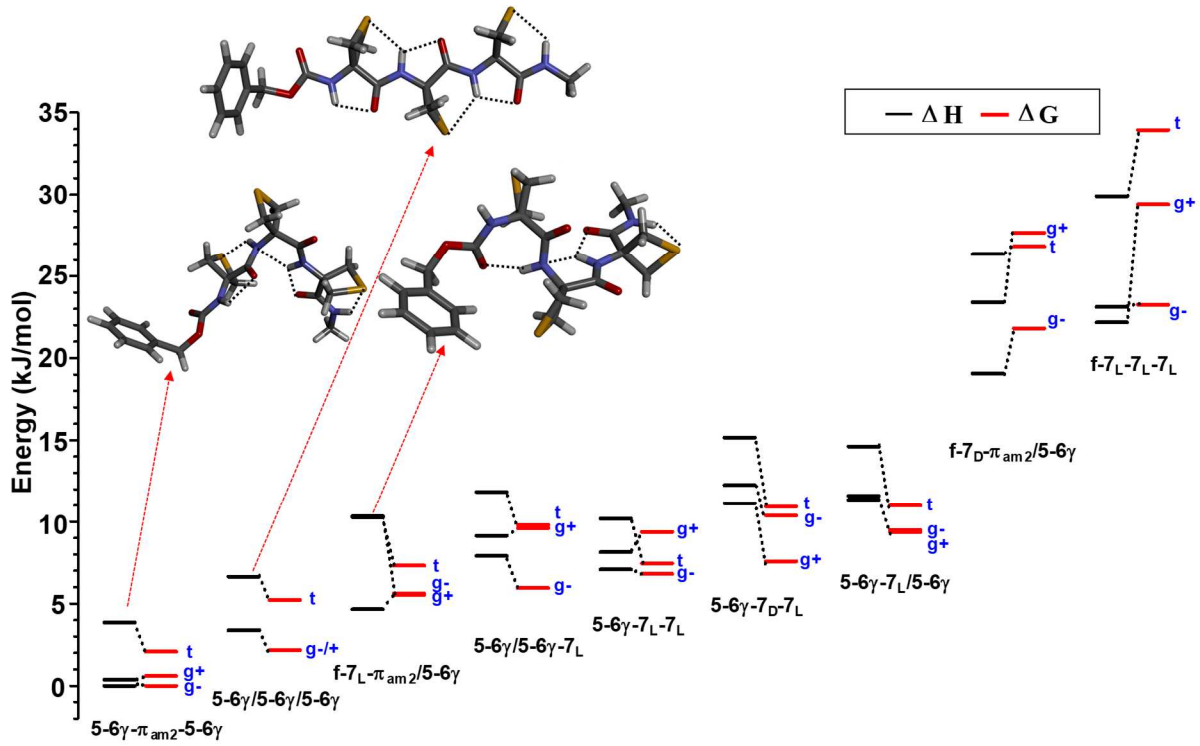

Figure S7. Conformational landscape of Cbz-(Attc)$_3$-NHMe **(3)**. Only one Cbz-cap rotamer is shown for each backbone family. Only one member of each enantiomer pair is shown (when such pairs exist).

IR Spectroscopy. The conformer-specific IR/UV spectra in the Amide A and Amide I regions, recorded on the three UV bands A, A' and A_1 (Figure S8) are again very similar, providing evidence for a same backbone. The spectral proximity of the UV bands A and A' (3 cm^{-1} apart; Figure S1), however, makes improbable their assignment to a same Cbz-cap rotamer. Theoretical spectra for the most stable half-extended form fitted the experimental data best, as illustrated by its modest deviations (av. & max. deviations 9 and 21 cm^{-1}, 10 and 25 cm^{-1}, 8 and 25 cm^{-1}, respectively) when compared with other forms and in particular with its closest competitor, the fully extended form (Table S4). This allowed us to conclude that in the supersonic expansion the most abundant conformer had the half-extended C5-C6$^{\gamma}$-π_{am2}/C5-C6$^{\gamma}$ backbone.

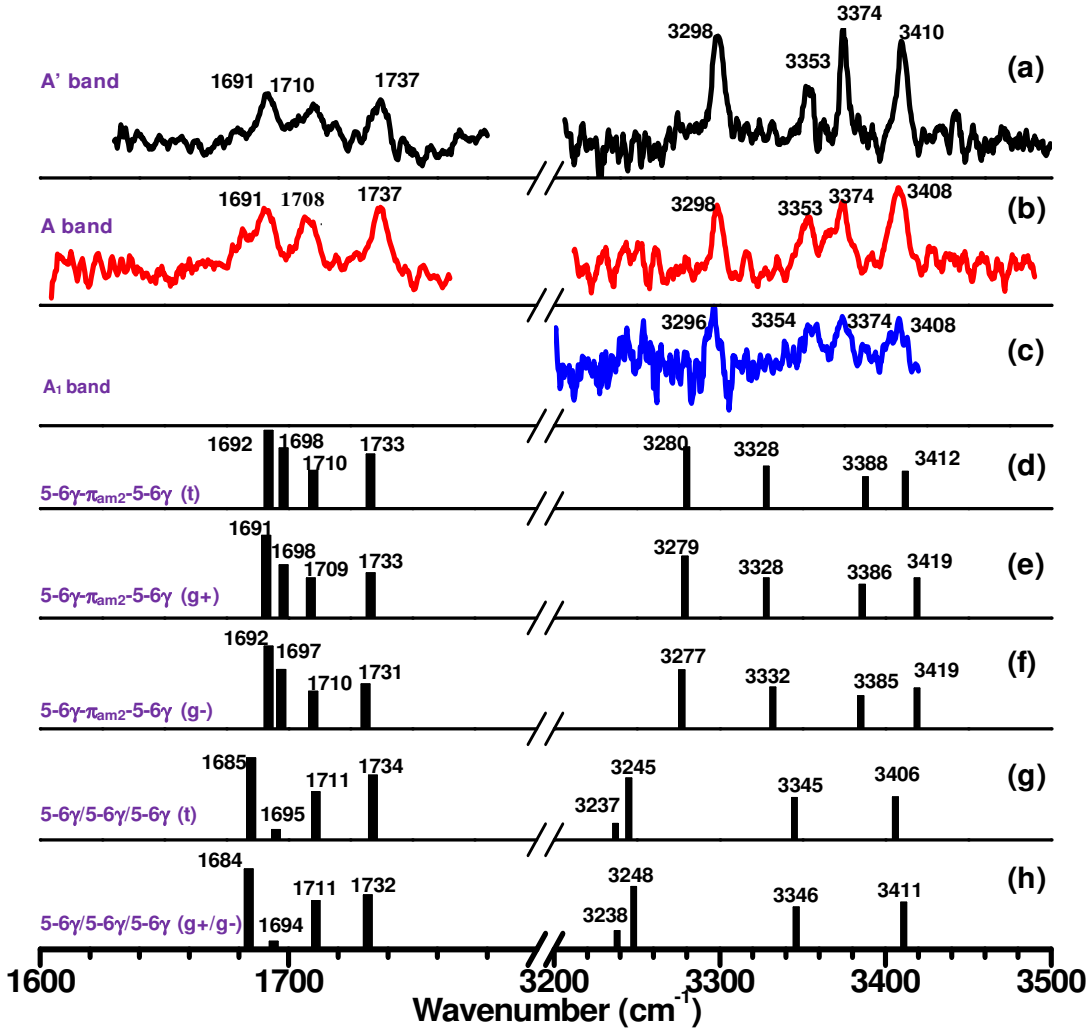

Figure S8. (a-c) Experimental conformer-specific IR/UV spectra of **3** obtained by probing the UV A, A' and A_1 bands. (d-f) Theoretical IR spectra of half-extended conformers. (g-h) Theoretical IR spectra of fully extended conformers.

Table S4. For compound **3**: relative enthalpies (ΔH, 0 K) in kJ/mol; relative Gibbs free energies (ΔG, 300 K) in kJ/mol; experimental and theoretical vibrational frequencies (cm^{-1}) in the N-H stretch, Amide I and Amide II regions and average and maximum deviation of the theoretical frequencies with respect to experimental spectra on A (the average deviation was calculated by considering all the frequencies). Best fits to experiment are highlighted in grey.

Conformers	Type of H-bonding	ΔH	ΔG	N-H Stretching frequency				Amide I				Amide II				With respect to A'	
				ν_{NH1}	ν_{NH2}	ν_{NH3}	ν_{NH4}	ν_{CO1}	ν_{CO2}	ν_{CO3}	ν_{CO4}	ν_{NH1}	ν_{NH2}	ν_{NH3}	ν_{NH4}	Average deviation	Max. deviation
Exp.A'				3410	3374	3353	3296	1737	1719	1710	1692	1550	1524	1498	1483		
Theory																	
3-01_g^-	5-6γ-π_{am2}/5-6γ	0.4	0	3419	3385	3332	3277	1731	1710	1697	1692	1551	1535	1492	1476	9	21
3-01_g^+	5-6γ-π_{am2}/5-6γ	0	0.6	3419	3386	3328	3279	1733	1709	1698	1691	1550	1541	1490	1477	10	25
3-01_t	5-6γ-π_{am2}/5-6γ	3.9	2.1	3412	3388	3328	3280	1733	1710	1698	1692	1546	1532	1497	1478	8	25
3-02_g^-/g^+	5-6γ/5-6γ/5-6γ	3.4	2.2	3411	3346	3248	3238	1732	1711	1694	1684	1550	1509	1500	1482	21	105
3-02_t	5-6γ/5-6γ/5-6γ	6.7	5.2	3406	3345	3245	3237	1734	1711	1685	1555	1509	1497	1490	1475	38	137
3-03_g^+	f-7_L-π_{am2}/5-6γ	4.6	5.5	3498	3391	3326	3261	1714	1709	1692	1690	1546	1545	1503	1485	21	88
3-03_g^-	f-7_L-π_{am2}/5-6γ	10.3	5.6	3497	3386	3329	3263	1712	1705	1692	1690	1546	1545	1509	1482	21	87
3-03_t	f-7_L-π_{am2}/5-6γ	12.3	9.4	3496	3387	3326	3258	1712	1707	1692	1691	1551	1548	1504	1492	22	86
3-04_g^-	5-6γ/5-6γ-7_L	7.9	5.9	3418	3338	3271	3240	1733	1709	1694	1677	1553	1550	1505	1479	22	82
3-04_g^+	5-6γ/5-6γ-7_L	9.1	9.6	3414	3342	3272	3250	1735	1710	1694	1676	1561	1548	1515	1477	22	81
3-04_t	5-6γ/5-6γ-7_L	11.8	9.8	3415	3343	3272	3241	1734	1710	1694	1677	1554	1547	1510	1488	22	81
3-05_g^-	5-6γ-7_L-7_L	7.1	6.8	3434	3315	3271	3250	1734	1707	1682	1664	1574	1563	1542	1480	33	82
3-05_t	5-6γ-7_L-7_L	10.2	7.4	3431	3321	3275	3239	1734	1709	1681	1664	1566	1561	1544	1489	32	78
3-05_g^+	5-6γ-7_L-7_L	8.1	9.4	3430	3319	3277	3242	1734	1710	1681	1664	1566	1560	1550	1479	32	76
3-06_g^+	5-6γ-7_D-7_L	11.1	7.6	3430	3324	3266	3242	1732	1708	1680	1665	1562	1561	1554	1477	32	87
3-06_g^-	5-6γ-7_D-7_L	12.3	10.4	3436	3323	3272	3246	1733	1708	1681	1665	1564	1560	1551	1486	33	81
3-06_t	5-6γ-7_D-7_L	15.1	10.9	3432	3326	3273	3243	1732	1708	1682	1666	1570	1559	1555	1489	33	80
3-07_g^-	5-6γ-7_L/5-6γ	11.3	9.4	3410	3348	3319	3282	1732	1713	1696	1684	1545	1534	1505	1482	11	34
3-07_t	5-6γ-7_L/5-6γ	14.6	11.0	3410	3344	3325	3275	1730	1713	1697	1684	1545	1536	1504	1475	12	30
3-07_g^+	5-6γ-7_L/5-6γ	11.6	9.5	3412	3344	3325	3283	1731	1713	1696	1684	1546	1534	1503	1482	11	30
3-08_g^-	f-7_D-π_{am2}/5-6γ	19.1	21.8	3467	3396	3307	3257	1712	1701	1693	1683	1552	1549	1527	1485	24	57
3-08_t	f-7_D-π_{am2}/5-6γ	26.4	26.8	3490	3410	3318	3246	1713	1703	1692	1682	1556	1542	1519	1487	26	80
3-08_g^+	f-7_D-π_{am2}/5-6γ	23.4	27.7	3438	3388	3313	3298	1721	1712	1697	1691	1554	1550	1516	1484	14	40
3-09_g^-	f-7_L-7_L-7_L	23.2	26.0	3446	3294	3274	3208	1709	1703	1679	1661	1571	1559	1558	1530	46	88
3-09_t	f-7_L-7_L-7_L	29.9	33.9	3392	3302	3269	3228	1710	1705	1680	1662	1568	1561	1559	1522	42	84
3-09_g^+	f-7_L-7_L-7_L	22.9	24.4	3463	3300	3255	3209	1709	1705	1679	1662	1565	1559	1556	1534	48	98

4.4. NBO analysis

The stability of extended planar structures in compounds **1-3** was rationalized in the light of a NBO analysis of hyperconjugation (HC) and H-bond (HB) interactions. For a sake of simplification, this analysis was carried out on related model systems, *viz.* compounds in which the N-terminal cap was a methoxycarbonyl group instead of a Cbz group. Indeed, these related model systems exhibited conformational and energy landscapes equivalent to those observed for **1**-**3** except of course for the absence of three Cbz-cap rotamers. For example, the relative enthalpy between the half-extended and the extended conformers was 1.9 kJ/mol in the related model systems compared to 3.4 kJ/mol in **3**. In the following, the related model systems are denoted as compounds **1-3**.

Relevant HC and HB interactions between donor and acceptor NBOs and their corresponding stabilization energies are reported in Table S5. The H-bond-induced stabilizations (given in the Table of the manuscript) were estimated by summing the interactions energies between donor NBOs corresponding to carbonyl O atom or sulfur atom lone pairs (noted lp(1) O/S and lp(2) O/S) and the σ^*_{NH} antibonding acceptor NBO.

In **1**, the strong hyperconjugative HCa interactions (~90 (2*45) kJ/mol range) between the donor NBO of the amide N atom lone pair [lp(1) N1] and the acceptors σ* NBO on the two vicinal Cα1–Cβ1a/b covalent bonds played a major shaping role, since the planar backbone structure maximizes the corresponding NBO overlap. The N–H···S H-bonding interaction was significant but made a relatively weaker contribution (~32 kJ/mol), followed by the much weaker C5 H-bonding interaction (~14 kJ/mol) resulting in a total HB(**1**) contribution for the monomer of ~46 kJ/mol. As far as the thietane ring was concerned, its puckering was also controlled by strong HCc interactions (~52(2*26) kJ/mol) between two vicinal side chain covalent bonds (σCβ1a/b-S1) and a backbone bond (σ*N1-Cα1), which favor the presentation of the S atom towards its N–H hydrogen bonding partner. Furthermore, strong HCf interactions inside the thietane ring were also present (~76 kJ/mol).

In **2**, where the extended planar structure was formed by a juxtaposition of two C5-C6$^\gamma$ monomer motifs, similar HC and HB interactions were at play. However, although their structure was very similar to that of **1**, the two monomer motifs exhibited HC and HB interactions somewhat different from that observed in **1**. The two N-H2/3···S1/2 H-bonding interactions were weaker than in **1** (~27 (S1) and ~29 (S2) kJ/mol) but the C5 H-bonding

interaction involving the O2 atom was stronger (~19 kJ/mol). This leads to a total HB contribution (C5 and C6$^{\gamma}$) for *motif 1* in **2** (noted HBm$_1$(**2**)) weaker by 6 kJ/mol than in **1,** but to a total HBm$_2$(**2**) for *motif 2* (~48 kJ/mol) stronger by 2 kJ/mol, leading to the following ranking: HBm$_2$(**2**) > HB$_1$(**1**) > HBm$_1$(**2**) with HB$_{S1}$(**1**) > HB$_{S2}$ (**2**) > HB$_{S1}$(**2**) and HB$_{O2}$(**2**) > HB$_{O1}$(**1**) > HB$_{O1}$(**2**). The two HCa interactions between the donor NBOs of the amide N atoms lone pairs [lp(1/2) N1/2] and the acceptor σ* NBOs on the vicinal covalent bonds (Cα1/2–Cβ1/2a/b) in these motifs (~88 and 84 kJ/mol) were weaker than in **1.** On the contrary, whereas the HCc interactions between the two vicinal side chain and the backbone covalent bonds were weaker for the first monomer motif (~50 kJ/mol) than in **1**, these interactions were stronger in the second monomer motif (~53 kJ/mol). Furthermore, the strong HCf interactions within the thietane rings are both stronger than those of **1** (82 kJ/mol for the first monomer motif and 77 kJ/mol for the second monomer motif).

In **3**, unsurprisingly, the extended C5-C6$^{\gamma}$/C5-C6$^{\gamma}$/C5-C6$^{\gamma}$ form exhibited similar trends showing that the same interaction types prevail and contribute to the stability of the structure. The case of the half-extended C5-C6$^{\gamma}$-π_{am2}/C5-C6$^{\gamma}$ form appeared different. The extended form presented three HB contributions of ~41, ~43 and ~48 kJ/mol, close to that for **1**. On the contrary, the central C5 and C6$^{\gamma}$ H-bonds (in blue) missed in the half extended form but the two remaining HB contributions were significantly stronger than in **1** (~54 kJ/mol for *motif 1* and ~50 kJ/mol for *motif 3*). This was mainly due to the N-H2···S1 H-bonding interaction being 10 kJ/mol stronger than in **1**, commensurate with the shortened H-bond distance of 236 pm (compared to 240 pm in **1**). Moreover, in the half-extended form, most types of HC contributions were comparable to their counterpart in the extended form, namely about +2 kJ/mol for HCa, –8 for HCc, +4 for HCd, +7 for HCe and –1 for HCf, except the HCb interactions between vicinal thietane CC and backbone CO bonds, whose sum was stronger by 16.0 kJ/mol (100.9 vs. 84.8 kJ/mol). This is essentially due to the existence of a strong HC between the σ NBO of one of the thietane ring Cα–Cβ covalent bonds and the σ* NBO of the vicinal C1–N2 bond (E(2) ~18 kJ/mol, HCb highlighted in red in Table S5), which favored the planar *trans* conformation of the C1–N2–Cα–Cβ chain of the half-extended form. Anecdotally, a weak $\pi_{am2} \rightarrow \sigma^*_{N3\text{-}H3}$ H-bond type interaction (3.1 kJ/mol) was also detected by the NBO analysis, but it is evidently not the principal reason for the stability of the half-extended structure.

Table S5. Interactions between donor and acceptor NBOs and corresponding stabilization energies (noted $E^{(2)}$, given in kJ/mol) in compounds **1**, **2**, extended **3** and half-extended **3** (the atom numbering for this table is given below). Interactions are sorted according to type and strength (> 8.4 kJ/mol, except for H-bonds), giving rise to 6 families of hyperconjugative interactions, noted HCa-f, whose individual sum is given in italics. For compound **3**, when strong interactions are found for one form, they are also given for the other form; interactions which are significantly stronger in the fully extended form are in blue while those stronger in the half-extended form are in red. They appear in bold font when the difference is > 7 kJ/mol. Interactions relevant to the discussion of the NBO analysis are highlighted (grey background).

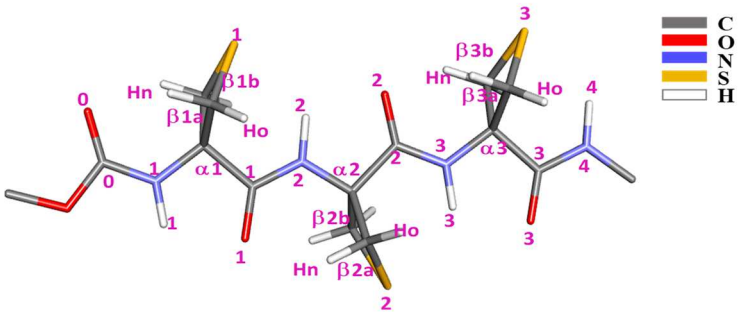

1		2		3_extended		3 half-extended	
Donor → Acceptor	**$E^{(2)}$**	**Donor → Acceptor**	**$E^{(2)}$**	**Donor → Acceptor**	**$E^{(2)}$**	**Donor → Acceptor**	**$E^{(2)}$**
Hyperconjugation from backbone to thietane ring : HCa							
lp(1) N1 → σ* Cα1-Cβ1a	45.2	lp(1) N1 → σ* Cα1-Cβ1a	44.5	lp(1) N1 → σ* Cα1-Cβ1a	44.3	lp(1) N1 → σ* Cα1-Cβ1a	45.0
lp(1) N1 → σ* Cα1-Cβ1β	45.2	lp(1) N1 → σ* Cα1-Cβ1β	43.5	lp(1) N1 → σ* Cα1-Cβ1b	43.9	lp(1) N1 → σ* Cα1-Cβ1b	44.4
		lp(1) N2 → σ* Cα1-Cβ1a	42.2	lp(1) N2 → σ* Cα2-Cβ2a	41.0	lp(1) N2 → σ* Cα2-Cβ2a	37.7
		lp(1) N2 → σ* Cα1-Cβ1β	41.5	lp(1) N2 → σ* Cα2-Cβ2b	40.7	lp(1) N2 → σ* Cα2-C3	36.1
				lp(1) N3 → σ* Cα3-Cβ3a	42.0	lp(1) N3 → σ* Cα3-Cβ3a	46.8
				lp(1) N3 → σ* Cα3-Cβ3b	41.4	lp(1) N3 → σ* Cα3-Cβ3b	38.6
				σC2-O2 → σ* Cα2-Cβ2a	**2.3**	**σC2-O2 → σ* Cα2-Cβ2a**	**9.5**
				sum	*255.6*	*sum*	*258.1*
Hyperconjugation interactions from thietane ring to backbone							
HC interactions between vicinal ring CC and backbone CO bonds : HCb							
σCα1-Cβ1a → σ* C1-O1	13.6	σCα1-Cβ1a→σ*C1-O1	14.8	σCα1-Cβ1a→σ*C1-O1	14.4	σCα1-Cβ1a→σ*C1-O1	12.7
σCα1-Cβ1b → σ* C1-O1	13.3	σCα1-Cβ1b→σ*C1-O1	14.4	σCα1-Cβ1b→σ*C1-O1	14.3	σCα1-Cβ1b→σ*C1-O1	17.4
		σCα2-Cβ2a→σ*C2-O2	13.4	σCα2-Cβ2a→σ*C2-O2	14.5	σCα2-Cβ2a→σ*C2-O2	14.9
		σCα2-Cβ2b→σ*C2-O2	13.4	σCα2-Cβ2b→σ*C2-O2	14.2	σCα2-Cβ2b→σ*C2-O2	10.4
				σCα3-Cβ3a→σ*C3-O3	13.4	σCα3-Cβ3a→σ*C3-O3	11.4
				σCα3-Cβ3b→σ*C3-O3	13.2	σCα3-Cβ3b→σ*C3-O3	16.2
				σCα2-Cβ2a → σ* C1-N2	**0.8**	**σCα2-Cβ2a → σ* C1-N2**	**17.9**
				sum	*84.8*	*sum*	*100.9*
HC interactions involving sulfur between vicinal ring CS and backbone CN bonds : HCc							
σCβ1a-S1 → σ* N1-Cα1	26.0	σCβ1a-S1 → σ* N1-Cα1	24.9	σCβ1a-S1 → σ* N1-Cα1	25.0	σCβ1a-S1 → σ* N1-Cα1	26.8
σCβ1b -S1→ σ* N1-Cα1	26.0	σCβ1b -S1 → σ* N1-Cα1	24.9	σCβ1b-S1 → σ* N1-Cα1	25.0	σCβ1b-S1 → σ* N1-Cα1	26.7
		σCβ2a-S2 → σ* N2-Cα2	26.6	σCβ2a-S2 → σ* N2-Cα2	25.5	σCβ2a-S2 → σ* Cα2-C3	20.3
		σCβ2b -S2 → σ* N2-Cα2	26.6	σCβ2b -S2 → σ* N2-Cα2	25.4	σCβ2b -S2 → σ* Cα2-C3	19.2
				σCβ3a-S3 → σ* N3-Cα3	26.7	σCβ3a-S3 → σ* N3-Cα3	26.9
				σCβ3b-S3 → σ* N3-Cα3	26.7	σCβ3b-S3 → σ* N3-Cα3	26.8
				sum	*154.3*	*sum*	*146.7*
HC interactions between vicinal ring CH and backbone CC bonds : HCd							
σCβ1a-Hn → σ* Cα1-C1	12.4	σCβ1a-Hn → σ* Cα1-C1	15.4	σCβ1a-Hn → σ* Cα1-C1	12.5	σCβ1a-Hn → σ* Cα1-C1	13.5
σCβ1b-Hn → σ* Cα1-C1	12.3	σCβ1b-Hn → σ* Cα1-C1	15.4	σCβ1b-Hn → σ* Cα1-C1	12.4	σCβ1b-Hn → σ* Cα1-C1	12.9
		σCβ2a-Hn → σ* Cα2-C2	12.1	σCβ2a-Hn → σ* Cα2-C3	12.0	σCβ2a-Ho → σ* Cα2-N2	17.7
		σCβ2b-Hn → σ* Cα2-C2	12.0	σCβ2b-Hn → σ* Cα2-C3	11.9	σCβ2b-Ho → σ* Cα2-N2	15.0
				σCβ3a-Hn → σ* Cα3-C4	12.1	σCβ3a-Hn → σ* Cα3-C4	12.1
				σCβ3b-Hn → σ* Cα3-C4	12.0	σCβ3b-Hn → σ* Cα3-C4	13.5
				sum	*72.9*	*sum*	*84.7*
Intra-backbone hyperconjugation : HCe							
				σCα2-C2 → σ* N2-H2	**1.5**	**σCα2-C2 → σ* N2-H2**	**9.0**

Hyperconjugation within the thietane ring : HCf							
lp(2) S1 →σ* Cβa/b-Hn/o	75.6	lp(2) S1 →σ* Cβ1a/b-Hn/o	82	**lp(2) S1 →σ* Cβ1a/b-Hn/o**	**81.4**	**lp(2) S1 →σ* Cβ1a/b-Hn/o**	**72.9**
		lp(2) S2 →σ* Cβ2a/b-Hn/o	76.9	lp(2) S2 →σ* Cβ2a/b-Hn/o	83.4	lp(2) S2 →σ* Cβ2a/b-Hn/o	82.9
				lp(2) S3 →σ* Cβ3a/b-Hn/o	77.1	lp(2) S3 →σ* Cβ3a/b-Hn/o	75.4
				σS2-Cβ2β → σ* Cβ2a-Hn	**0.6**	**σS2-Cβ2b → σ* Cβ2a-Hn**	**9.9**
				sum	*242.5*	*sum*	*241.1*
Hydrogen bonding							
C5 interaction							
lp(1) O1 → σ* N1-H1	2.9	lp(1) O1 → σ* N1-H1	2.7	lp(1) O1 → σ* N1-H1	2.8	lp(1) O1 → σ* N1-H1	2.4
lp(2) O1 → σ* N1-H1	11.1	lp(2) O1 → σ* N1-H1	10.4	lp(2) O1 → σ* N1-H1	10.6	lp(2) O1 → σ* N1-H1	9.0
		lp(1) O2 → σ* N2-H2	5.8	lp(1) O2 → σ* N2-H2	5.6		
		lp(2) O2 → σ* N2-H2	12.8	**lp(2) O2 → σ* N2-H2**	**12.1**		
				lp(1) O3 → σ* N3-H3	5.9	lp(1) O3 → σ* N3-H3	4.4
				lp(2) O3 → σ* N3-H3	13.3	lp(2) O3 → σ* N3-H3	14.1
NH – S							
lp(1) S1 → σ* N2-H2	30.7	lp(1) S1 → σ* N2-H2	2.1	lp(1) S1 → σ* N2-H2	2.2	lp(1) S1 → σ* N2-H2	2.7
lp(2) S1 → σ* N2-H2	1.7	lp(2) S1 → σ* N2-H2	24.8	**lp(2) S1 → σ* N2-H2**	**25.6**	**lp(2) S1 → σ* N2-H2**	**40.0**
		lp(1) S2 → σ* N3-H3	1.5	lp(1) S2 → σ* N3-H3	2.0		
		lp(2) S2 → σ* N3-H3	27.7	**lp(2) S2 → σ* N3-H3**	**22.8**		
				lp(1) S3 → σ* N4-H4	1.5	lp(1) S3 → σ* N4-H4	1.6
				lp(2) S3 → σ* N4-H4	27.2	lp(2) S3 → σ* N4-H4	29.5
NH -π_{amide} interaction						π_{amide2} → σ*N3-H3	3.1

4.5. UV spectroscopy and Cbz-cap rotamerism

IR spectroscopic absorptions are particularly sensitive to the *backbone* structure. For each compound **1-3**, the fact that the IR/UV data recorded on bands A and A_1 (and A' in the case of **3**) were so similar led us to assigned them to molecular structures having the same backbone. But regarding the orientation of the phenyl ring of the Cbz-cap (Cbz-rotamerism), they can be assigned to different rotamers, or alternatively to different vibronic transitions of a same Cbz-cap rotamer. The structures of **1** and **2** (apart from the Cbz-cap) exhibit a symmetry plane; only two Cbz-rotamers are therefore expected: a unique *trans* rotamer [C_{sp2}–C_{sp3}–O–C(=O) dihedral φ = 180°] and two *gauche* conformers (φ = ± 60°), with undistinguishable UV spectra due to the backbone symmetry plane. This symmetry is lifted in compound **3** due to the central (chiral) fold so the *gauche* rotamers should now exhibit non-identical UV spectral characteristics; however, due to the distance between the chiral backbone fold and the Cbz-cap, the difference is expected to be small. In contrast, the spectroscopic features of the *trans* form should remain unique with small changes along the *trans* series. In such a context, the UV spectroscopy can be revisited and interpreted in terms of Cbz-rotamerism (Figure S1).

Apart from the B band, assigned to a C7-C7 folded backbone, all the UV bands were observed in the same spectral range (37575-375600 cm^{-1}) suggesting that this range is the UV spectral signature of a Cbz-cap in close contact with a first Attc residue in a planar configuration. The series of A bands, whose frequency does not evolve significantly (37582 ± 3 cm^{-1}; Figure S1), shows a splitting in compound **3** (bands A and A'), whose backbone is no longer planar at the level of the second residue. This enabled us to assign this A, A' series to *gauche* rotamers. The series of A_1 bands (Figure S1), which also remained in a same range (37594 ± 4 cm^{-1}) and whose IR/UV spectra are identical to those obtained on the A, A' bands (within the experimental accuracy), are consistent with vibronic bands of the same *gauche* rotamers, involving a low frequency torsional mode of the benzyl moiety relative to the backbone. The *trans* rotamers, found to be less stable at low temperature (See Tables S2, S3 and S4) probably interconvert to the *gauche* forms in the late expansion.

4.6. Structure coordinate files

Table S6. Most stable structure coordinate files for **1-3** with their Cbz-cap rotamers, Ac-Aib-NHMe and *N*-methylacetamide·SMe_2 model compounds at the B97-D3(BJ)-abc/def2-TZVPPD level of theory; xyz format, coordinates in Å.

1_t				**1**-g$^-$				**1**-g$^+$			
C	0.7641599	-1.2641717	4.7662375	C	0.1139205	-1.5368665	5.4129009	C	0.1346924	-1.3068439	5.2364935
O	0.7396488	-2.0488260	3.8313798	O	0.1474468	-1.7588020	4.2124586	O	0.2367481	-1.4591025	4.0292048
N	1.6681842	-1.2607289	5.7835111	N	1.1700991	-1.6205200	6.2652262	N	1.1290197	-1.4872364	6.1465221
C	2.7421912	-2.2011225	5.9286824	C	2.5069588	-1.9704740	5.8772915	C	2.4682974	-1.8906283	5.8244728
C	3.4779172	-1.7784892	7.2382684	C	3.3449154	-1.9012149	7.1897982	C	3.2181299	-1.9459128	7.1901291
O	3.0961307	-0.8146257	7.8997824	O	2.8274002	-1.5856821	8.2599533	O	2.6437965	-1.6773280	8.2439754
N	4.5393403	-2.5369450	7.5787992	N	4.6522351	-2.2068011	7.0618502	N	4.5162802	-2.3062172	7.1261655
O	-0.1273333	-0.2457062	4.9463165	O	-1.0045795	-1.1763750	6.1094033	O	-1.0038819	-0.9128324	5.8801914
C	-1.1516296	-0.1355943	3.9157036	C	-2.1860442	-0.8882080	5.3037665	C	-2.1967528	-0.8101203	5.0475278
C	-2.0597928	0.9969322	4.2951075	C	-2.2026725	0.5469222	4.8516703	C	-2.8975693	-2.1358496	4.9234247
C	-1.7673085	2.3065188	3.8982033	C	-1.6840474	0.9091760	3.6021951	C	-3.7658839	-2.5696477	5.9327877
C	-3.2021590	0.7610552	5.0676935	C	-2.7157531	1.5439413	5.6904281	C	-2.6736190	-2.9622005	3.8154302
C	-2.5997552	3.3624974	4.2674553	C	-1.6786114	2.2452097	3.2014347	C	-4.3993589	-3.8083199	5.8399218
C	-4.0379975	1.8139877	5.4384350	C	-2.7106398	2.8801227	5.2917904	C	-3.3084013	-4.2009111	3.7195578
C	-3.7372163	3.1173019	5.0389835	C	-2.1907711	3.2328351	4.0449282	C	-4.1708683	-4.6266347	4.7315092
C	5.3260831	-2.2654875	8.7716365	C	5.5610898	-2.1777900	8.1968736	C	5.3446791	-2.4046175	8.3173184
C	2.3459440	-3.7088530	5.9478064	C	2.6802566	-3.3372066	5.1472987	C	2.6151382	-3.2244615	5.0294320
S	3.8292569	-4.1590570	4.9369218	S	3.9236993	-2.6116421	3.9842965	S	3.9720989	-2.5109998	3.9926615
C	3.7265227	-2.3232896	4.7258465	C	3.1430299	-1.1133352	4.7396236	C	3.2247213	-1.0128129	4.7816167
H	1.6088763	-0.5650541	6.5202420	H	1.0530057	-1.3982183	7.2484594	H	0.9492767	-1.3443743	7.1349646
H	4.7809134	-3.3132081	6.9679417	H	4.9953310	-2.4463253	6.1355082	H	4.9082405	-2.5079693	6.2103417
H	-1.6913092	-1.0850510	3.8554625	H	-3.0191620	-1.1002777	5.9769405	H	-1.9111447	-0.4164335	4.0702163
H	-0.6610384	0.0416101	2.9536956	H	-2.2095890	-1.5751741	4.4554206	H	-2.8180722	-0.0822554	5.5737150
H	-0.8811649	2.4968334	3.2976501	H	-1.2760723	0.1393750	2.9545045	H	-3.9430102	-1.9313339	6.7950522
H	-3.4353234	-0.2542480	5.3787890	H	-3.1207806	1.2685380	6.6613528	H	-1.9895832	-2.6330724	3.0395102
H	-2.3634041	4.3749187	3.9523322	H	-1.2757609	2.5162038	2.2293677	H	-5.0728681	-4.1337821	6.6278964
H	-4.9238665	1.6182486	6.0360650	H	-3.1142552	3.6443213	5.9501879	H	-3.1296058	-4.8343998	2.8551608
H	-4.3887636	3.9383593	5.3247389	H	-2.1880870	4.2729501	3.7307920	H	-4.6656577	-5.5910085	4.6562851
H	5.7799931	-1.2703757	8.7227154	H	5.2175467	-2.8537021	8.9860498	H	4.9084086	-3.1048899	9.0364947
H	4.7004508	-2.3083265	9.6687130	H	6.5494170	-2.4923991	7.8574949	H	6.3339459	-2.7593952	8.0231940
H	6.1139185	-3.0170384	8.8457582	H	5.6280165	-1.1702113	8.6201252	H	5.4418280	-1.4315032	8.8098031
H	1.4315567	-3.8914631	5.3847739	H	1.7765970	-3.6241375	4.6109462	H	1.7352108	-3.4285702	4.4206578
H	2.3044126	-4.1792445	6.9319280	H	3.0531345	-4.1613009	5.7585574	H	2.9007103	-4.0998377	5.6156135
H	4.6773995	-1.7976173	4.8312381	H	3.8488037	-0.3444321	5.0590861	H	3.9476383	-0.3032569	5.1887756
H	3.2422624	-2.0740397	3.7822862	H	2.3841226	-0.7013992	4.0760190	H	2.5367168	-0.5224408	4.0942768
2-t				**2**-g$^-$				**2**-g+			
C	1.4655361	-2.3507768	1.1620178	C	-2.1791151	-2.4538937	0.2076392	C	0.5801516	-2.0661899	-0.1658472
C	2.8327030	-2.9270396	0.6871062	C	-3.1744016	-3.1526595	-0.7652264	C	1.4190244	-2.5412611	-1.3885628
O	3.8273284	-2.2109748	0.6044022	O	-4.1344701	-2.5454100	-1.2325929	O	2.0385251	-1.7377187	-2.0810685
N	2.8376723	-4.2425932	0.3860092	N	-2.9052242	-4.4449802	-1.0460924	N	1.4118277	-3.8706514	-1.6204283
C	4.0463880	-4.9204994	-0.0567818	C	-3.7443503	-5.2219866	-1.9455335	C	2.1542231	-4.4568949	-2.7259717

C	0.8760540	-3.1719133	2.3480813	C	-0.7052917	-2.5908275	-0.2799167	C	0.9750578	-2.8301193	1.1339850
S	-0.2515955	-4.0928488	1.2072844	S	-0.4000499	-3.9870280	0.8950710	S	-0.4778849	-3.9626315	0.9624439
C	0.3164290	-2.6767335	0.1617658	C	-1.9854715	-3.2673759	1.5222154	C	-0.8827616	-2.5999133	-0.2210194
H	1.9682880	-4.7591056	0.4834440	H	-2.0824231	-4.8651010	-0.6241646	H	0.8735713	-4.4626537	-0.9948359
H	4.4093996	-4.4988156	-0.9994091	H	-4.7827719	-5.2214186	-1.6011709	H	1.8133434	-4.0496138	-3.6828816
H	4.8424249	-4.8186465	0.6872594	H	-3.7244881	-4.8070662	-2.9587355	H	3.2245891	-4.2476158	-2.6319617
H	3.8181465	-5.9780293	-0.1993688	H	-3.3715130	-6.2473341	-1.9686190	H	1.9955062	-5.5364914	-2.7161769
H	0.3044848	-2.5490115	3.0340160	H	-0.1020521	-1.7247631	-0.0120723	H	0.8729523	-2.2075830	2.0214062
H	1.5876568	-3.8001885	2.8868264	H	-0.5784567	-2.8478046	-1.3331592	H	1.9453597	-3.3292153	1.1123135
H	0.6302959	-2.9522152	-0.8466098	H	-2.7619542	-4.0019314	1.7416496	H	-1.2261881	-2.9358981	-1.2008143
H	-0.4368400	-1.8909200	0.1385989	H	-1.8007568	-2.6214664	2.3791114	H	-1.5897498	-1.9017344	0.2243805
C	0.0888368	3.4433780	2.7810400	C	-2.2686410	3.3484470	2.3012569	C	-0.2701234	3.6701235	1.9380199
O	1.0444729	4.1999929	2.7269566	O	-3.1992407	4.0044750	1.8624470	O	0.2547127	4.5232576	1.2407989
N	0.1035466	2.1131923	2.4925297	N	-2.0092750	2.0443026	2.0167066	N	-0.2305056	2.3285843	1.7199415
C	1.2612708	1.3852475	2.0512895	C	-2.7991273	1.2243579	1.1401022	C	0.4375867	1.6966247	0.6158872
C	0.7691218	-0.0769991	1.8452118	C	-2.0905217	-0.1615885	1.1319902	C	0.1587039	0.1750899	0.7917680
O	-0.4028520	-0.3826853	2.0681193	O	-1.0682280	-0.3498075	1.7922489	O	-0.5443270	-0.2316727	1.7173552
N	1.7061543	-0.9510327	1.4160014	N	-2.6733422	-1.1071290	0.3626189	N	0.7280190	-0.6313785	-0.1308397
O	-1.1745294	3.8164549	3.1455161	O	-1.3259837	3.8168185	3.1742084	O	-0.9825821	3.9210232	3.0780052
C	-1.3205380	5.2264663	3.4815394	C	-1.3714254	5.2496279	3.4404232	C	-1.2580548	5.3256274	3.3552729
C	1.9792672	1.9404047	0.7835326	C	-4.3138983	1.1030439	1.4878544	C	0.0376312	2.1908566	-0.8088378
S	3.6403740	1.6254144	1.5250974	S	-4.7843054	1.2340095	-0.2926549	S	1.7967028	2.1449197	-1.3702257
C	2.5137577	1.4512997	2.9779768	C	-3.0173986	1.7710100	-0.3043108	C	1.9576134	2.0043971	0.4637085
H	-0.7476986	1.5674429	2.5705490	H	-1.1968773	1.5897513	2.4183563	H	-0.7298893	1.6991430	2.3388301
H	2.6669040	-0.6379508	1.2502709	H	-3.5219694	-0.8902295	-0.1687186	H	1.3014451	-0.2347849	-0.8813544
H	-0.7074438	5.4414971	4.3621533	H	-2.4148849	5.5684936	3.4797130	H	-1.3674552	5.3615616	4.4412376
H	1.8016722	3.0077595	0.6567446	H	-4.6654340	1.9667256	2.0509605	H	-0.3408468	3.2119332	-0.7860330
H	1.7869836	1.3989889	-0.1453463	H	-4.6171531	0.1713286	1.9701454	H	-0.6342106	1.5349426	-1.3661743
H	2.6975456	0.5661146	3.5906832	H	-2.4079833	1.3088816	-1.0839792	H	2.6375885	1.2193003	0.8011098
H	2.5156661	2.3549021	3.5864203	H	-2.9361368	2.8568571	-0.3384656	H	2.2184149	2.9637288	0.9094960
H	-0.9427261	5.8249064	2.6476114	H	-0.9167052	5.3453696	4.4287285	H	-0.3952884	5.9213477	3.0501560
C	-2.7748931	5.4892140	3.7395591	C	-0.5974393	6.0216749	2.4064430	C	-2.5152102	5.7815195	2.6653740
C	-3.6364015	5.7972068	2.6803434	C	0.7941682	6.1376940	2.5103568	C	-2.4567571	6.4051402	1.4129520
C	-3.2936587	5.4180863	5.0367164	C	-1.2494002	6.6078517	1.3148626	C	-3.7643390	5.5604264	3.2583383
C	-4.9915151	6.0280597	2.9119468	C	1.5239403	6.8248754	1.5415111	C	-3.6280264	6.7991843	0.7659115
C	-4.6486295	5.6499883	5.2733187	C	-0.5212356	7.2975834	0.3452097	C	-4.9362809	5.9528423	2.6128534
C	-5.5001429	5.9547431	4.2103050	C	0.8659992	7.4066053	0.4558481	C	-4.8693040	6.5731433	1.3636633
H	-3.2395494	5.8558170	1.6698812	H	1.3062410	5.6850852	3.3562471	H	-1.4896815	6.5669614	0.9470837
H	-2.6300427	5.1800408	5.8643398	H	-2.3266420	6.5071612	1.2252346	H	-3.8155111	5.0767464	4.2309105
H	-5.6499645	6.2691035	2.0821005	H	2.6031057	6.9102756	1.6341837	H	-3.5721057	7.2840323	-0.2048202
H	-5.0391099	5.5950570	6.2855953	H	-1.0369472	7.7497500	-0.4974904	H	-5.8998281	5.7786251	3.0837183
H	-6.5552063	6.1384742	4.3930671	H	1.4324646	7.9445221	-0.2993158	H	-5.7811390	6.8818747	0.8598735

3-Extended-t				**3**-Extended-g$^-$				**3**-Extended-g+			
C	0.5206127	3.1459062	6.6246808	C	0.4047322	3.1171632	6.6137432	C	0.4167208	3.1639565	6.6474598
C	-0.3911614	3.6744686	7.7688664	C	-0.4111526	3.6724481	7.8163590	C	-0.5504405	3.5639546	7.7986536
O	-1.3444858	4.4110168	7.5209479	O	-1.2830747	4.5225702	7.6428537	O	-1.6217869	4.1153516	7.5512729
N	-0.0538904	3.2656430	9.0120073	N	-0.0857142	3.1576983	9.0226025	N	-0.1278958	3.2589984	9.0455679
C	-0.7631708	3.6290807	10.2149330	C	-0.7041672	3.5361967	10.2703042	C	-0.8757962	3.5284112	10.2505166
C	0.6956532	1.5989691	6.6838806	C	0.3832696	1.5596562	6.5640806	C	0.7693415	1.6462399	6.7002366
S	2.3575222	1.7695711	7.4691388	S	2.0685000	1.4660451	7.3129996	S	2.4007450	2.0053661	7.4849168
C	2.0202764	3.4860185	6.8804500	C	1.9399137	3.2479349	6.8488596	C	1.8680482	3.6724129	6.8944253
H	0.7584385	2.6589624	9.1566334	H	0.6530089	2.4532082	9.1039772	H	0.7703869	2.7891352	9.1888908
H	0.7727768	1.1589258	5.6906786	H	0.3843416	1.1849394	5.5415603	H	0.8953593	1.2236965	5.7044273
H	-0.0384976	1.0667824	7.2919801	H	-0.4002354	1.0821616	7.1557907	H	0.1025739	1.0294472	7.3061664
H	2.2053625	4.2633598	7.6247006	H	2.2364908	3.9424302	7.6375810	H	1.9689044	4.4677509	7.6358243
H	2.5538568	3.6980226	5.9549539	H	2.4777356	3.4545617	5.9248113	H	2.3701700	3.9390488	5.9656970
C	0.0235920	4.0970413	0.5474606	C	-0.0962935	4.5563333	0.6347856	C	-0.2019875	4.1648461	0.5895862

O	-0.9308438	4.7923786	0.2398646	O	-0.9586836	5.3907841	0.4113286	O	-1.2458566	4.7270925	0.3006329
N	0.3735188	3.7295998	1.8103777	N	0.2257903	4.0530233	1.8561442	N	0.1908104	3.8105855	1.8423913
C	-0.3365015	4.1092297	3.0001409	C	-0.3970911	4.4392618	3.0916280	C	-0.5711612	4.0485940	3.0370579
C	0.4483949	3.4438610	4.1698911	C	0.3218019	3.5961867	4.1871855	C	0.2973503	3.4759265	4.1954365
O	1.4498204	2.7640336	3.9467769	O	1.2232599	2.8138028	3.8872077	O	1.3753544	2.9297863	3.9612076
N	-0.0487785	3.6703892	5.4054364	N	-0.1170266	3.7937288	5.4495687	N	-0.2185290	3.6246890	5.4350415
O	0.9121400	3.5639496	-0.3435896	O	0.7090677	3.9900774	-0.3137742	O	0.7538529	3.7820282	-0.3099923
C	0.6441430	3.8846765	-1.7394276	C	0.3930617	4.3284799	-1.6963031	C	0.5494696	4.2408687	-1.6788834
C	-0.5329961	5.6392461	3.2267302	C	-0.3800486	5.9621777	3.4265730	C	-0.9961966	5.5254388	3.2981595
S	-2.2643979	5.3789107	3.8148065	S	-2.1178170	5.8938351	4.0486890	S	-2.6727166	4.9944664	3.8648370
C	-1.8537337	3.7529846	3.0418703	C	-1.9469591	4.2841925	3.1597825	C	-2.0175984	3.4656491	3.0629173
H	1.1888718	3.1456075	1.9622021	H	0.9570268	3.3555209	1.9419813	H	1.0811520	3.3459046	1.9835816
H	-0.8833579	4.2509416	5.5236553	H	-0.8682193	4.4645517	5.6321327	H	-1.1282730	4.0765934	5.5606196
H	-0.3505025	3.5113238	-1.9996864	H	0.0503061	5.3644406	-1.7343885	H	1.0889904	3.5075612	-2.2819039
H	-0.5179603	6.1873525	2.2856152	H	-0.3103443	6.5696354	2.5252059	H	-1.0574431	6.0951045	2.3721556
H	0.1318009	6.0997458	3.9606822	H	0.3559663	6.2758677	4.1698476	H	-0.4117505	6.0606893	4.0493678
H	-2.1211255	2.8823177	3.6448046	H	-2.3116750	3.4186191	3.7168912	H	-2.1498779	2.5533579	3.6484629
H	-2.2758100	3.6784141	2.0402181	H	-2.4004806	4.3302655	2.1702579	H	-2.4203135	3.3472877	2.0577122
H	0.6420374	4.9726988	-1.8532551	H	1.3498432	4.2351122	-2.2144217	H	-0.5168934	4.1977089	-1.9097905
C	-0.0098129	2.9064152	11.3714611	C	0.0089583	2.6783688	11.3583276	C	0.0177236	3.0136259	11.4174087
O	0.9765587	2.2095939	11.1450988	O	0.8960178	1.8838590	11.0560597	O	1.1106783	2.4973173	11.1971870
C	-0.9141180	5.1555787	10.4874996	C	-0.6742173	5.0551337	10.6153750	C	-1.3183582	5.0061844	10.4669916
H	-0.2327247	5.5727424	11.2310686	H	0.0764276	5.3589180	11.3470175	H	-0.7227944	5.5775841	11.1810231
H	-0.8980104	5.7377507	9.5676304	H	-0.6279773	5.6757071	9.7221184	H	-1.4264725	5.5432134	9.5262655
S	-2.6513296	4.9215964	11.0794751	S	-2.4030927	4.9842985	11.2702099	S	-2.9701311	4.4644590	11.1011299
C	-2.2893740	3.3176291	10.2321225	C	-2.2536974	3.3919565	10.3409963	C	-2.3113888	2.9258854	10.3140150
H	-2.7173382	3.3079413	9.2307736	H	-2.7188883	3.4739917	9.3596956	H	-2.7409837	2.7886240	9.3229509
H	-2.5845095	2.4298696	10.7945592	H	-2.6218661	2.5168986	10.8794361	H	-2.4180491	2.0238667	10.9188692
N	-0.5122326	3.1039691	12.6075871	N	-0.4144792	2.8739362	12.6240788	N	-0.4917320	3.1746853	12.6561646
H	-1.3314632	3.6975098	12.7010423	H	-1.1557060	3.5509107	12.7807307	H	-1.4041959	3.6125535	12.7437735
C	0.0906175	2.4963551	13.7841754	C	0.1561826	2.1414947	13.7443542	C	0.2325083	2.7446887	13.8425141
H	0.0853020	1.4047589	13.7048589	H	-0.0048376	1.0647363	13.6301427	H	0.4370843	1.6701190	13.8056642
H	1.1291518	2.8214306	13.9021840	H	1.2341415	2.3169862	13.8146933	H	1.1902736	3.2680988	13.9251354
H	-0.4836062	2.7971002	14.6619923	H	-0.3254889	2.4824105	14.6622419	H	-0.3771852	2.9663077	14.7199277
C	1.7148158	3.2404806	-2.5700887	C	-0.6310057	3.3874843	-2.2711520	C	1.1026430	5.6255777	-1.8815236
C	1.5298742	1.9598216	-3.1019601	C	-1.9934538	3.7092935	-2.2397501	C	2.4668968	5.8072770	-2.1391518
C	2.9215794	3.9064285	-2.8119785	C	-0.2333028	2.1641942	-2.8241875	C	0.2722034	6.7491390	-1.7891421
C	2.5314979	1.3541754	-3.8604383	C	-2.9396335	2.8215693	-2.7521886	C	2.9955036	7.0873216	-2.2994096
C	3.9259634	3.3045018	-3.5687100	C	-1.1777321	1.2749868	-3.3360618	C	0.7988193	8.0307969	-1.9508812
C	3.7321316	2.0259032	-4.0947148	C	-2.5343349	1.6031108	-3.3002672	C	2.1605766	8.2026401	-2.2050025
H	0.5947036	1.4353420	-2.9206263	H	-2.3043455	4.6519312	-1.8002491	H	3.1166681	4.9384672	-2.2136131
H	3.0723596	4.9027152	-2.4033133	H	0.8234806	1.9088838	-2.8525316	H	-0.7833384	6.6116028	-1.5765642
H	2.3746897	0.3602276	-4.2701308	H	-3.9943238	3.0814732	-2.7250065	H	4.0554453	7.2153787	-2.5010669
H	4.8574843	3.8331250	-3.7510569	H	-0.8562046	0.3301538	-3.7653978	H	0.1459303	8.8961736	-1.8779521
H	4.5121601	1.5567979	-4.6877824	H	-3.2720474	0.9134056	-3.7009928	H	2.5698320	9.2011812	-2.3314632

3-Half-extended-t				**3**-Half-extended-g$^-$				**3**-Half-extended-g+			
C	1.2250462	1.5457492	6.5360818	C	1.2581670	1.5722130	6.5240565	C	1.3227459	1.5111708	6.5468253
C	1.1631849	2.2646382	7.9040919	C	1.2743628	2.3346309	7.8698390	C	1.1561808	2.2475137	7.8972538
O	2.0994105	2.2073117	8.6933145	O	2.2641215	2.3199037	8.5932596	O	2.0574493	2.2543212	8.7281765
N	-0.0279116	2.8588577	8.1604207	N	0.0914280	2.9128414	8.1899598	N	-0.0738352	2.7833032	8.0874849
C	-0.3397716	3.6684053	9.3062613	C	-0.1722202	3.7240879	9.3464357	C	-0.4742787	3.6048439	9.1971053
C	0.8936183	0.0348741	6.6473864	C	0.9979654	0.0548141	6.7105182	C	1.0989199	-0.0178748	6.6747289
S	2.2709330	-0.4068563	5.5026808	S	2.3021326	-0.3758618	5.4794877	S	2.5522783	-0.3759984	5.5963274
C	2.6602911	1.3354834	5.9957173	C	2.6541614	1.3980564	5.8779144	C	2.7911986	1.3979533	6.0701547
H	-0.7304416	2.9079761	7.4294021	H	-0.6626149	2.9224960	7.5104168	H	-0.7441224	2.7820462	7.3253533
H	-0.1047101	-0.2530065	6.3102396	H	-0.0106154	-0.2809944	6.4586216	H	0.1394990	-0.3849848	6.3031866
H	1.0749754	-0.3467762	7.6539386	H	1.2675179	-0.2855414	7.7120353	H	1.2655617	-0.3681830	7.6950778

H	3.3990283	1.3704118	6.7957755	H	3.4503323	1.4934175	6.6153353	H	3.4895957	1.5008819	6.8998761
H	2.9417096	1.9919897	5.1744371	H	2.8413369	2.0338441	5.0147662	H	3.0589843	2.0602154	5.2490193
C	-0.6177607	5.9874230	2.6911891	C	-1.0781048	5.7298271	2.6258854	C	-0.6915952	5.7004816	2.5077324
O	-1.5201916	5.6440589	1.9453875	O	-2.0362309	5.3068013	1.9989875	O	-1.5334665	5.2609766	1.7411327
N	-0.0376034	5.2162965	3.6523407	N	-0.3785413	5.0386918	3.5665563	N	-0.0901604	5.0043048	3.5100772
C	-0.4080779	3.8603995	3.9447137	C	-0.6728636	3.6930599	3.9716174	C	-0.3706983	3.6339977	3.8330956
C	0.5361132	3.4174960	5.0971755	C	0.3844026	3.3482837	5.0569925	C	0.5623051	3.2943959	5.0286854
O	1.3860355	4.1731760	5.5613798	O	1.2437656	4.1549717	5.4025259	O	1.3399644	4.1219779	5.4969433
N	0.3466459	2.1544642	5.5478541	N	0.2792360	2.1066588	5.5888826	N	0.4431682	2.0348262	5.5124853
O	-0.0316896	7.2205834	2.6834947	O	-0.5509162	6.9825266	2.4955345	O	-0.1977083	6.9735844	2.4808211
C	-0.5643335	8.1459788	1.6911320	C	-1.1272772	7.8017086	1.4339961	C	-0.8331393	7.8792522	1.5294402
C	-1.9065576	3.6074824	4.2937149	C	-2.1248759	3.4179272	4.4693127	C	-1.8586799	3.2846587	4.1408776
S	-1.9012449	2.0137791	3.3486970	S	-2.1548812	1.7782306	3.6084204	S	-1.7097243	1.6716738	3.2428254
C	-0.3605166	2.8515942	2.7560247	C	-0.6946563	2.6170350	2.8422150	C	-0.2082712	2.5956613	2.6803779
H	0.7142215	5.5934351	4.2185725	H	0.4098132	5.4725312	4.0329813	H	0.6030475	5.4562270	4.0955889
H	-0.3376367	1.5792881	5.0570054	H	-0.4275322	1.4872495	5.1928306	H	-0.1813294	1.4004879	5.0146662
H	-1.6229931	8.3180150	1.9062667	H	-0.9567835	8.8250404	1.7748779	H	-1.0914802	7.3178514	0.6292513
H	-0.4865979	7.6803450	0.7043963	H	-2.1991775	7.6020875	1.3799435	H	-0.0520749	8.6072968	1.3018812
H	-2.5532082	4.3328611	3.8016274	H	-2.8365146	4.0991366	4.0052422	H	-2.5373582	3.9505746	3.6098228
H	-2.1514481	3.5207128	5.3527804	H	-2.2676583	3.3791283	5.5495814	H	-2.1316833	3.2086672	5.1938802
H	0.5192201	2.2064176	2.7073130	H	0.1967111	1.9920265	2.7569132	H	0.7148537	2.0123362	2.6864367
H	-0.5380832	3.3493962	1.8034747	H	-0.9628370	3.0540542	1.8813024	H	-0.3801312	3.0506165	1.7057637
C	-1.7644832	4.2320360	9.0243069	C	-1.6263507	4.2465798	9.1460242	C	-1.9096549	4.0916892	8.8395603
O	-2.3365273	4.0035731	7.9565382	O	-2.2607600	3.9796821	8.1233917	O	-2.4240229	3.8063892	7.7561900
C	-0.2238161	2.9696887	10.6902745	C	0.0389430	3.0377158	10.7258462	C	-0.3871885	2.9463403	10.6026601
H	-1.1612152	2.6377528	11.1399348	H	-0.8636553	2.6890221	11.2307417	H	-1.3270125	2.5812395	11.0204107
H	0.5105220	2.1651280	10.6696610	H	0.7879769	2.2487510	10.6683191	H	0.3838503	2.1770369	10.6343323
S	0.5048420	4.4925258	11.4480898	S	0.7752747	4.5813875	11.4320929	S	0.2378098	4.5189027	11.3503254
C	0.6651782	4.8159271	9.6325435	C	0.8220514	4.8967608	9.6082130	C	0.4599628	4.8071254	9.5354086
H	1.6704847	4.5832074	9.2855309	H	1.8109984	4.6851447	9.2051584	H	1.4891673	4.6161147	9.2366074
H	0.3634982	5.8161309	9.3178741	H	0.4789151	5.8875774	9.3065853	H	0.1240173	5.7835184	9.1830402
N	-2.3033187	4.9790266	10.0057413	N	-2.1200952	4.9998779	10.1458904	N	-2.5260683	4.8390220	9.7740567
H	-1.7350737	5.1509708	10.8316195	H	-1.5078788	5.1955975	10.9339259	H	-2.0059156	5.0636229	10.6186280
C	-3.6052208	5.6133142	9.8642773	C	-3.4488670	5.5896221	10.0827129	C	-3.8491056	5.4044959	9.5557220
H	-3.8419178	6.1302734	10.7955265	H	-3.6289580	6.1376899	11.0088098	H	-4.1545775	5.9312262	10.4610486
H	-3.6035949	6.3346489	9.0402063	H	-3.5329996	6.2755821	9.2335451	H	-3.8437209	6.1045883	8.7135746
H	-4.3768891	4.8659597	9.6589845	H	-4.2110291	4.8131702	9.9677633	H	-4.5727274	4.6146319	9.3350525
C	0.2331481	9.4139628	1.7744327	C	-0.4531277	7.5500737	0.1128445	C	-2.0412578	8.5479718	2.1276184
C	-0.2065108	10.4813228	2.5647769	C	0.7318785	8.2208514	-0.2119007	C	-3.3216686	8.0129663	1.9397604
C	1.4381861	9.5394308	1.0733024	C	-0.9863431	6.6314288	-0.7998654	C	-1.8941099	9.7057782	2.9011955
C	0.5438426	11.6540825	2.6545703	C	1.3765563	7.9788720	-1.4240161	C	-4.4337702	8.6264072	2.5164759
C	2.1921668	10.7088921	1.1619548	C	-0.3436650	6.3888371	-2.0136419	C	-3.0044489	10.3199522	3.4792357
C	1.7453776	11.7691949	1.9535381	C	0.8387683	7.0607091	-2.3277197	C	-4.2776657	9.7798140	3.2874222
H	-1.1422860	10.3915577	3.1110271	H	1.1495288	8.9381578	0.4909129	H	-3.4361131	7.1084922	1.3508034
H	1.7848850	8.7139593	0.4566363	H	-1.8989147	6.1016635	-0.5452451	H	-0.9024807	10.1269814	3.0490655
H	0.1906706	12.4778131	3.2686138	H	2.2942125	8.5080785	-1.6656530	H	-5.4232795	8.2046381	2.3630237
H	3.1250903	10.7952870	0.6121312	H	-0.7664501	5.6749735	-2.7152839	H	-2.8782179	11.2206353	4.0736379
H	2.3294896	12.6826736	2.0203057	H	1.3380065	6.8724149	-3.2742191	H	-5.1449912	10.2587063	3.7335419

Ac-Aib-NHMe				*N*-methylacetamide··SMe_2			
C	-2.2880107	0.5997462	0.8260274	C	2.0826698	1.3325270	0.7181326
O	-2.9957616	-0.3573927	0.5166920	H	1.2215728	1.9350090	0.4161154
N	-0.9558667	0.6778623	0.5585557	C	1.7011016	-0.0097978	1.3268615
C	-0.1565723	-0.3304573	-0.1321325	O	2.5376252	-0.7618267	1.8196187
C	1.2796422	0.2697047	-0.1675136	N	0.3724606	-0.3096967	1.2905887
O	1.5402597	1.3795258	0.2948224	H	-0.2647305	0.3095725	0.7985092
N	2.2249527	-0.5080687	-0.7467415	C	-0.1400271	-1.5621362	1.8168797
C	-2.8606253	1.8095333	1.5527814	H	2.7228835	1.1568502	-0.1519976

C	3.6138818	-0.0855732	-0.8539574	H	2.6726123	1.8899510	1.4503688	
C	-0.1631348	-1.6557729	0.6565946	H	0.1018740	-2.4104450	1.1635937	
C	-0.6739671	-0.5360703	-1.5711038	H	-1.2252242	-1.4860170	1.9168450	
H	-0.4233808	1.4969226	0.8292239	H	0.3001937	-1.7625825	2.7970576	
H	1.9654837	-1.4150141	-1.0961022	C	-0.2948025	0.9433165	-2.1964012	
H	3.6893148	0.8554878	-1.4066274	H	0.2335606	1.8990374	-2.2160472	
H	4.0543513	0.0657960	0.1367993	H	-0.6544706	0.7135927	-3.2032218	
H	4.1738290	-0.8594369	-1.3820286	S	-1.6887203	1.1219837	-1.0464086	
H	0.4119788	-2.4301655	0.1394266	C	-2.4003601	-0.5421370	-1.1961091	
H	-1.1924941	-2.0023629	0.7593980	H	-3.2553282	-0.5927092	-0.5180019	
H	-0.0919324	-1.2992136	-2.0965635	H	0.3906377	0.1618768	-1.8563988	
H	-0.6109173	0.3987726	-2.1350181	H	-1.6695697	-1.3041899	-0.9115642	
H	-3.3321617	1.4684584	2.4787182	H	-2.7439586	-0.7221786	-2.2184203	
H	-3.6435364	2.2520019	0.9297997					
H	-2.1159472	2.5744283	1.7888142					
H	0.2659505	-1.5097700	1.6520912					
H	-1.7153362	-0.8589418	-1.5319562					

5. Solution state conformational analysis

5.1 Infrared spectroscopy

Solution state infrared spectra were recorded in $CHCl_3$ (see section 1.1 for instrumentation).

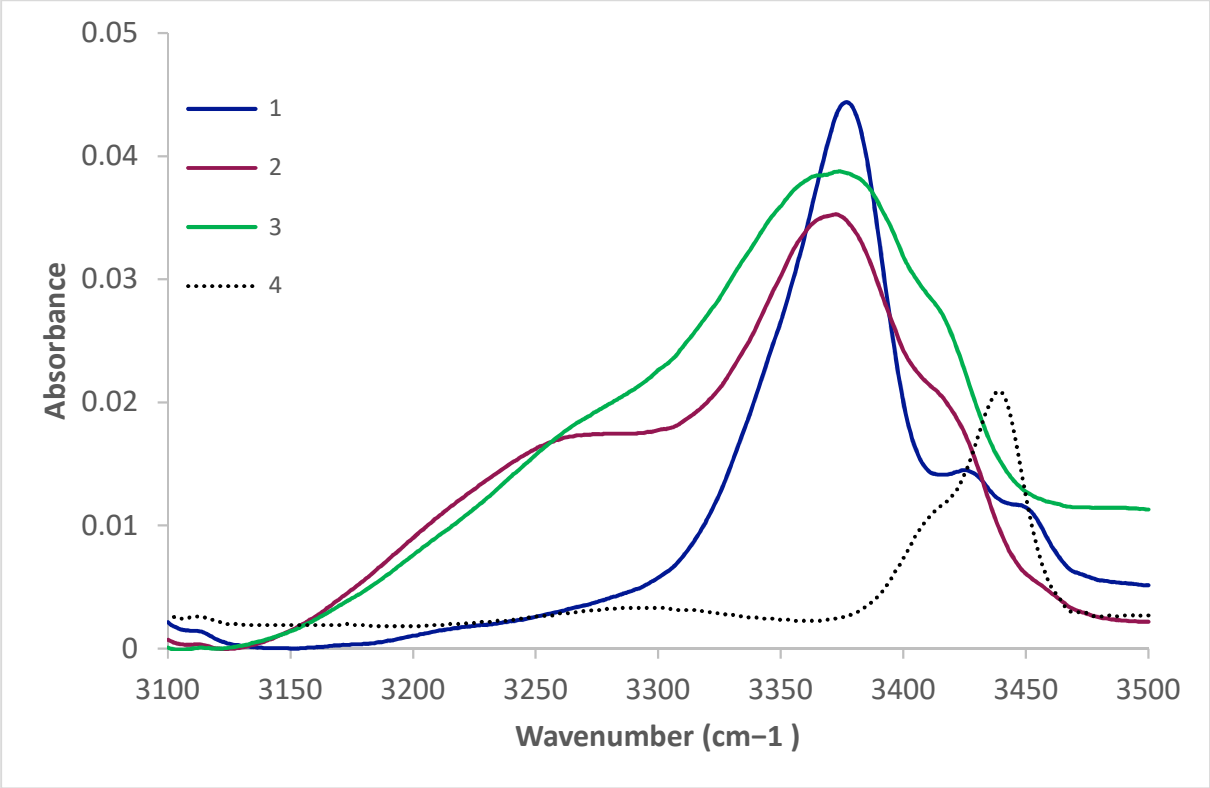

Figure S9. Solution state IR absorption spectra in the NH stretch region for **1-4** (5 mM in $CHCl_3$).

Cbz-Attc-NHMe **1**

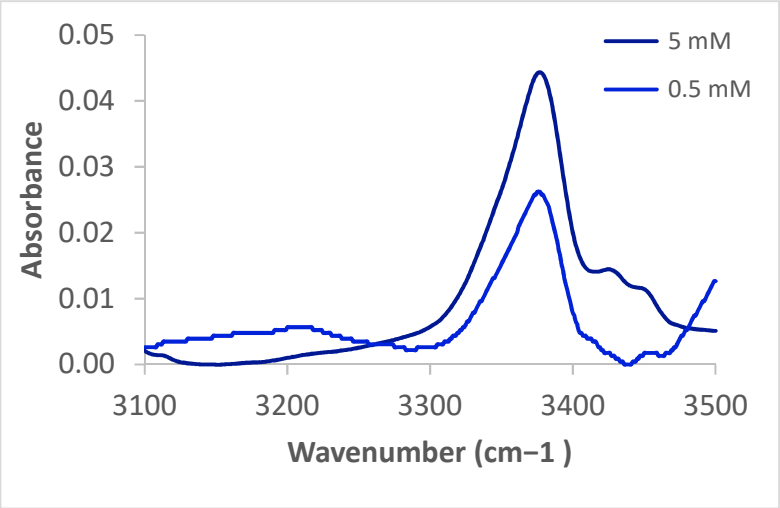

Cbz-(Attc)$_2$-NHMe **2**

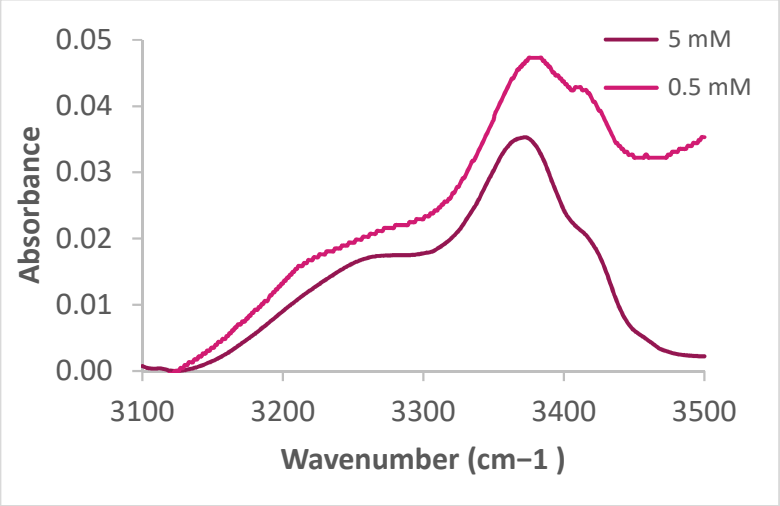

Cbz-(Attc)$_3$-NHMe **3**

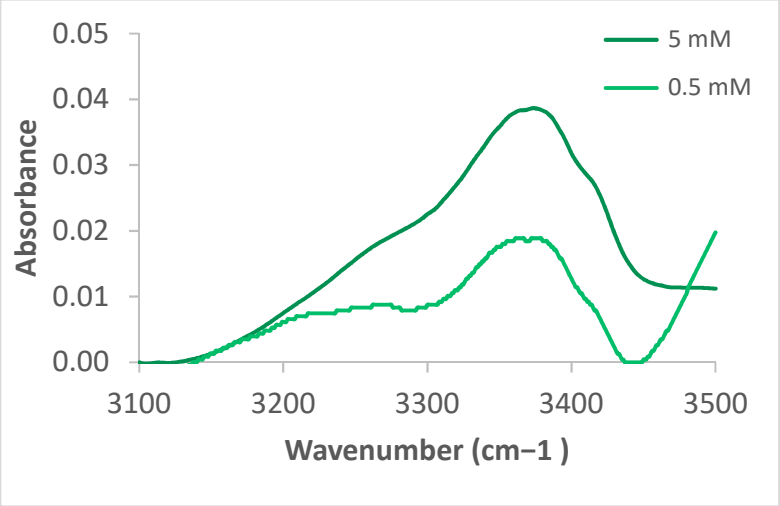

Figure S10. Solution state IR absorption spectra in the NH stretch region for **1-3** at two different concentrations (0.5 mM and 5 mM) in $CHCl_3$. Absorbance is not to scale for the ten-fold diluted sample solutions.

5.2 ^{1}H NMR: DMSO-d_6 titrations

^{1}H spectra of **1-4** were recorded at 300 K on a 400 MHz spectrometer (see section 1.1). Samples were dissolved in $CDCl_3$ (400 µL) to give solutions of concentration 5 mM. Aliquots of DMSO-d_6 (6 × 2 µL, 2 × 4 µL, 2 × 10 µL) were added successively to the NMR tube followed, after each addition, by rapid agitation then re-recording of the ^{1}H spectra.

Cbz-Attc-NHMe 1

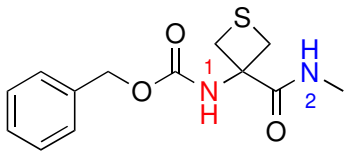

	DMSO-d_6 (%, v/v)											
NH	*0*	*0.5*	*1*	*1.5*	*2*	*2.5*	*3*	*4*	*5*	*7.5*	*10*	**Δδ**
NH^1	6.45	6.49	6.54	6.58	6.62	6.66	6.70	6.77	6.83	6.95	7.05	0.60
NH^2	7.98	7.93	7.88	7.83	7.79	7.75	7.70	7.63	7.55	7.41	7.29	-0.68

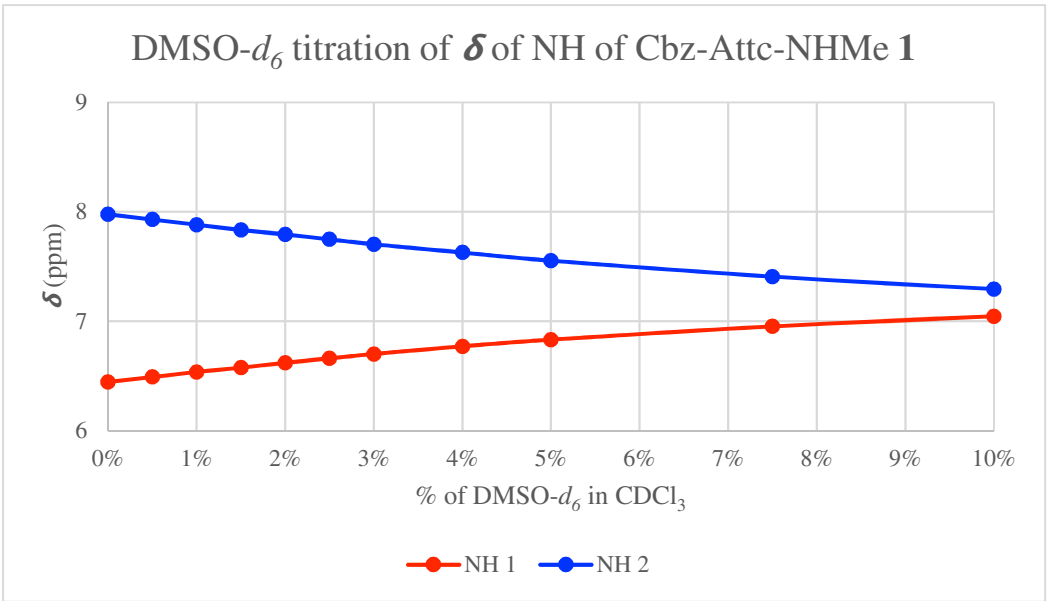

Cbz-(Attc)$_2$-NHMe 2

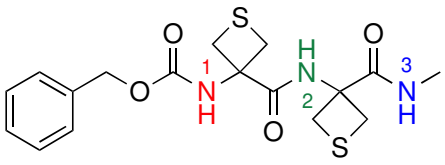

	DMSO-d_6 (%, v/v)											
NH	*0*	*0.5*	*1*	*1.5*	*2*	*2.5*	*3*	*4*	*5*	*7.5*	*10*	**Δδ**
NH^1	6.23	6.43	6.59	6.73	6.84	6.93	7.03	7.18	7.26	7.49	7.61	1.38
NH^2	8.95	8.78	8.65	8.54	8.45	8.37	8.31	8.20	8.13	8.01	7.96	-0.79
NH^3	7.84	7.76	7.69	7.63	7.57	7.52	7.47	7.38	7.30	7.20	7.96	-0.99

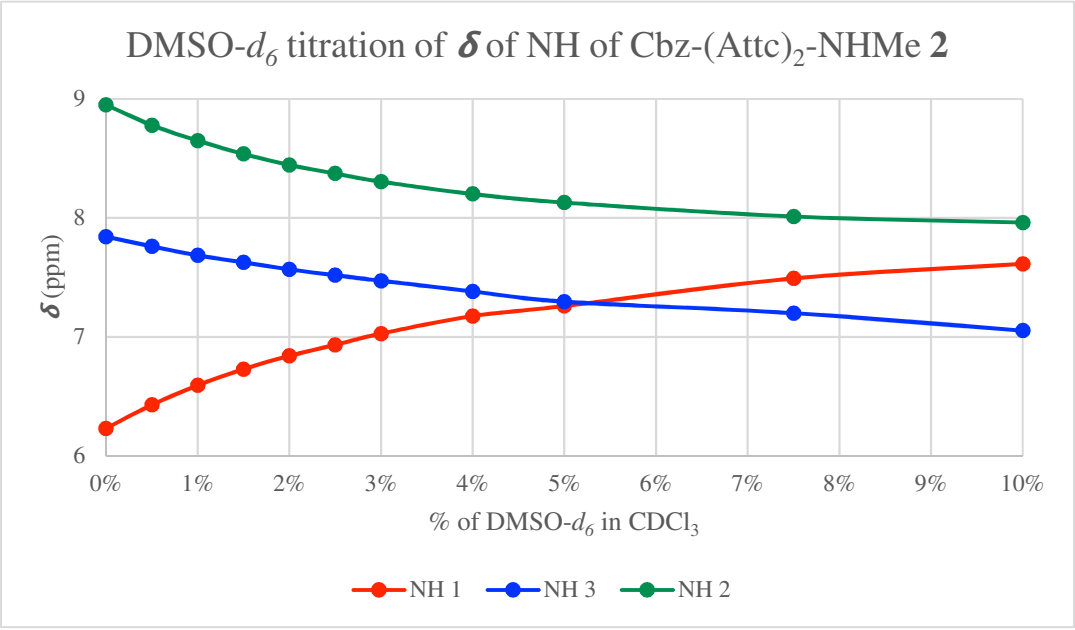

Cbz-(Attc)$_3$-NHMe 3

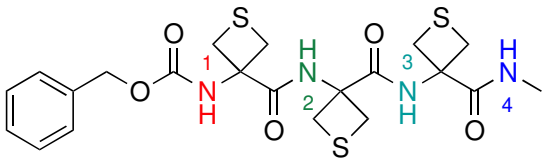

	DMSO-d_6 (%, v/v)											
NH	*0*	*0.5*	*1*	*1.5*	*2*	*2.5*	*3*	*4*	*5*	*7.5*	*10*	**Δδ**
NH^1	6.26	6.81	7.12	7.31	7.47	7.58	7.67	7.79	7.90	8.05	8.15	1.89
NH^2	8.32	8.24	8.21	8.22	8.24	8.26	8.29	8.35	8.42	8.53	8.62	0.30
NH^3	8.39	8.10	7.94	7.84	7.77	7.72	7.67	7.63	7.58	7.51	7.45	-0.94
NH^4	7.52	7.36	7.15	7.06	7.00	6.94	6.91	6.85	6.81	6.72	6.63	-0.89

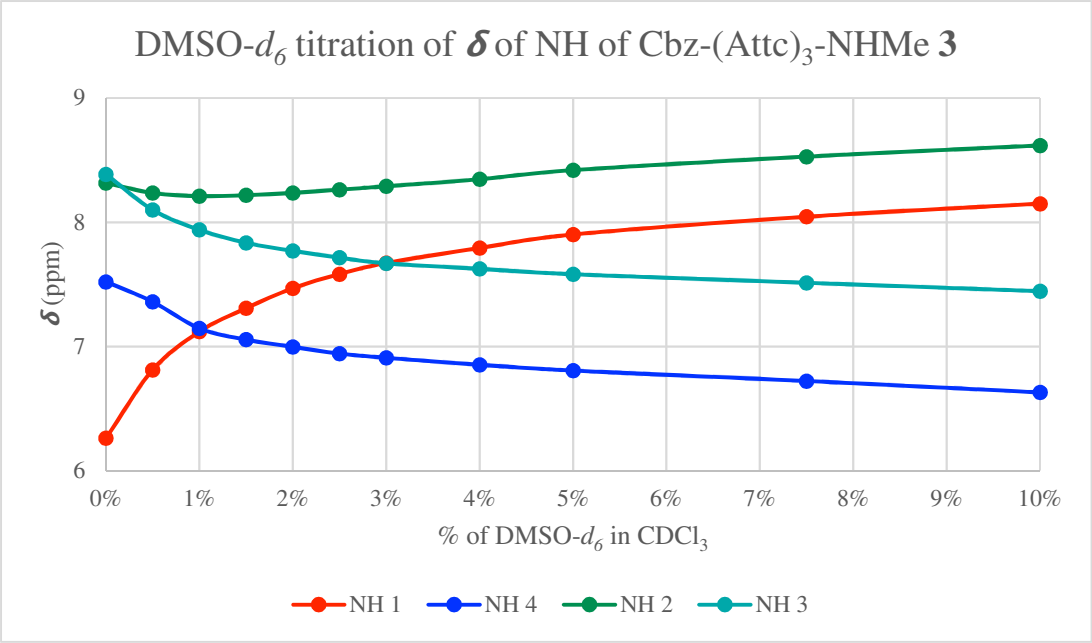

Cbz-Attc-OMe 4

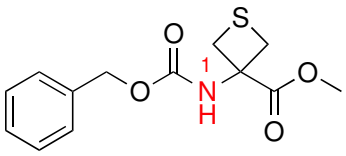

	DMSO-d_6 (%, v/v)											
NH	*0*	*0.5*	*1*	*1.5*	*2*	*2.5*	*3*	*4*	*5*	*7.5*	*10*	Δδ
NH[1]	5.59	5.82	6.00	6.17	6.32	6.45	6.56	6.76	6.92	7.18	7.38	1.79

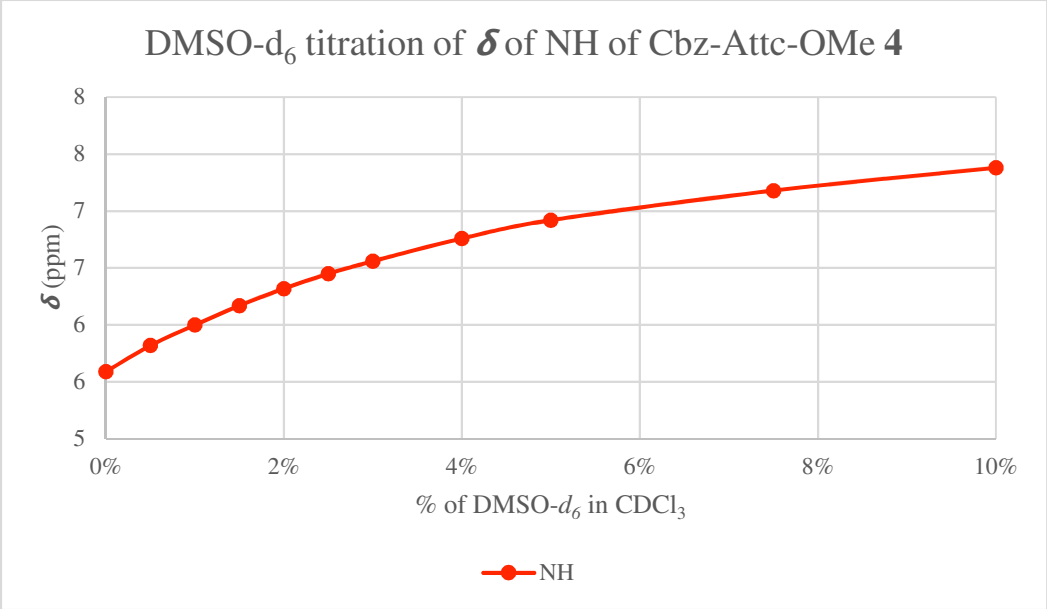

5.3 2D NOESY NMR of compound 2

A NOESY experiment was performed on compound **2** (20 mM solution in $CDCl_3$); data were acquired at 300 K on a 400 MHz spectrometer (see section 1.1). The pulse sequence was noesygpph, and the mixing time was 800 ms. The experiment was performed by collecting 1024 points in f2 and 256 points in f1.

Spectral correlations in the NH resonance region are shown below. 3D projections of NH correlations are illustrated in Figure S11 and are strength-qualified in Table S7.

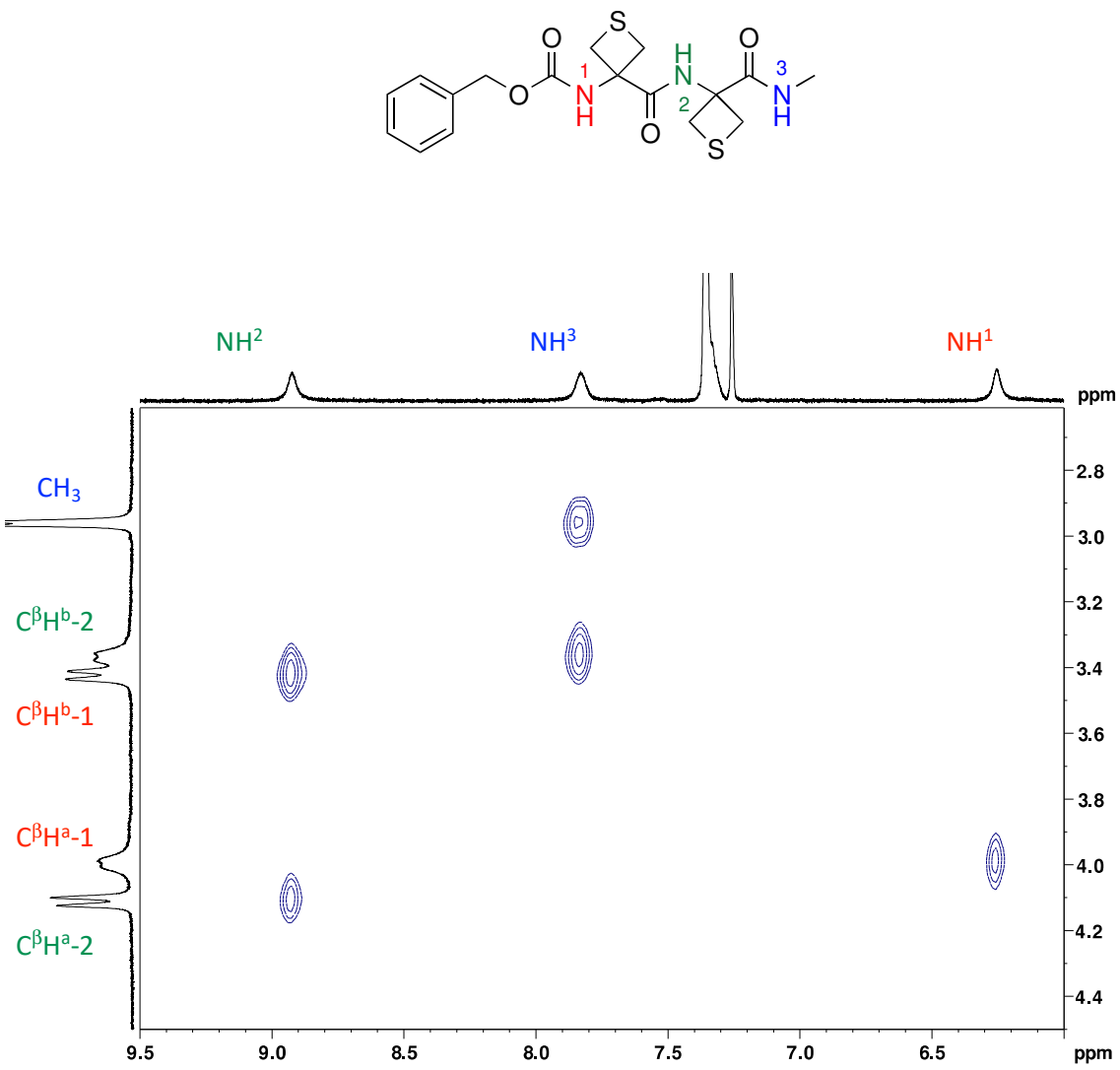

NH	NH^1	NH^2	NH^3
3D projection of NOE correlations	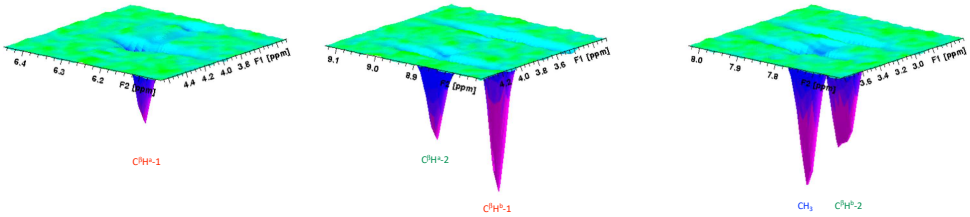		

Figure S11. 3D projections of NOE correlations for NH(1), NH(2) and NH(3) in compound **2**.

Table S7. Strengths of NOE correlations for NH(1), NH(2) and NH(3) in compound **2**.

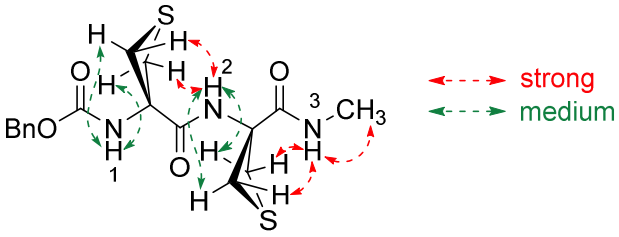

NH	NOE correlation	Strength (by volume) of NOE correlation
NH(1)	$C^{\beta}H$(a)-Attc(1)	medium
NH(2)	$C^{\beta}H$(b)-Attc(1)	strong
	$C^{\beta}H$(a)-Attc(2)	medium
NH(3)	$C^{\beta}H$(b)-Attc(2)	strong
	CH_3	strong

6. X-Ray single crystal structures

A crystal of **1** suitable for X-ray diffraction was obtained by slow evaporation of a $CHCl_3$ solution at ambient temperature. A crystal of **2** suitable for X-ray diffraction was obtained by slow evaporation of an EtOH solution at ambient temperature. A crystal of **3** suitable for X-ray diffraction was obtained by slow evaporation of an acetonitrile solution at ambient temperature.

X-ray diffraction data for compounds **1** and **3** were collected on a VENTURE PHOTON100 CMOS Bruker diffractometer equipped with a Micro-focus IuS source using Mo Kα radiation. X-ray diffraction data for compound **2** were collected on the same instrumental set-up using Cu Kα radiation. Crystals were mounted on a CryoLoop (Hampton Research) with Paratone-N (Hampton Research) as cryoprotectant and then flashfrozen in a nitrogen-gas stream at 100 K. The temperature of the crystal was maintained at the selected value by means of a 700 series Cryostream (for compounds **2** and **3**) or N-Helix (for compound **1**) cooling device to within an accuracy of ±1 K. The data were corrected for Lorentz polarization and absorption effects. The structures were solved by direct methods using SHELXS-97[S16] and refined against F^2 by full-matrix least-squares techniques using SHELXL-2018[S17] with anisotropic displacement parameters for all non-hydrogen atoms. Hydrogen atoms were located on a difference Fourier map and introduced into the calculations as a riding model with isotropic thermal parameters. All calculations were performed by using the Crystal Structure crystallographic software package WINGX.[S18]

The crystal data collection and refinement parameters are given in Table S8.

CCDC 1985233-1985235 contain the supplementary crystallographic data for this paper. These data can be obtained free of charge from the Cambridge Crystallographic Data Centre via http://www.ccdc.cam.ac.uk/Community/Requestastructure.

Table S8. Crystallographic data and structure refinement details.

Compound	**1**	**2**	**3**
CCDC	1985234	1985233	1985235
Empirical Formula	$C_{13}H_{16}N_2O_3S$	$C_{17}H_{21}N_3O_4S_2$	$C_{21}H_{26}N_4O_5S_3$
M_r	280.34	395.49	510.64
Crystal size, mm^3	$0.12 \times 0.08 \times 0.03$	$0.24 \times 0.03 \times 0.02$	$0.16 \times 0.14 \times 0.04$
Crystal system	triclinic	triclinic	monoclinic
Space group	*P* -1	*P* -1	*P* $2_1/n$
a, Å	8.685(3)	11.823(11)	9.3649(6)
b, Å	8.736(4)	14.91(2)	16.1291(11)
c, Å	9.845(4)	17.77(3)	15.8386(8)
α, °	93.793(12)	66.73(6)	90
β, °	115.772(9)	84.29(5)	103.398(2)
γ, °	100.572(12)	75.73(5)	90
Cell volume, $Å^3$	652.2(5)	2789(7)	2327.3(2)
Z ; Z'	2 ; 1	6 ; 3	4 ; 1
T, K	100(1)	100(1)	100(1)
Radiation type; wavelength Å	MoKα; 0.71073	CuKα; 1.54178	MoKα; 0.71073
F_{000}	296	1248	1072
μ, mm^{-1}	0.254	2.843	0.360
θ range, °	2.329 - 31.562	2.706 - 67.658	2.319 - 30.562
Reflections collected	52 952	30 314	85 926
Reflections unique	4 369	9 707	7 138
R_{int}	0.0762	0.0724	0.1345
GOF	1.024	1.045	0.997
Refl. obs. $I > 2\sigma(I)$	3 437	7 902	4 971
Parameters	173	706	287
wR_2 (all data)	0.0990	0.1779	0.0802
R value $I > 2\sigma(I)$	0.0377	0.0605	0.0376
Largest diff. peak and hole ($e^-.Å^{-3}$)	0.494 ; –0.381	1.240 ; –0.707	0.375 ; –0.376

Compound **1** (Figure S12) showed only intermolecular N–H···O=C interactions in the lattice, implicating both NH and both carbonyl groups of each molecule, with the molecules being linked in infinite 1D H-bonding networks (Figure S13). The closest contact for the sulfur atom was an aromatic hydrogen atom on the Cbz-cap of a molecule in a neighboring network, with a H···S distance of 293 pm (Figure S14).

In compound **2** the asymmetric unit contained three molecules (Figure S15 shows one molecule). In the lattice, networks of N–H···O=C interactions connected molecules of types **2**(a) and **2**(b) in alternation while molecules of type **2**(c) were paired symmetrically through intermolecular N–H···O=C H-bonds between NH(1) and the carbonyl oxygen of Attc(2). In all three types of molecule (a-c) an intramolecular C10 interaction was observed between the Cbz-cap C=O and NH(3), with N–H···O=C distances of 219, 233 and 230 pm, respectively (Figure S16). Sulfur-aromatic interactions were apparent between Attc(2) residues and Cbz-caps of pairs of **2**(a) molecules, with a H···S distance of 280 pm. The sulfur atom of Attc(1) of each **2**(a) molecule was oriented towards NH(2) of each **2**(c) molecule, with a N–H···S distance of 294 pm (Figure S17).

In compound **3** both NH(3) and NH(4) of the molecule made C10 interactions to provide a short 3_{10}-helix (Figure S18). The former interacts with the Cbz-cap C=O and the latter with the carbonyl of Attc(1), with N–H···O=C distances of 208 and 218 pm respectively. The remaining backbone groups were engaged in intermolecular interactions linking molecules in 1D networks (Figure S19). Sulfur-aromatic interactions were again apparent: each Cbz-cap's phenyl ring shows two such interactions, implicating the Attc(3) sulfur atom of two consecutive molecules of **3** in an adjacent H-bonded network, with H···S distances of 288 and 293 pm (Figure S20).

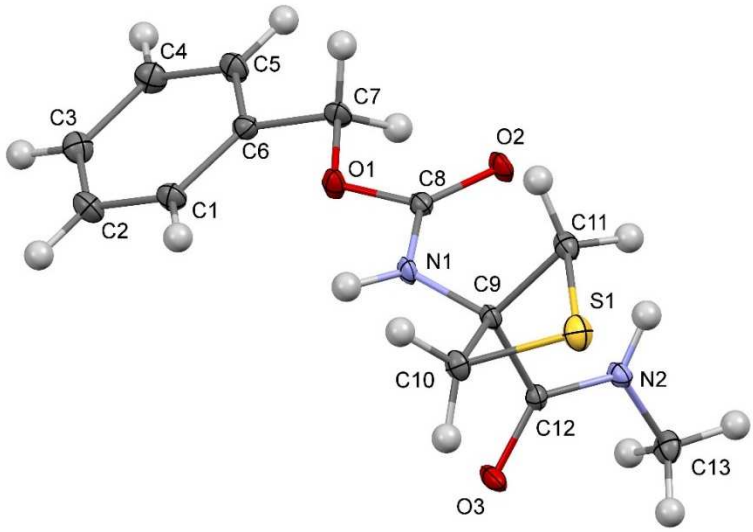

Figure S12. ORTEP drawing of compound **1**. Thermal ellipsoids are shown at the 30% level.

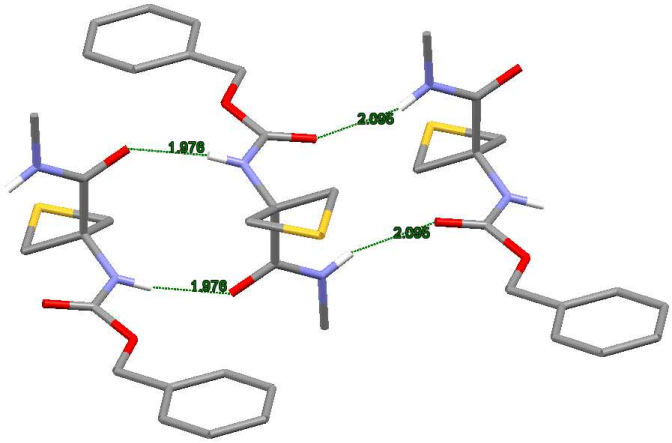

Figure S13. Hydrogen bonding network of **1** in the crystal structure. Each molecule forms four intermolecular H-bonds. Only NH hydrogen atoms are shown for clarity.

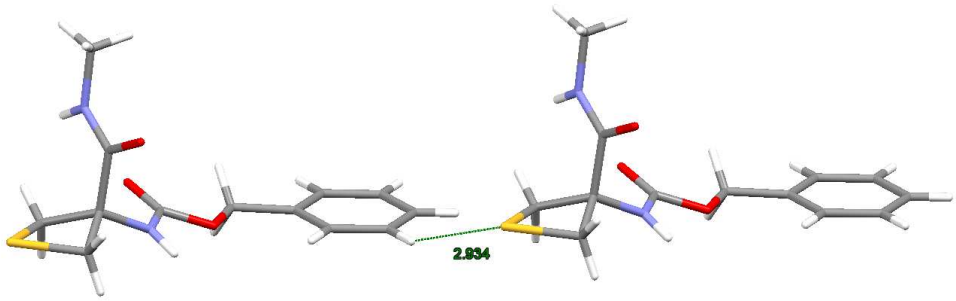

Figure S14. Sulfur-aromatic interaction between two neighboring molecules of **1** in the crystal structure.

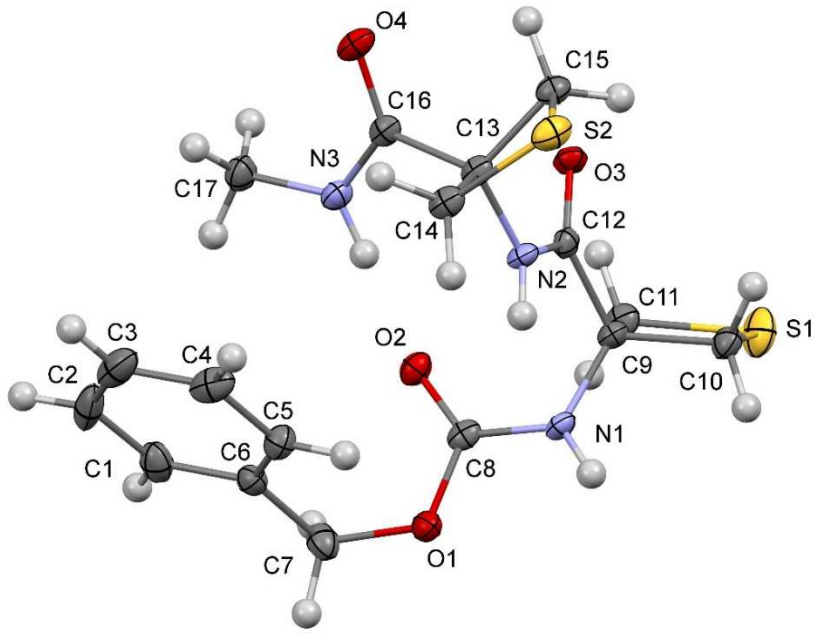

Figure S15. ORTEP drawing of **2** showing only one molecule of the three in the asymmetric unit. Thermal ellipsoids are shown at the 30% level.

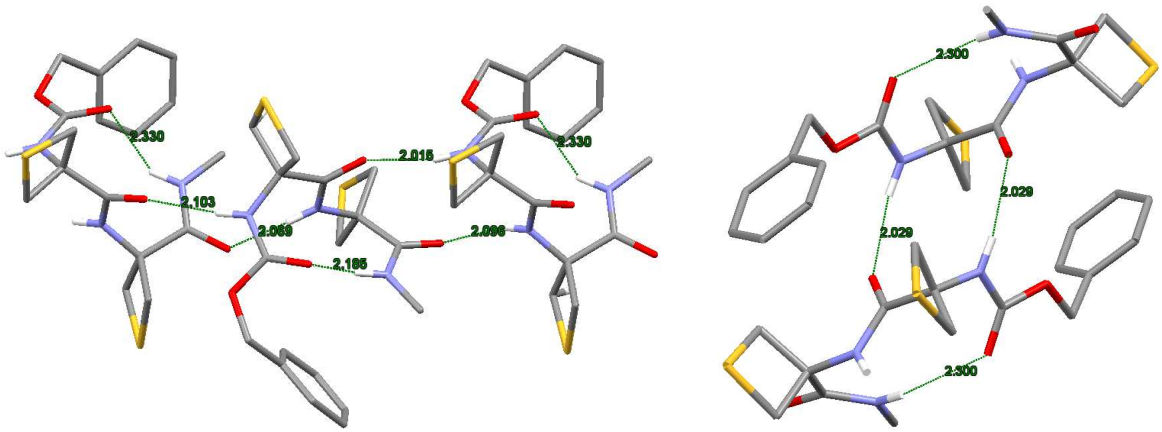

Figure S16. Hydrogen bonding networks of **2** in the crystal structure. Each of the three molecules in the asymmetric unit also forms one intramolecular C10 H-bond. Left: four intermolecular H-bonds linking molecules **2**(a) and molecules **2**(b) alternately in infinite chains. Right: two intermolecular H-bonds linking molecules **2**(c) in pairs. Only NH hydrogen atoms are shown for clarity.

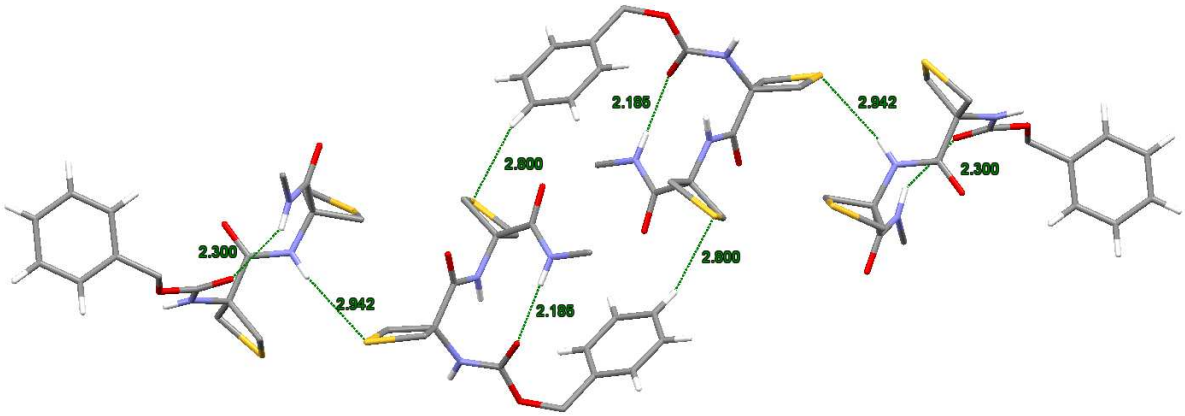

Figure S17. Close contacts for sulfur atoms in the crystal structure of **2**. Sulfur-aromatic interactions between pairs of **2**(a) molecules (which are not connected through N–H···O=C H-bonds) implicating the Attc(2) residues. The sulfur atom of each Attc(1) residue is oriented towards NH(2) of neighboring **2**(c) molecules. Each molecule in shown with its intramolecular C10 H-bond. Aliphatic hydrogens have been removed for clarity.

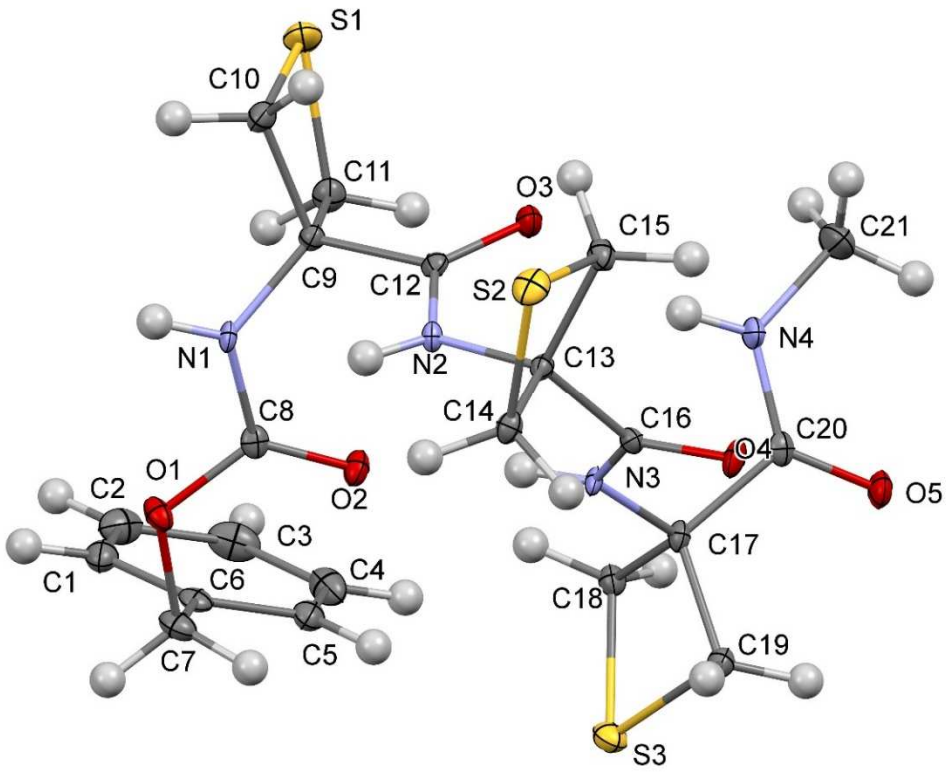

Figure S18. ORTEP drawing of compound **3**. Thermal ellipsoids are shown at the 30% level.

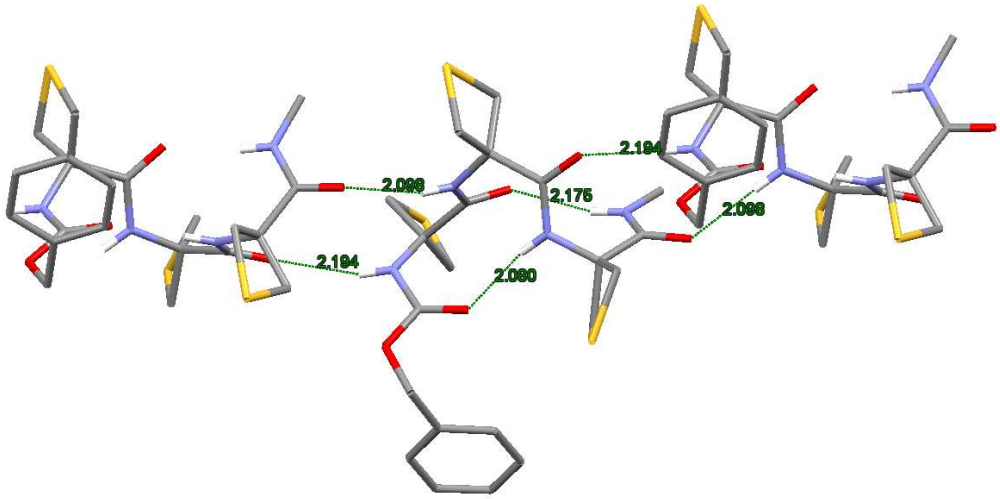

Figure S19. Hydrogen bonding network of **3** in the crystal structure. Each molecule forms two intramolecular C10 H-bonds, making a 3_{10}-helix conformer, and four intermolecular H-bonds. Only NH hydrogen atoms are shown for clarity.

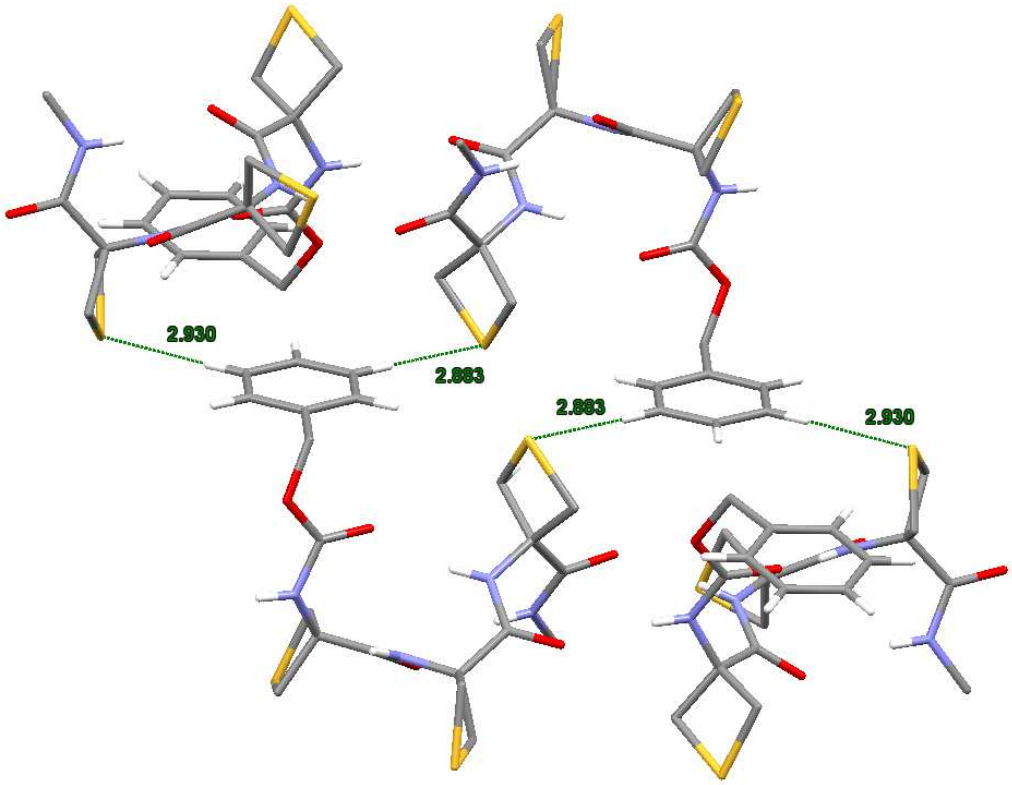

Figure S20. Intermolecular sulfur-aromatic interactions between Attc(3) sulfur atoms and Cbz-caps of neighboring molecules in the crystal structure of **3**. Aliphatic hydrogens have been removed for clarity.

7. References

[S1] A. P. Kozikowski and A. H. Fauq, *Synlett*, 1991, 783-784.

[S2] E. Gloaguen, H. Valdes, F. Pagliarulo, R. Pollet, B. Tardivel, P. Hobza, F. Piuzzi and M. Mons, *J. Phys. Chem. A*, 2010, **114**, 2973-2982.

[S3] E. Gloaguen and M. Mons, *Top. Curr. Chem.*, 2015, **364**, 225-270.

[S4] Macromodel Schrödinger, LLC,: New York, NY, USA, Schrödinger Release 2019-3.

[S5] S. Grimme, J. Antony, S. Ehrlich and H. Krieg, *J. Chem. Phys.*, 2010, **132**, 154104.

[S6] D. Rappoport and F. Furche, *J. Chem. Phys.*, 2010, **133**, 134105.

[S7] K. Eichkorn, F. Weigend, O. Treutler and R. Ahlrichs, *Theor. Chem. Acc.*, 1997, **97**, 119-124.

[S8] Turbomole V7.2 2017, a development of University of Karlsruhe and Forschungszentrum Karlsruhe GmbH, 1989-2007, Turbomole GmbH, since 2007; available from http://www.turbomole.com.

[S9] H. S. Biswal, E. Gloaguen, Y. Loquais, B. Tardivel and M. Mons, *J. Phys. Chem. Lett.*, 2012, **3**, 755-759.

[S10] A. E. Reed, L. A. Curtiss and F. Weinhold, *Chem. Rev.*, 1988, **88**, 899-926.

[S11] F. Weinhold, *J. Comput. Chem.*, 2012, **33**, 2363-2379.

[S12] I. V. Alabugin, G. dos Passos Gomes and M. A. Abdo, *WIREs Comput. Mol. Sci.*, 2019, **9**, e1389.

[S13] F. Weinhold, A. E. Reed, J. E. Carpenter and E. D. Glendening NBO version 3.1.

[S14] M. J. Frisch, G. W. Trucks, H. B. Schlegel, G. E. Scuseria, M. A. Robb, J. R. Cheeseman, G. Scalmani, V. Barone, G. A. Petersson, H. Nakatsuji, X. Li, M. Caricato, A. V. Marenich, J. Bloino, B. G. Janesko, R. R. Gomperts, B. B. Mennucci, H. P. Hratchian, J. V. Ortiz, A. F. Izmaylov, J. L. Sonnenberg, D. Williams-Young, F. Ding, F. Lipparini, F. Egidi, J. Goings, B. Peng, A. Petrone, T. Henderson, D. Ranasinghe, V. G. Zakrzewski, J. Gao, N. Rega, G. Zheng, W. Liang, M. Hada, M. Ehara, K. Toyota, R. Fukuda, J. Hasegawa, M. Ishida, T. Nakajima, Y. Honda, O. Kitao, N. Nakai, T. Vreven, K. Throssell, J. A. Montgomery, J. E. Peralta, F. Ogliaro, M. J. Bearpark, J. J. Heyd, E. N. Brothers, K. N. Kudin, V. N. Staroverov, T. A. Keith, R. Kobayashi, J. Normand, K. Raghavachari, A. P. Rendell, J. C. Burant, S. S. Iyengar, J. Tomasi, M. Cossi, J. M. Millam, M. Klene, C. Adamo, R. Cammi, J. W. Ochterski, R. L. Martin, K. Morokuma, O. Farkas, J. B. Foresman and D. J. Fox, Gaussian 16, Revision A.03; Gaussian, Inc., Wallingford CT, USA, 2016.

[S15] E. Gloaguen, V. Brenner, M. Alauddin, B. Tardivel, M. Mons, A. Zehnacker-Rentien, V. Declerck and D. J. Aitken, *Angew. Chem. Int. Ed.*, 2014, **53**, 13756-13759.

[S16] G. M. Sheldrick SHELXS-97, Program for Crystal Structure Solution, University of Göttingen: Göttingen, Germany, 1997.

[S17] G. M. Sheldrick, *Acta Crystallogr. A*, 2008, **64**, 112-122.

[S18] L. J. Farrugia, *J. Appl. Cryst.*, 1999, **32**, 837-838.